Master of Science (Medicine)

Establishment of enhanced protein purification strategies for recombinant immunotherapeutics

Valentine Amanda Shangase

Supervisor:

Prof. Dr. Dr. Stefan Barth

Medical Biotechnology and Immunotherapy
Research Unit, Department of Integrative
Biomedical Sciences, University of Cape Town

This dissertation is submitted to the Faculty of Health Sciences, University of Cape Town, in fulfilment of the requirements for the degree of Master of Science

DECLARATION

1. This thesis/dissertation has been submitted to the Turnitin module (or equivalent similarity and originality checking software) and I confirm that my supervisor has seen my report, and any concerns revealed by such have been resolved with my supervisor.
2. I know that Plagiarism is wrong. Plagiarism is to use another's work and pretend that it is one's own.
3. I have used the Vancouver referencing style for citation and referencing. Each significant contribution to, and quotation in, this research project proposal obtained from the work or works, of other people has been attributed, cited, and referenced.
4. This research project proposal is my work.
5. I have not allowed and will not allow anyone to copy my work to pass it off as his or her work.

Signed: Signed by candidate

Date: 20 March 2025

In loving memory of my grandmother, TayiTayi Ngenisile Shangase intombi kamaDube noMaweshe, umthaphuna nyosi othaphuna ngesamba kwezinye izimpisi. Iyobonana kwelizayo. Ngiyabonga angiphezi Shuku omhlophe ngenhliziyo.

ACKNOWLEDGEMENTS

To my dear parents, Mrs. MaHlophe and Mr Justic Mzelemu, for investing all you have and beyond in me. I would also like to extend my heartfelt thanks to my siblings, Paris, Ayanda, and Awandamadoda, for being my biggest cheerleaders.

I am very thankful to my supervisor Prof Dr Dr Stefan Barth, for granting me the opportunity to be part of the Medical Biotechnology and Immunotherapy (MB&I) Research Unit. I will always appreciate your patience, constant support, and belief in me, especially in challenging times.

I am thankful to the MB&I for the wonderful experience and valuable knowledge you have shared with me. Thank you for all the warm hugs and laughter we shared and the constant support, encouragement, and all the fun memories we created together.

To my dear friends Nhlanhla Khumalo, Sizalobuhle Masuku, and Chardae Friedberg, thank you for making every challenge I encountered throughout this study more bearable. I will forever be in debt to your kindness and support. Finally, thanks to Marc Henry, Emmanuel Fajemisin, Dr Taiwo Aruleba, and Dr Nkhasi Lekena for always offering a helping hand.

CONTENTS

TABLE OF FIGURES

List of tables

List of Abbreviations

Abs	Absorbance
ADC	Antibody-Drug Conjugate
AGT	O6 -Alkylguanine-DNA alkyltransferase
AML	Acute Myeloid Leukemia
BG	Benzyl guanine
BG-Alexa 488	BG-modified SNAP-Surface® Alexa Fluor® 488
BG-Alexa 647	BG-modified SNAP-Surface® Alexa Fluor® 647
(BrA)	Biotin ligands
BSA	Bovine Serum Albumin
dH2O	deionized H2O
DMEM	Dulbecco's Modified Eagle's Medium
DNA	Deoxyribonucleic acid
eGFP	Enhanced Green Fluorescent Protein
FBS	Fetal Bovine Serum
FDA	Food and Drug Administration (United States)
HEK293T	Human Embryonic Kidney cells
IEX	Ion Exchange Chromatography
IMAC	Immobilized Metal Affinity Chromatography
LMIC	Low and Middle-Income Countries
mAb	Monoclonal antibody
MB&I	Medical Biotechnology and Immunotherapy Research

	Unit
NHS	N-hydroxy succinimide
NSNLC	non-small cell lung cancer
ORF	Open Reading Frame
PVDF	Polyvinylidene Fluoride
Rcf	Relative centrifugal force
RE	Restriction Enzyme
RMT	Receptor-Mediated Transcytosis
Rpm	Revolutions per minute of the rotor
RT	Room temperature
scFv	Single-chain variable fragment
SDS-PAGE	Sodium Dodecyl-Sulfate Polyacrylamide Gel Electrophoresis
SEC	Size Exclusion Chromatography
UV	Ultraviolet

ABSTRACT

Antibody-based diagnostic and therapeutic agents play a substantial role in modern medicine, particularly for cancer management. The use of monoclonal antibodies (mAbs) and their derivatives to fight cancer demonstrates a significant impact on both laboratory research and clinical applications. This is largely attributed to their ability to recognize specific antigens. The enhancement of these well-characterized mAbs with effector molecules with desirable, tailored properties. This further gives the product to homogeneous antibody conjugates and improves their potency while reducing toxic side effects. An efficient and cost-effective protocol to produce high-quality recombinant proteins play a pivotal role in supporting both lab-scale research and pharmaceutical applications. Although relying on the limited availability of resources, the MB&I research unit successfully employs a single IMAC step to purify mammalian and bacterially expressed recombinant proteins to successfully supporting a decent number of student projects per year. Such enriched protein preparation does allow preliminary qualitative analysis of such highly active immunotherapeutics; however, expanding this research into future readiness levels needs further expansion.

The main objective of this study was to reestablish and develop an improved protein purification strategy by exploring Immobilized Metal Affinity Chromatography (IMAC), Ion Exchange Chromatography (IEX), and Size Exchange Chromatography (SEC) and further strategically integrating these purification techniques to improve protein purity. Intrinsic properties of the proteins of interest, such as the affinity tag incorporated in the recombinant antibody, and its Isoelectric value (pI), largely contribute to the choice of purification technique as demonstrated by the well-characterized mammalian-expressed SNAP tag-based antibody fusion protein αASPH(scFv)-SNAP and the bacterially expressed recombinant immunotoxin

H22(scFv)-ETA. IMAC was employed as the initial purification step to recover the full-length histidine-tagged recombinant proteins. The Ni^{2+} immobilized on the matrices in columns has a high affinity for Histidine incorporated, which allows the capture of the target protein. The remaining host proteins were removed by IEX, which excludes charge-based impurity and isolates the target protein. SEC was used as the last polishing step to remove remaining aggregates and contaminants. Each purification strategy was independently enhanced by optimizing purification conditions such as the flow rate and the buffer system and subsequently integrated to achieve improved resolution.

The data analysis showed that optimizing running conditions for each purification technique enhanced protein purity. A lower flow rate improved protein retention, thus reducing the loss of target protein. The buffer conditions also played a substantial role in achieving improved protein purity. The integrated purification strategy yielded a higher protein purity compared to the conventional single-step methods. on the contrary, a significant amount of the target protein is lost in each purification technique. An adaptable combinatory chromatography technique was established. The established purification workflow was successfully applied to a variety of other recombinant proteins. This was achieved by careful consideration of the unique physiochemical characteristics of recombinant protein. The established purification techniques can be expanded to a wider variety of fusion proteins. The protein purity and recovery following the application of the combinatory purification technique varied with the combination of chromatography and the nature of the protein. Bacterially expressed proteins require a more expensive wash step compared to mammalian-expressed proteins. However, higher protein yield was obtained from bacterially expressed proteins compared to mammalian-expressed proteins. The findings suggest that the choice of chromatography combination techniques should be based on the nature of the protein, yield, and purity requirement.

The limited capacity to produce cost-effective recombinant immunotherapeutics significantly restricts the accessibility of antibody-based treatments such as monoclonal antibodies for cancer treatment. This study outlines the technology that can be a baseline for advancing lab-based research and local continuous production of recombinant biopharmaceuticals and offers a great opportunity to close the existing gap in developing countries.

Chapter 1: LITERATURE REVIEW

1.1 The Global Burden of Cancer

For decades, cancer has been a major public and economic challenge globally, accounting for more than 10 million deaths to date. Previously, the cancer burden dominated Europe, China, and Northern American countries, however, a spiral increase is observed in underdeveloped and developing nations such as some African and Asian regions (1,2). Among many factors contributing to the global shift of cancer cases is caused by some major risk factors, such as environmental factors, lifestyle, growth, and aging of the population in developing countries, and the slower decline in cancers related to infectious aetiologies in low-resource countries than in high-resource countries (3–5). The milestone fight against cancer has led to several cancer therapies such as surgery, chemotherapy, radiation therapy, targeted therapy, immunotherapy, stem cell or bone marrow transplant, and hormonal therapy. Though these therapies have spared some lives, they have several drawbacks that limit their efficacy in the clinic, which may be direct or indirect. Some of these limitations include damage to healthy tissues, systemic toxicities, the development of drug resistance, and remaining an affliction known to humanity (6–8).

Many cancers can be prevented by avoiding risk factors, and most cancers have a promising chance of cure; however, this depends on early detection of cancer and appropriate treatment and care of patients who develop cancer. The majority of the high-income countries have access to comprehensive treatment. Whereas less than 15% of the low-income countries have access. The lack of infrastructure, Poor access to epidemiological data, research, treatment, and cancer control and prevention combine to result in significantly poorer survival rates in developing countries for a range of specific malignancies compared to those of developed nations (9). This situation demands for even greater effort to develop more inclusive and effective

cancer therapies thus improving patient care. Achieving this heavy relay on an establishment of a much more cost-effective therapy production, that may either enhance already existing therapies or through the development of more effective therapies (6,10,11).

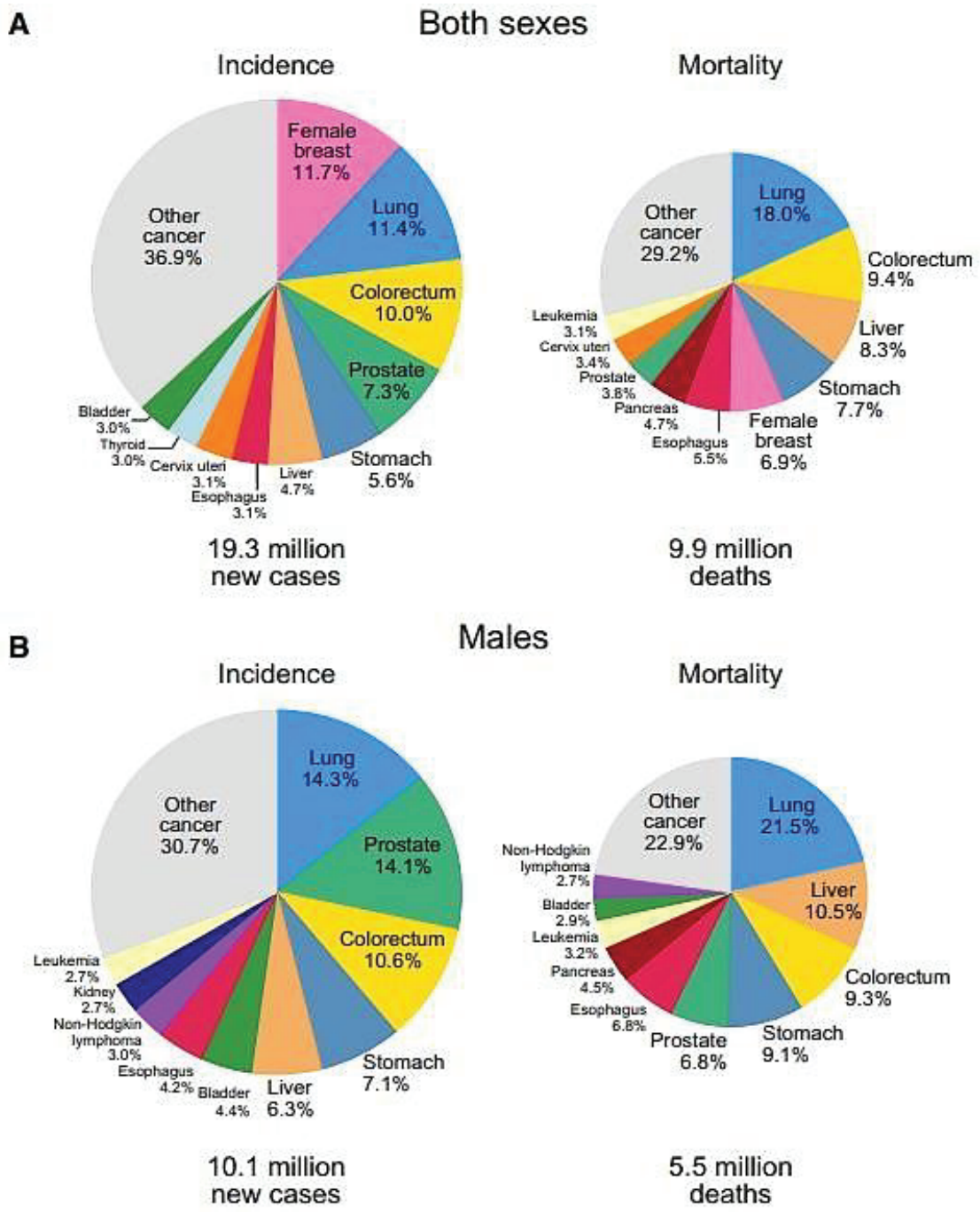

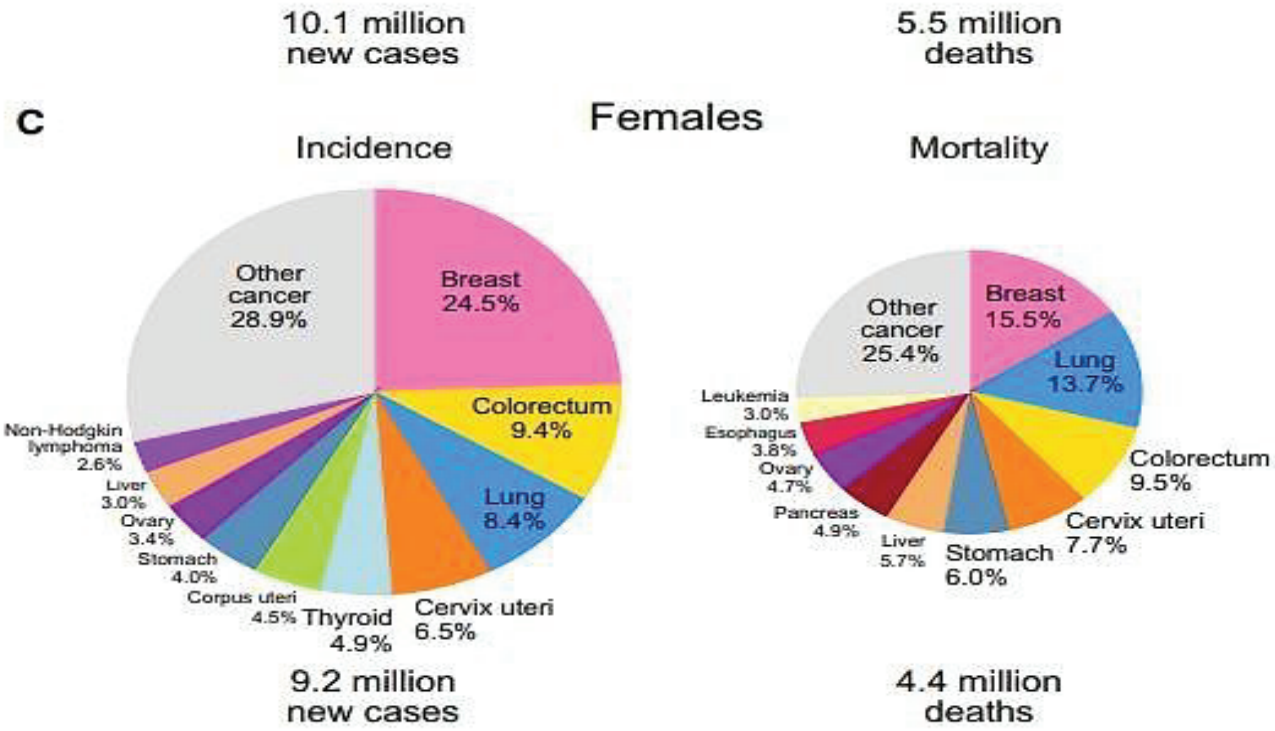

Figure 1. Estimated number of cancer cases: A) represents both Sexes, (B) represents only men, and (C) represents only women (Source: GLOBOCAN 2020).

1.2 Background overview of immunotherapy

For many years, non-specific cancer therapies such as chemotherapy and radiation have been a major setback in treating cancer. While these traditional therapies aim to destroy cancer cells, they also affect healthy body cells (12). Chemotherapy drugs work by interfering with the process of cell division, which is a characteristic feature of both healthy and cancer cells, and because of the non-specificity limitation, healthy cells that divide rapidly, such as those in the bone marrow, hair follicles, and the lining of the digestive tract are also destroyed by the chemo-drugs. While radiotherapy uses high-energy radiation to destroy cancer cells in specific body areas, surrounding healthy cells can also be affected (13). This may lead to side effects like anaemia, hair loss, nausea, vomiting, digestive issues, and damage to body organs (14,15). Specificity plays a pivotal role in effective and more reliable cancer therapy. The discovery and development of immunotherapy marked a significant turning point in cancer treatment addressing some of the setbacks of traditional therapy.

Immunotherapy harnesses the body's own immune system to recognize and attack cancer cells while sparing healthy ones (14,16). This approach is more targeted and can have fewer side effects compared to traditional treatments. Immunotherapy includes various approaches like T-cell therapy, oncolytic virus therapy, cancer vaccines, checkpoint inhibitors and monoclonal antibodies (16–18). Although immunotherapy may be seen as an apparent solution to some of the setbacks of traditional therapy, it is worth mentioning that the efficacy of immunotherapy can be improved in combination with other therapeutic strategies such as Antibody Drug Conjugates technology (ADC) (19–21).

1.3 Targeted therapeutic approach for cancer treatment

1.3.1 Antibody-drug conjugate

The development of monoclonal antibodies, which are a derivative of antibody technology, has gained much attention in the development of cancer therapy. They are a type of targeted cancer therapy that is designed to interact with specific targets(22,23). Substantial advancement has been made in the past few years in the development of anti-drug conjugates as part of the broader effort to advance precision medicine (24). As a result, mAbs have subsequently been conjugated with toxic payloads to form antibody-drug conjugates (ADCs) (21, 25, 26). Antibody-drug conjugation is a therapeutic approach that combines the specificity of monoclonal antibodies (mAbs) with the potency of cytotoxic drugs to ensure specific targeted drug delivery into the cancerous cells through the antibody-antigen interaction (27–29). The cytotoxic drug payload is released, leading to cell death, and thus, normal tissues are spared from chemotherapeutic damage (21,27). To produce uniform ADCs with low aggregation levels site-specific drug conjugation methods such as the SNAPtag technology are used for the combination of different anticancer drugs with complementary, and non-overlapping toxicity profiles that show a promising potency of anticancer activity (30,31). SNAP-tag, which is a human DNA-repair enzyme

O6alkylguanine DNA alkyltransferase (AGT) derived self-labelling protein covalently binds the benzyl ring of a BG-modified molecule to a thiol group on a cysteine residue in the SNAPtag's active site (Figure 2) (32), giving rise to ADC with added advantage solution to the challenge of increasing the therapeutic index of cell-killing agents for treating cancer and represent an important development in the armamentarium of anticancer therapies (33–35). Monoclonal antibodies (mAbs) have demonstrated considerable utility in the clinical management of cancer (36,37).

The ADC consists of three separate key components, a monoclonal antibody that binds to a tumor-associated cancer antigen with high specificity, an effector molecule that has a high potency to kill the cancer cells, and a chemical linker that will ensure that the effector does not separate from the antibody during transit (**Figure 3**) (38–40). The high-affinity antibody-antigen interaction of immunoconjugates allows for the selective delivery of synthetic small effector molecules such as fluorophores, toxins, radionuclides, drugs, and nanoparticles to the targeted cancer cells. Even though most unconjugated antibodies do have a high affinity for cancer targets, their therapeutic potential is boosted by repurposing these antibodies as delivery machinery for more effective effectors (41–43).

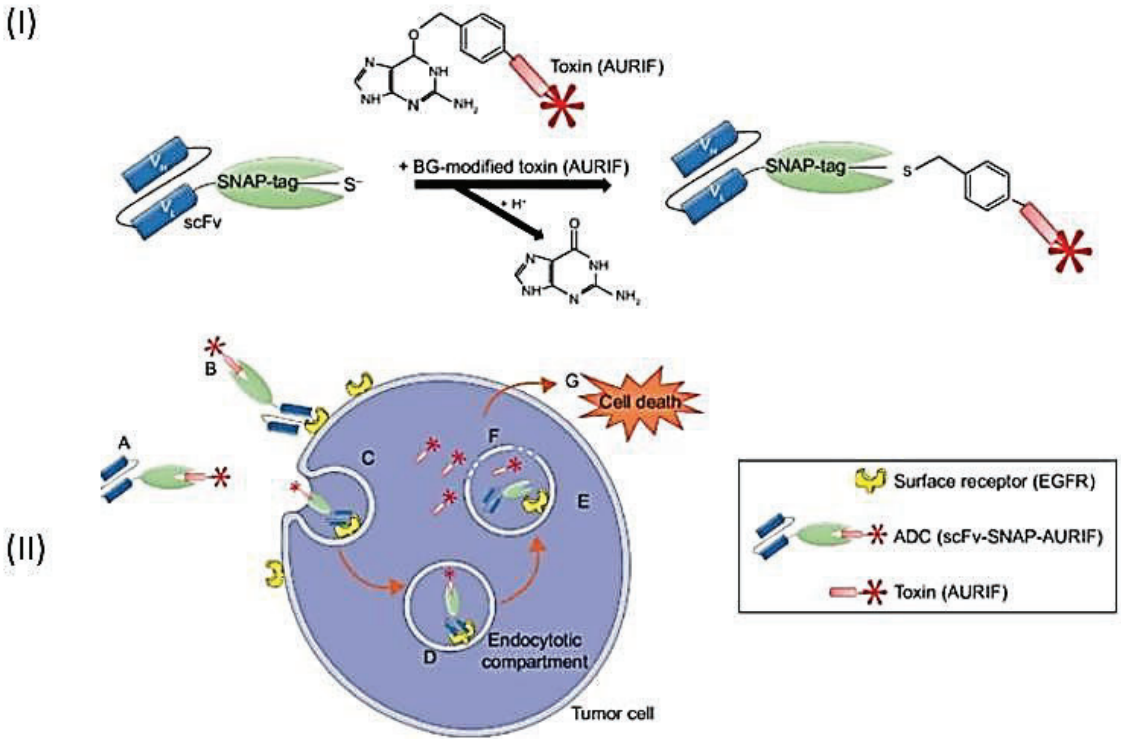

Figure 2: SNAP-tag technology and the mechanism of action of the scFv-SNAP-aUriF ADCs. (A) The SNAP tag undergoes a self-labelling reaction to form a covalent bond with BG derivatives. (B) (I and II) The scFv-SNAP-AURIF ADC binds via its scFv specifically to the extracellular receptor of the target tumor cell, and (C and D) is internalized receptor-mediated into the lysosomal compartment. (E and F) Due to acidification and enzymatic reactions within the lysosomes, the fusion protein is degraded, and the toxin (AURIF) is set free into the cytosol. (G) Auristatin-based toxins influence the microtubule structure and cause cell death by apoptosis (44*)*.

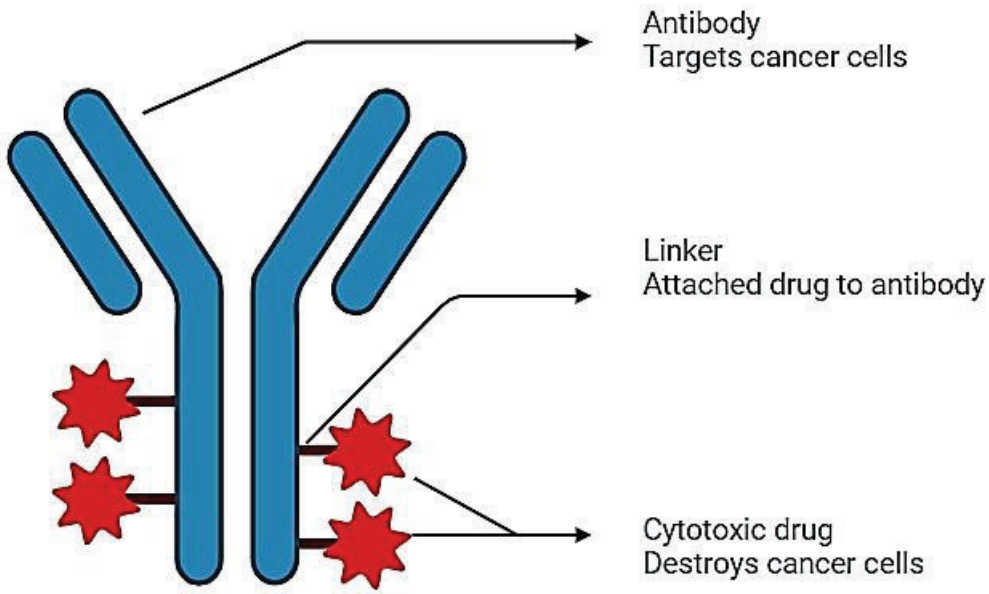

Figure 3: Schematic structure of an Antibody Drug Conjugate. The ADC is composed of three key components. The antibody provides the targeting specificity, the linker ensures stable circulation and

controlled release of the drug at the target site, and the payload provides the cell-killing activity. (Created with BioRender.com).

1.3.2 Recombinant Immunotoxins

Malignant cells are well known for their potency to invade the immune surveillance by producing several immune suppressing cytokines, creating an environment that will allow the cancer cells to thrive and proliferate uncontrollably (26) An approach such as targeted therapy, whereby drug or protein molecules are delivered to specific cells, is a compelling approach to treating malignant diseases. Similarly, like Antibody Drug Conjugates, recombinant immunotoxins are chimeric proteins composed of a truncated, binding-deficient, catalytically active toxin directly linked to a scFv or natural ligand. These fusion gene products are highly homogenous, much easier to modify and more economical to produce than chemical conjugates. Immunotoxins typically use a smaller antibody fragment, such as a single-chain variable fragment (scFv) rather than a full monoclonal antibody, immunotoxins often use smaller antibody fragments to maintain specificity and facilitate internalization, fused directly to a cytotoxic protein or toxin that inhibits protein synthesis the entire molecule including the antibody fragment and the toxin is taken up by target cells, causing the death of the cell to cell death (29,30).

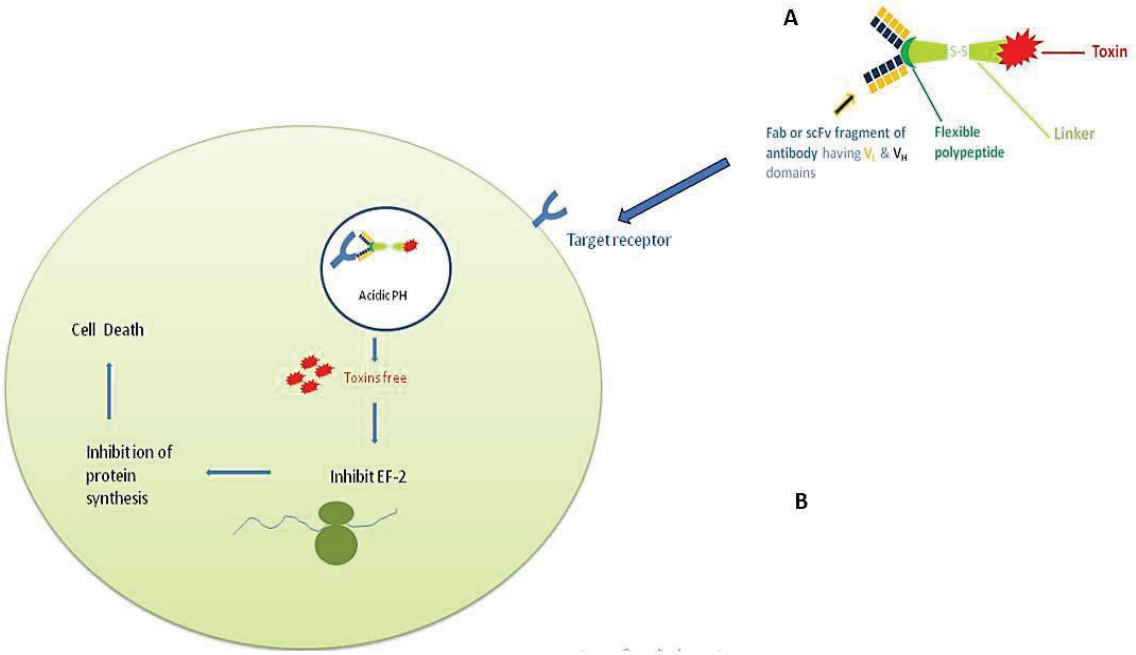

Figure 4: Mechanism of Immunotoxins. (A) The Fab portion of the antibody attaches to the receptor on the cell surface. (B) The immunotoxin and receptor form a complex that undergoes internalization through endocytosis, subsequently localizing to an acidified endosome, the endoplasmic reticulum, or the trans-Golgi apparatus. Within a reducing environment, the disulfide bond in the linker is disrupted. Consequently, the linker connecting the toxin to the antibody is cleaved, allowing the liberated toxin to exert its cytotoxic effect by impeding the protein synthesis of the cell (Medicalverg.in, 2020).

1.4 Targeting cancer via differentially expressed tumour-associated antigens

Cancer cells often have altered signalling pathways and gene expression profiles compared to normal cells. This can lead to the upregulation of Tumor-Associated Antigens (TAAs) and differentially upregulated cell surface receptors that are not as abundant in healthy cells (43,45). These factors are crucial in discriminating between normal and diseased cells, particularly in the context of cancer therapies such as vaccines and the use of human-specific immune cells to recognize malignant cells (46). Overexpression of immune checkpoint molecules affects tumor-specific T-cell immunity in the cancer microenvironment and can reshape tumor progression and metastasis (47). Antibodies targeting checkpoints could restore antitumor immunity by blocking the inhibitory receptor-ligand interaction (48,49). Immunotherapy enhances the body's natural ability to identify and inhibit these receptors in the context of cancer, disrupting the signalling pathways that promote cancer growth.

Additionally, differentially upregulated receptors can serve as diagnostic markers, allowing for the identification of cancer cells. Potential cancer markers identified for molecular targeted therapy include growth factors, signalling molecules, cell-cycle proteins, modulators of apoptosis, and molecules that promote angiogenesis (48,49). The approach of targeted therapy uses antibodies or antibody fragments that recognize differentially upregulated tumor-associated antigen (21,50). TAAs are proteins expressed on the surface of cancer cells, and they serve as targets for ADCs and play a crucial role in the development and improvement of antibody-drug conjugate technology.

1.4.1 ASPH

Aspartate β-hydroxylase (ASPH) is an embryonic transmembrane enzyme aberrantly upregulated in cancer cells, associated with malignant transformation, and plays a role in the post-translational modification of proteins (51). It catalyses the hydroxylation of specific aspartate residues in target proteins. One well-known target of aspartyl β-hydroxylase is Notch, a transmembrane receptor involved in cell communication and development. The hydroxylation of Notch by ASPH is part of the regulatory mechanism that controls Notch signalling (52). The activity of aspartate β-hydroxylase has been implicated in various physiological and pathological processes, including cancer progression, angiogenesis, and cell fate determination. Dysregulation of ASPH has been associated with certain cancers, making it a potential target for therapeutic interventions (53,54). αASPH(scFv)-SNAP is composed of a recombinant single-chain antibody fragment (scFv) targeting ASPH fused with a SNAP-tag. This fusion could be used for specific and controlled labelling or imaging of the target protein in various experimental or therapeutic contexts. This study explores an optimum purification approach for SNAP-tag fusion antibody proteins exemplified by mammalian expressed αASPH(scFv) -SNAP.

1.4.2 CD64

Acute Myeloid Leukaemia (AML) monocytic differentiation is the 72-kDa glycoprotein, CD64. The expression of CD64 is typically restricted to activated cells of the myeloid lineage and is highly pronounced on monocytic blast cells observed in individuals with AML. This receptor is involved in various biological functions, encompassing the mediation of superoxide and cytokine production (tumor necrosis factor α, IL-1, and IL-6), cytotoxicity,

endocytosis/phagocytosis, and the facilitation of antigen presentation. This makes CD64 a good target for AML. Furthermore, its rapid internalization makes it well-suited for ligand-based targeted therapies. Previously, CD64 has been targeted using a chemically coupled immunotoxin based on ricin A. However, undesired off-target effects, including the induction of vascular leakage syndrome, occurred due to nonspecific binding to epithelial cells. Clinical studies have shown that recombinant immunotoxin αH22(scFv)-ETA, comprising a truncated Pseudomonas exotoxin A (PE) and a humanized scFv antibody against CD64, exhibits a reduced nonspecific toxicity while maintaining an antigen-dependent toxicity toward target cells (55–58). αCD64 (H22(scFv)-ETA) is one of the studied recombinant immunotoxins in the MB&I research group. While a highly effective bacterial expression system has been established for producing H22(scFv)-ETA, there is a requirement to enhance the purification process. This optimization is crucial to facilitate ongoing research endeavours at the MB&I lab, aiming to uncover insights into the immune response mechanism (59,60).

1.5 Production of recombinant immunotherapeutic

Africa faces an increased burden of diseases such as cancer due to several factors such including environmental factors, economics, and the health system. Affordability plays a pivotal role in the accessibility to healthcare. Investing in low-cost production of immunotherapeutics fosters the potential to narrow the existing gap between

developed and developing nations. The upstream production of immunotherapeutics, which involves cell culture and fermentation, influences the scalability and efficiency of protein expression. The choice of expression host has a direct impact on the yield, ease of protein extraction, and relative protein purity; therefore, it is crucial to carefully consider the complexity associated with this choice (61). Furthermore, the development of an efficient purification strategy is required to address a resource-intensive and complex purification process. Efforts to incorporate cost-effective technologies and innovation for optimizing expression and purification can enhance production efficiency at a low cost. While finding a balance between the production of high-quality therapeutic products with cost-effectiveness is a constant challenge, advances in these areas can lead to long-term savings thus allowing more accessibility, affordability, and equity in low-income nations.

1.5.1 Expression of recombinant immunotherapeutic

The choice of expression host influences the quality of the end protein product. Different types of expression systems can be used to express therapeutic recombinant proteins. The most commonly used expression hosts include bacterial, plant, insect, yeast, and mammalian expression systems (62). Key elements to be considered when choosing an expression system include intended protein yield, quality, scalability, regulatory considerations, and ensuring cost-effectiveness in the production process (63–65). Moreover, different proteins may be favoured by different expression systems, other factors such as the post-translational modifications, and the destination of the expressed protein should a determining factors (66). In this study, two well-defined expression systems were explored to yield recombinant immunotherapeutic agents exemplified for establishing optimum purification recombinant immunotherapeutic studied at the MB&I unit of recombinant immunotherapeutic proteins that will be utilized.

Mammalian expression systems are commonly favoured for the expression of recombinant proteins used in the production of immunotherapeutic proteins. This is due to their ability to properly fold and modify complex proteins, such as antibodies, cytokines, and other biologically active molecules (64,67,68). These systems ensure that the expressed proteins maintain their proper conformation and post-translational modifications, crucial for their biological activity and therapeutic efficacy. While this expression system offers advantages, inconveniences associated include higher production costs, longer production timelines, and the potential for viral contamination due to the use of animal-derived cell lines 69,70). On the other hand, a bacterial expression system may be a convenient choice of an expression system for therapeutic antibodies due to its rapid growth, rapid expression, ease of culture, and high product yields, and is excellent for functional expression of non-glycosylated proteins (71,72). It is rather desirable for the expression of recombinant immunotoxins (73,74). Using *E. coli* to produce recombinant proteins eliminates the issue of glycosylation and potential interactions with lectin receptors (75–77). This can result to the generation of non-glycosylated proteins that are more predictable in terms of their structure and function. Thus, reduces adverse immunogenicity and side effects related to glycan-lectin interactions, which is particularly important in therapeutic applications (78).

1.5.2 Purification of immunotherapeutic

Purification of antibodies is an important step in the production process and is typically carried out to remove any impurities or contaminants that may interfere with the activity or specificity of the antibody and are suitable for use in humans (79–81). The choice of purification technique explores the biophysiological characteristics of the protein to be purified, such as size, charge, and the presence of any affinity tags or other modifications. The downstream application of the purified protein may also influence the choice of purification technique (82). In this case, the study focuses on

the optimum purification strategies to produce pure and functional immunotherapeutic agents; for this reason, it is crucial to employ purification techniques that preserve the integrity of the target for high-quality recombinant immunotherapeutic agents (83,84).

Chromatography is widely used for the purification of immunotherapeutic agents. It involves the separation of components in a mixture based on their interaction with a stationary phase and a mobile phase (85,86). Chromatography provides tailored flexibility for specific properties of the protein of interest. Different chromatography techniques are employed depending on the properties of the compounds being purified. Three chromatography techniques, including IMAC, IEC, and are exploited to improve protein purity (88,89).

1.5.2.1 Immobilized Metal Affinity Chromatography

Recombinant proteins are commonly expressed with an affinity tag, which is a peptide or protein tag, fused to either the N- or C-terminus to facilitate protein purity (89). Such tags include histidine, glutathione S-transferase (GST), maltose binding protein (MBP), or Streptag II (90–92). IMAC is a type of affinity chromatography that is commonly used to purify recombinant proteins engineered to include polyhistidine tags (86,93). The histidine tag linked to the target protein will bind to the metal ion attached to a solid support matrix (in this case Ni^{2}) while contaminants lacking the poly-histidine tag are excluded and the target protein can be isolated from the selectively eluted from the column using a chelating agent, such as imidazole which competes with the histidine residues for binding to the metal ion (**Figure 5**). In addition, histidine tags are small and less likely to interfere with the natural properties of the proteins to which they are fused. Therefore, their removal may not be necessary post-purification (86,90). Though IMAC can provide a stable binding interaction between the His-tagged protein and the Ni column, contaminating substances may also bind onto the column contributing to poor overall protein purity (82,86,93). However, advantageous this technique can be improved by optimizing the buffer system and

overall running conditions that will favor selective binding of the target protein, thus reducing contamination (89,94).

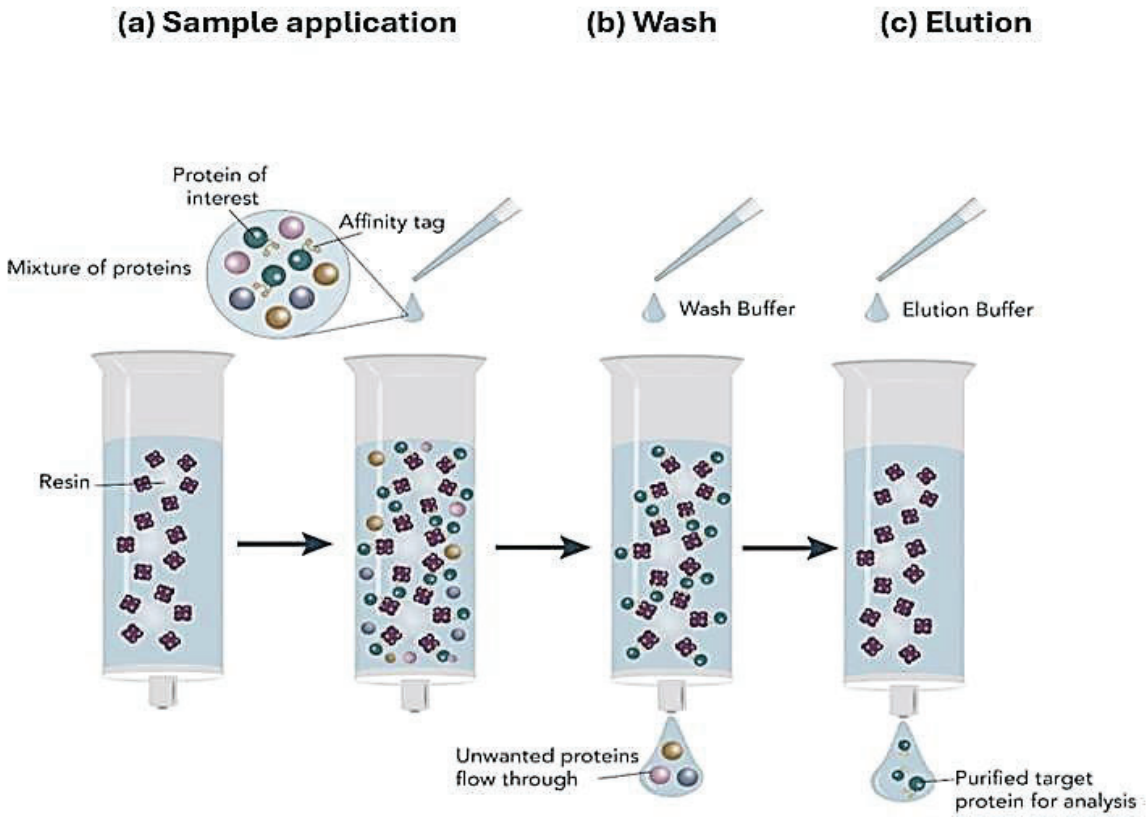

Figure 5: Principle of the Immobilized Metal Affinity Chromatography. IMAC purification involves three main steps (a). Sample application: Following column equilibration, a protein sample containing the histidine-tagged target protein is applied to the IMAC column. (b) After binding, the column is washed with a buffer containing imidazole to remove weakly bound or non-specifically bound proteins and contaminants. (c) The target protein is eluted from the column by increasing the imidazole concentration in the elution buffer, which competes with the histidine residues for binding to the metal ions, thereby releasing the bound protein. (source: ba-lifesciences)

1.5.2.2 Ion Exchange Chromatography

Ion exchange chromatography is influenced by the charge of the target protein. The target protein is isolated from impurities based on differences in its net charge. The technique can be performed using either a positively charged (anion exchange) or negatively charged (cation exchange) stationary phase, depending on the charge of the protein being purified (94). Like the IMAC method, this purification process consists of three primary stages: sample loading onto the column, a washing step, and ultimately, an elution step (**Figure 6).** The net surface charge of a protein is highly influenced by the pH of the solution. This characteristic is exploited to separate

molecules based on their interaction with the oppositely charged particles of the stationary phase and subsequent release from the column by modifying the pH or the ionic strength of the mobile phase (33–35).

The pI of the protein, which is the pH at which the net charge of a protein is neutral, is an important factor to consider when selecting ion exchange chromatography conditions. If the pH of the buffer used for the chromatography is below the protein's pI, the protein will have a net positive charge and bind to negatively charged ion exchange resin. Conversely, if the buffer pH is above the protein's pI, the protein will have a net negative charge and will bind to positively charged ion exchange resin (98). Optimization of the pH and salt concentration of the buffer makes it possible to selectively elute the protein of interest from the ion exchange resin while leaving impurities bound to the resin (99-100). Other less demanding elements that can be considered for the optimization of IEC are running conditions such as the flow rate of the sample application step, wash step, and elution step (97).

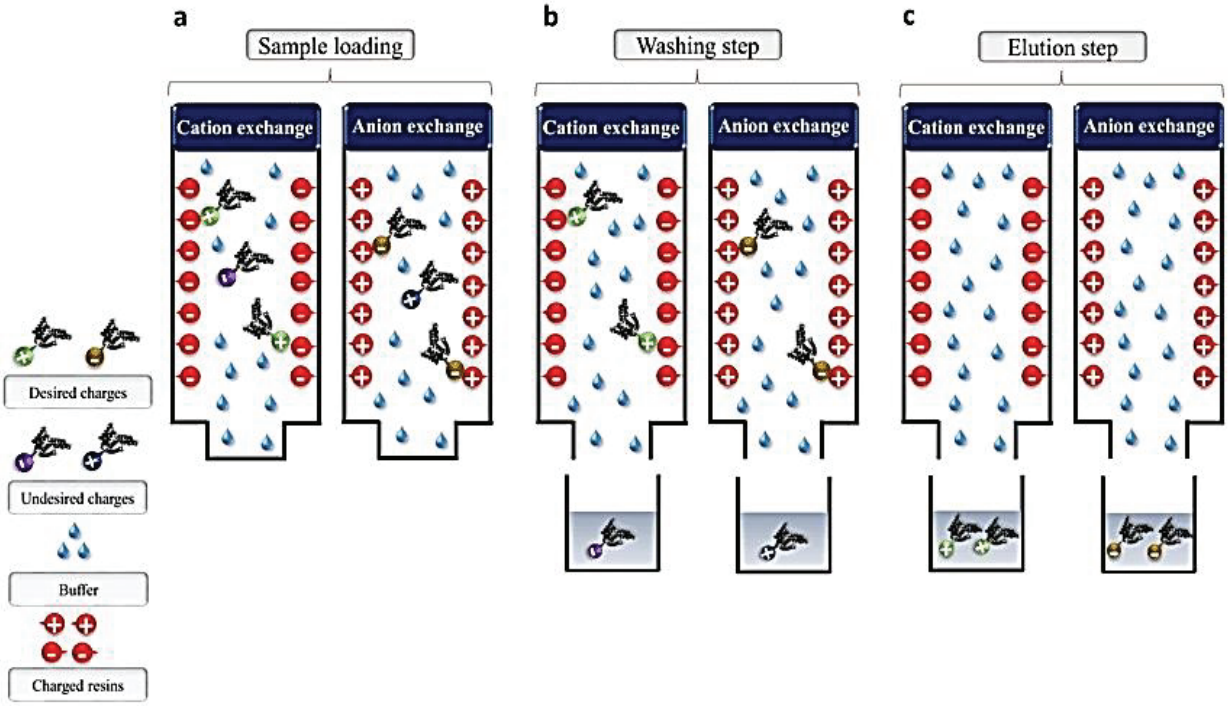

Figure 6: Schematic illustration of ion-exchange Chromatography. (a) Crude extracts are introduced to the columns (cation/anion exchange) of the fusion protein, depending on the charge of the protein, positively charged proteins will bind to the cation, and negatively charged proteins will bind to the anion. (b) The column is washed with a wash buffer of pH that will allow the removal of unwanted contaminants with minimum yield

loss. (c) Finally, the target protein is eluted by weakened ion exchanger-tag interactions via an optimized pH-assisted elution strategy (97*).*

1.5.2.3 Size Exclusion Chromatography

The principle of Size Exclusion Chromatography is that when samples containing the target protein to be purified are applied to the column, as the sample mixture moves down the column, components in the sample move down the column at different rates depending on their size, this means that different molecules will have different elution rates (100-101). It takes a longer period for smaller molecules to be eluted from the column, while the larger molecules are eluted faster. This is because the column in the size exclusion chromatography consists of porous beads. These pores allow the trapping of smaller molecules into the stationary phase while larger molecules pass through. Samples are eluted isostatically using a mild buffer system like phosphate-buffered saline (PBS), which helps maintain the stability and integrity of the biomolecules being separated (102-103). Advantageously, SEC can be employed as the last purification step, improving protein purity by excluding possible larger aggregates formed by interaction with other molecules or impurities (101,104–106).

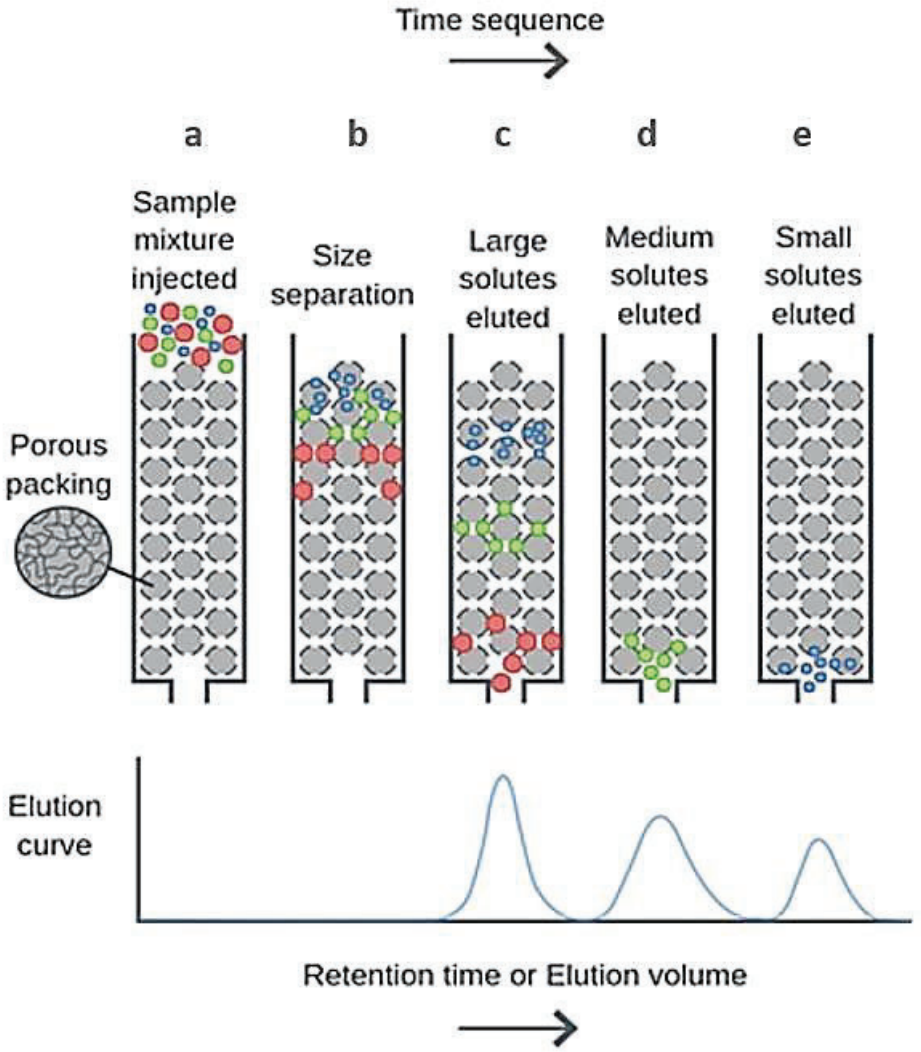

Figure 7: Mechanism of Size Exclusion Chromatography. (A) The sample is added onto the column at a stationary phase. (B) Sample separated based on size (C), larger molecules, which cannot enter the pores, travel through the column more quickly via the shorter interstitial paths. (D) smaller molecules enter the pores of the stationary phase beads, causing them to take longer paths through the column (Source: Labster Theory).

1.6 Aims

Proteins play a significant role in biological functions, the key being that proteins do not function in isolation; rather, they interact with other proteins and other molecules such as DNA and RNA that mediate metabolic and signalling pathways, cellular processes, and organismal systems. Many diseases are a result of protein malfunction or a lack of protein control. Precise studies involving the network of protein interactions can give a clear molecular basis for diseases, which may translate to prevention, diagnosis, and treatment. Because proteins are biological molecules, their functionality greatly relies on their natural structure. Therefore, sufficient protein

purification is vital for characterizing individual proteins and protein complexes and identifying interactions with other proteins, DNA, or RNA.

Currently, the Medical Biotechnology and Immunotherapy (MB&I) research unit at UCT focuses to a greater extent on biotechnological methods that involve antibody technologies, protein engineering & expression, to enhance current immunodiagnostic therapies and develop new effective immunodiagnostic and therapeutics, thus improving patient care. Such studies require precise identification and evaluation of potential targets and their role in diseases such as cancer. However, the expression of such recombinant biopharmaceutics can be challenging based on the yield achieved in different hosts of expression. Currently, at the MB&I research lab Immobilized Metal Affinity Chromatography (IMAC) is employed as the main initial purification technique for engineered antibody fusion proteins, including SNAP tag or protein toxins. However, protocols initially established deliver full-length proteins not only upon elution but already in washing steps. Studies conducted by former PhD and MSc students yielded protein purity from 8.5 – 36% for both mammalian and bacterially expressed proteins (107–109). While such initial studies may not demand very high levels of purity for proof of concept, extending successfully confirmed research into more quantitative preclinical studies needs improved purification. Research applications can be demanding, with a requirement of high purity, respectively. The primary aim of this study is to establish improved cost-effective and time-efficient purification strategies yielding quality protein products after extraction from mammalian and bacterial expression systems.

1.7 Objectives

The aim of this research will be achieved through experimenting with the following objectives:

1) Expression of recombinant protein in HEK293T mammalian cell culture and H22(scFv)-ETA in *E. coli*.

2) Optimizing the Immobilized Metal Affinity Chromatography (IMAC) for the polyHis-tagged recombinant proteins extracted from both expression hosts. The goal here is to improve the binding, washing, and elution of our target proteins using IMAC by optimizing the concentrations of buffers.
3) The successful expression of the full-length protein will be determined through SDS-PAGE and western blot analysis.
4) Combine multiple chromatography techniques for a comprehensive purification process. The purification process will involve IMAC, Ion Exchange chromatography, and Size Exclusion Chromatography (SEC). IMAC and Ion Exchange will be used for the initial separation, and SEC as the last polishing step.
5) The enzymatic functionality of the purified SNAP fusion protein will be determined by conjugating SNAP fusion to BG-modified fluorophores.
6) The binding activity of the purified protein will be analyzed using confocal microscopy and flow cytometry.
7) Finally, expand the application of the established protocol to other fusion antibodies.

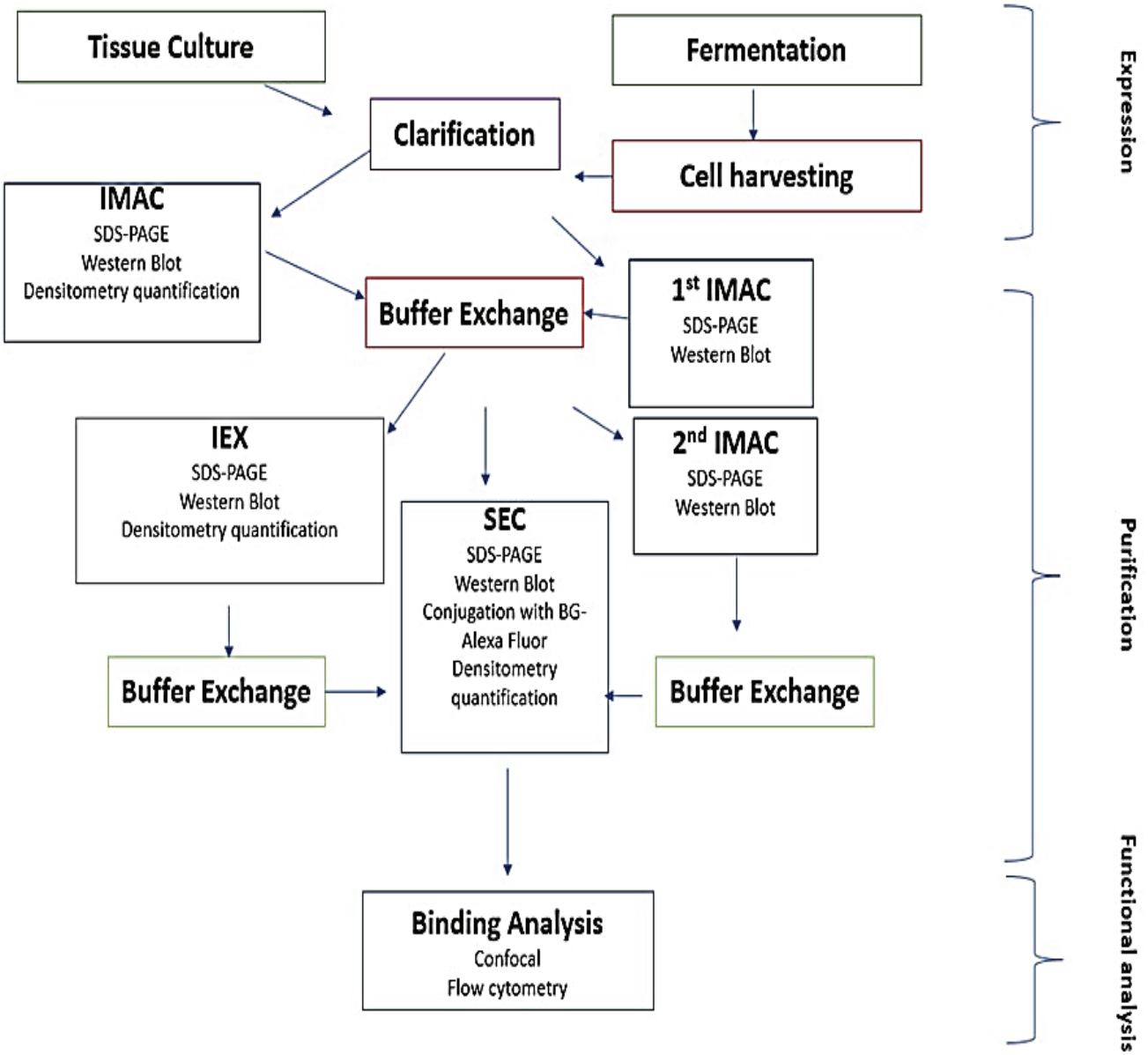

Figure 8: Research Workflow. This research initiative centres on enhancing the purification process for fusion proteins, specifically exemplified by ASPH(scFv)-SNAP. The study investigates various purification methods for the mammalian-expressed ASPH(scFv)-SNAP. It aims to extend the application of the optimized protocol to a wider array of fusion proteins. The exploration encompasses three purification techniques: IMAC, IEX, and SEC.

Chapter 2: METHODS AND MATERIALS

This chapter overviews the material and standard operating procedures initially employed at the Medical Biotechnology and Immunotherapy Research Unit (MB&I). It represents the MB&I background as documented by standard operating procedures, student theses, and original publications. These methods serve as a reference for the development of improved SOPs. Moreover, a recombinant protein used in this chapter was designed, successfully expressed, and characterized by former MB&I students, serving as a tool to establish and improve existing purification protocols.

2.1 Expression of fusion proteins

2.1.1 Mammalian expression

The insilico design of the mammalian expression vector was carried out by a member of the MB&I group and successfully transfected Human Embryonic Kidney (HEK293T) cells expressing the recombinant fusion protein were used to express the target protein by adhering to the optimized standard operating procedure (SOP) provided by the laboratory (109). The reagents used in this section were purchased from Gibco (Life Technologies, USA).

To maintain a controlled and sterile environment, tissue culture was performed in a Biosafety Level 2 (BSL-2) cabinet. HEK 293T cells were recovered by freeze-thawing of cell pellets that were stored and preserved at -80 °C. This process involved thawing the frozen cell pellets at room temperature (25 °C) until completely thawed. Once thawed, the cells were appropriately cultured on a T25, T75, and T125, respectively. Following this, the cells were cultured in RPMI-1640 media, supplemented with 1% U/ml penicillin-streptomycin and 10% fetal bovine serum (FBS) to support cell growth and proliferation. The cells were then placed in a controlled incubator environment with suitable temperature (37 °C), humidity, and 5% CO2 levels to promote optimal cell growth and were further regularly monitored for cell confluence and viability. Media changes and passaging of cells to fresh flasks were performed as needed to maintain the cells in their logarithmic growth phase and prevent over-confluence.

The HEK 293T cells were transfected with a plasmid containing the gene encoding the green protein (GFP). GFP is a protein that emits a bright green colour when exposed to UV light. This made it possible to assess the successful growth of transfected HEK 293T cells through the ZOE® microscopic visualization of the GFP expression (Bio-Rad Laboratories, USA). This also allows for assessing parameters

such as the overall appearance and morphology of the cells to ensure healthy growth and normal cellular characteristics. It also measures the transfection efficiency, cell density, and Fluorescence intensity, which indicates high levels of these parameters' strong protein expression. The cells were also treated with 100-300 µg/µL of Zeocin for the selection of eGFP-positive cells. The collected cell culture supernatant (CCSN) fusion protein was centrifuged at high speed (4300xg) for 30 minutes, this was done to remove any cell debris or particles upon storage at -4°C.

2.1.2 Expression in E. coli (BL21) under osmotic stress conditions in the presence of compatible solutes

The protein of interest was expressed by the *E. coli* BL21 strain, which was successfully transformed with a plasmid encoding this protein. To begin, 200 µl of glycerol stock of BL21 was allowed to thaw at room temperature, after which it was introduced into a 50 ml Terrific

Broth (TB) medium (Conda Laboratorios, Spain) supplemented with 50 µg/mL of Kanamycin. The mixture was incubated at 37°C with continuous shaking at 225 rpm for 16 hours. The starter culture was used to inoculate 4x 500 mL (total 2L) fresh TB culture media, each supplemented with 50 µg/uL of kanamycin. The new cultures were incubated at 26°C while shaking at 180 rpm. Once the OD_{600nm} reached 1.6, a volume of 100 mL of compatible solutes was added to each culture medium, followed by further incubation at 26°C for 30 minutes at 180 rpm. To initiate periplasmic expression, in each culture medium, 600 µl of a 1M IPTG stock solution was introduced to attain a final concentration of 1 mM (via a 1:1000 dilution) and incubated for 16 hours. Following 16 hours of incubation, the cells were harvested by centrifugation at 4000 g for 30 minutes at 4°C. The resulting supernatant was discarded, while the pellets were gathered and weighed. The weighed pellet was suspended in lysis buffer (100mM Tris-HCl, 300mM NaCl, 150mM imidazole and 10% glycerol),

maintaining a buffer-to-pellet ratio of 2:1. To facilitate protein release from the harvested cells, the sample was sonicated by, alternating between 15 seconds on and 15 seconds off at 30% amplitude for three minutes. The lysed cells were further subjected to centrifugation at 24,000 g for 30 minutes at 4 °C. The collected supernatant was filtered using a 0.45-micron syringe filter and stored in 1XPBS at -80°C until the purification process.

2.2 Initial IMAC protocol employed for protein purification

The MB&I research unit uses the ÄKTA Avant system (GE Healthcare, USA) for IMAC technique as the standard purification method for both mammalian-expressed proteins and bacterially expressed proteins. This purification approach consisted of three primary steps: column equilibration, sample loading, column wash, and a gradient elution step involving an increase in Imidazole concentration to elute the target protein. The flow rate for all IMAC purification steps was maintained at 5 ml/min. Although in previous studies at the MB&I unit, this strategy successfully recovered the target protein, the quality of the recovered protein often exhibited low purity as low as 8%. While some contaminants were successfully removed, the process was not consistently efficient. In addition, poor retention of the target protein was observed during both the sample application step and the wash step, therefore, the protein of interest was lost in the sample application and wash steps. **Figure 9** show's SDS gel of a 72 kDa protein purified by IMAC employing a protocol described above.

Table 2: Buffer system used for mammalian-expressed proteins.

As seen in **Figure 9**, although a visible band of the protein of interest is observed around 72 kDa, distinct protein bands are also observed in both the flowthrough waste and the wash waste. To address these challenges, efforts were made to enhance the overall purification strategy. This involved optimizing IMAC purification and introducing Ion Exchange Chromatography and Size Exclusion Chromatography, which were also optimized. To achieve optimal protein purity, various parameters

related to the running conditions of the purification system were examined. These included the buffer system (pH, concentration, and composition), sample loading, column wash, and protein elution. The impact of the choice of column, regeneration conditions, and protein concentration was also thoroughly evaluated.

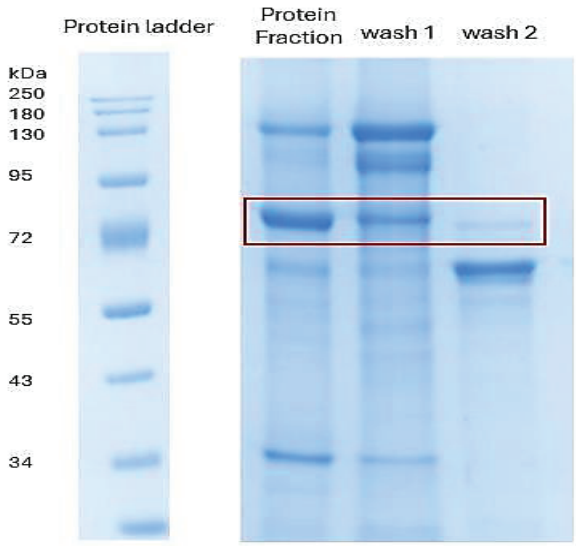

Figure 9: SDS-PAGE analysis of concentrated elutes containing SNAP-tag fusion protein (72 kDa) and wash waste

Table 1: Initial IMAC buffer system for mammalian-expressed protein

Buffer	Composition	Concentration
Buffer composition		
4X Incubation buffer	NaH2PO4 NaCl Imidazole	200 mM 1.2 M 40 mM
Equilibration/wash buffer	50 Mm NaH2PO4, 300 Mm NaCl, deionized H2O	50 Mm 300 mM
Elution buffer	NaH2PO4 NaCl Imidazole	50 mM 300 mM 500 mM

2.3 Protein characterization

2.3.1. SDS-PAGE analysis

The protein sample collected from the purification step was further analysed by Sodium dodecyl Sulphate-polyacrylamide gel electrophoresis (SDS-PAGE) to analyse

the purified protein. This analysis step involves denaturing the proteins and treating them with a reducing agent to break any disulfide bonds. This would allow the separation of the proteins based on their molecular weights. The principle of this technique is that the negatively charged SDS molecules bind to the proteins, causing them to denature and migrate toward the positive electrode (110). The proteins separate based on their molecular weight, with smaller proteins migrating faster through the gel

A volume of 15 µL of the protein sample was mixed with 5 µL of 4X LDS sample loading buffer (Bio-Rad, USA) and heated at 95 °C for 10 min. The samples were loaded into 10% SDS gel prepared on a precast NuPAGE Novex 12% Bis-Tris 1.0 mm mini gels (Invitrogen), along with 5 µL of Pre-stained SDS-PAGE Standards (Bio-Rad) were loaded in each gel run of known molecular weights for reference. The gels were placed in an electrophoresis apparatus and the electrophoresis was performed at room temperature for approximately 1h30 mins using a constant voltage (120V) in 1X solution of SDS running buffer until the dye front reached the end of the 60 mm gel. To allow protein band visualization, the gels were stained with Aqua stain solution (Bulldog Bio, UK).

2.3.2 Western Blot Analysis

The integrity of all the protein samples, which were purified and quantified, was detected through immunoassay. Two duplicate SDS gels were prepared as described above, of which one of the gels was used as a control and stained with aqua stain after electrophoresis, whereas the other duplicate SDS gel was used for western blot. The proteins to be detected were blotted onto an activated PVDF (polyvinylidene fluoride) membrane (Thermo Fisher Scientific, SA) using the western blotting filter paper stack (Thermo Fisher Scientific, USA) and the Bio-Rad Trans-Blot Turbo system (Bio-Rad, South Africa) set at 100V for 7 minutes thereafter rinsed the membrane 3X with Tris-

buffered saline –Tween (TBST) for 5 minutes post membrane transfer. To prevent non-specific binding, the membrane was also incubated with fat-free milk for 1 hour at room temperature. Post incubation, the PVDF membrane was rinsed 3X with TBST (Thermo Fisher Scientific, USA) and further incubated the membrane in dilutions of αHis-rabbit primary antibody in milk of where the rabbit αHis primary antibody = 1:1000, 10uL of antibody in 10 mL milk, overnight at 4 ºC.

After incubation, the membrane was washed with TBST 3X for 5 minutes each wash and incubated in a dilution of HRP-conjugated αrabbit secondary antibody (1:5000) for 1hr at room temperature. This was followed by a second wash with TBST (3X) to allow signal development, where 5 ml of TMB Blotting solution (Thermo Fisher Scientific, SA) was added onto the membrane. Once the bands developed, the substrate was removed and further washed with ultra-pure water to stop the reaction. The membrane was documented using a Gel DocTM XR documentation system (Bio-Rad, USA).

2.3.3 Densitometry

A densitometry technique employing ImageJ software was used to quantify the purified fusion proteins. A stock solution of 5 mg/ml Bovine Serum Albumin (BSA) was used to prepare standard concentrations of 8 µg, 4 µg, 2 µg, 1 µg, and 0.5 µg. Further, these BSA samples and 15 µl of the purified protein sample were mixed with 5 µl of the prepared 4X Laemmli sample loading dye. The mixture was then boiled at 95°C for 10 minutes before and loaded onto a 10% SDS gel. The gel was run as previously described in section 2.2.1, using an electrophoresis system. After running the gel, the gel image was captured using a Gel Doc XR+ system, which is a gel documentation system that allows for the visualization and imaging of protein gels. The gel image was then analysed using ImageJ software version 1.53e, which is an open-source image analysis program. Using ImageJ software, the band intensities of both the BSA standards and the protein samples were quantified. To calculate the

concentration of the fusion protein in each sample, a standard curve was constructed using the known concentrations of the BSA standards and their corresponding band intensities using Microsoft Excel software. The concentration of the target protein was calculated using the generated standard curve.

2.4 Conjugation of SNAP fusion protein to BG-modified Alexa Fluor 488

The functionality of the enzymatic SNAP-TAG was determined through conjugation of the SNAP-tagged fusion protein with BG-modified Alexa Fluor 488. Ideally, the BG-modified Alexa Fluor 488 would react specifically with the SNAP tag positioned at the N-terminal of the protein of interest. This would then conclude that the full-length protein recovered from the purification steps described above was achieved. The protein sample (3.5 μM) was mixed with 3.5 μM SNAP labelling reaction (scFv-SNAP: BG-Alexa = 1: 1), 1 mM dithiothreitol (DTT), and made to a total volume of 15 mL with 1X PBS. The mixture was incubated in the dark for 60 minutes at 37°C. Post incubation, 5uL of 4X Laemmli Sample Buffer (made up of β-mercaptoethanol) was added into the sample, then the sample was run on a 10% SDS gel in the dark at 100V-120V for 60-90 min. The fluorescence signal was detected by converting the emitted light from a fluorescent molecule into an electrical signal, which signals a bright green colour.

2.5 Surface binding analysis of purified (scFv)-SNAP-Alexa488 by confocal microscopy

Two cell lines, HEK 293 cells and MDA-MB-468A, were used in these experiments, where a total of 2.5 x 104 to 1 x 105 cells were seeded onto a cover slip placed in a 35 mm dish. The cells were then incubated in a medium at 37°C in a 5% CO2 environment overnight, allowing them to adhere and grow. The cells were treated with either 15 μg of mAb9.2.27(scFv)-SNAP-Alexa488, which is a specific antibody, in 100 μL of serum-free medium for 15-20 minutes at 37 ºC. This step allows the

antibodies to bind to the respective target proteins within the cells. Additionally, a 1:5000 dilution of Hoechst dye, a fluorescent nuclear stain, was added to the medium (200 μL). This dye helps visualize the cell nuclei. After incubation with the antibodies and counterstain, the excess dye and unbound antibodies were removed by washing the cells three times with a medium. The cells were further fixed by treating them with 4% paraformaldehyde (PFA) for 20 minutes. This step helps preserve the cellular structures and the antibody-protein interactions. The cells were washed with phosphate-buffered saline (PBS) to remove any residual PFA or other contaminants before they were mounted on a coverslip, with the cells attached for imaging purposes. Furthermore, the slide was left at room temperature for 24 hours, allowing the cells to settle and adhere to the slide. finally, the images were captured using a Ziess LSM880 Airyscan microscope with a 40X air objective. Confocal microscopy techniques were employed to visualize the fluorescent signals from the bound antibodies (scFv)-SNAP-Alexa488 and the Hoechst counter stain, providing information about the targeted protein binding.

CHAPTER 3: RESULTS

This chapter provides details on the development of improved protein purification techniques for SNAP-tag antibody fusion proteins, exemplified by mammalian-expressed αASHP(scFv)SNAP. The principles of the established purification protocol were subsequently applied to other mammalian-expressed SNAP-tag antibody fusion proteins and extended to the development of fusion antibody proteins expressed in bacteria. Consequently, this chapter is structured into three sections outlining the methods employed in the development of the optimum purification technique illustrated by αASPH(scFv)-SNAP expressed in HEK293 T. The established protocol was further applied as a baseline for the purification of an extended range of recombinant proteins. The downstream production of the proteins commenced with the expression of the fusion protein utilizing a well-defined expression vector system

introduced into low-density lab-scale cultures and protocols previously developed by former students of MB&I. The upstream development focused on optimizing three purification techniques, including IMAC, IEX, and SEC, to obtain full-length protein with high purity. All data obtained from the downstream purification steps were utilized to assess the effectiveness of the combination of these three distinct purification techniques.

3.1. Expression of αASPH(scFv)-SNAP by transfected HEK293T cells

The expression of ASPH(scFv)-SNAP after zeocin selection of successfully transfected cells was monitored through microscopic visualization of eGFP using a ZOE™ Fluorescent Cell Imager as described in section 2.1. **Figure 10** demonstrates GFP expression 3 months postseeding. The bright green, fluorescent signals emitted by the cells represent the level of protein expression by cells when the cell culture reached 90% confluency, which indicated efficient cell growth density and were ready for further processing. The supernatant, which contained the secreted protein, was harvested and further prepared for purification.

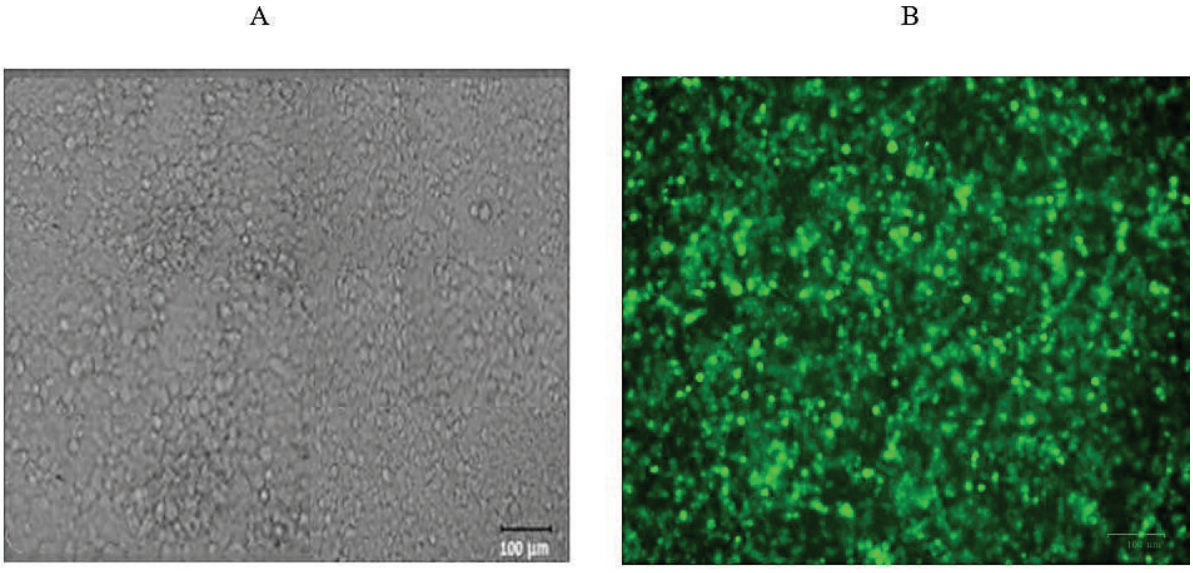

Figure 10: eGFP expression from αASPH(scFv)-SNAP positive HEK293T cells. (A) Shows transfected HEK293T cells viewed in phase contrast. (B) Green channel used to assess eGFP expression w and green

fluorescence channel three months post-seeding. The merged image was generated with the ZOE™ Fluorescent Cell Imager

3.2 Protocol re-establishment: IMAC purification of mammalian expressed exemplified by αASPH(scFv)-SNAP

Some of the major challenges observed by employing the initial IMAC protocol were poor protein retention during the sample application step and the column wash step, leading to protein loss. Furthermore, most of the target protein was eluted in two peaks with high levels of contaminants. To address these challenges, IMAC running conditions and buffer systems were adjusted.

3.2.1 Improving Protein Retention

To allow efficient binding of the target protein onto the column, the overall flow rate for all three major IMAC steps (Sample application step, column wash step, and the elution step) was reduced from 5 mL/min to 1 mL/min. Ideally, this would allow adequate time for the His-tagged target protein to interact with the immobilized metal (Nickel) ions on the column matrix, improving protein retention. In addition, a reduced wash flow rate allows for a gentler wash of nonspecific contaminants without interfering with the protein of interest pre-elution.

3.2.2 Improving elution

Based on the result generated by previous MB&I students, the major of the full-length target protein is eluted by gradually increasing imidazole concentration in the elution buffer. This elution strategy resulted in the protein of interest being eluted in two major elution peaks between (100 mM - 200 mM). A single-step elution at 250 mM imidazole was employed.

This generated a single elution peak of the full-length protein of interest.

3.2.3 Improving Protein Purity

Protein purity was further enhanced by eliminating non-specific binding. This was achieved by improving the buffer system. While all IMAC buffers were unchanged, a series of wash buffers containing different concentrations of Imidazole (**Table 2**) were prepared, and each was used to wash the column pre-protein elution. With each IMAC purification, the recovered target protein was characterized by SDS-PAGE and quantified. This approach aimed to identify the optimal Imidazole concentration that would effectively exclude impurities while ensuring the retention of the target protein. The wash step was maintained at a flow rate of 1 mL/min.

Table 2: IMAC buffer composition for mammalian-expressed protein

IMAC Purification	Wash buffer composition
A	50 Mm NaH2PO4, 300 Mm NaCl, Imidazole 10mM, deionized H2O
B	50 Mm NaH2PO4, 300 Mm NaCl, Imidazole 20mM deionized H2O
C	50 Mm NaH2PO4, 300 Mm NaCl, Imidazole 30 mM, deionized H2O

3.3 Proof of concept: Improving IMAC purification

3.3.1 Purification analysis improved IMAC

In a demonstration to verify if the concept discussed in **sections 3.1.2.1** and **3.1.2.2** has the potential for application, 1L Harvested CCSN was purified by IMAC using the ÄKTA Avant. A constant flow rate of 1 mL/min was maintained for all three major IMAC purification steps. Buffer conditions used in this purification strategy are summarized in **Table 4**. Figure 11 shows the chromatogram of the elution profile. Where 11A exhibits an elution profile implementing the initial MB&I protocol (in **section 2.2**). As shown in Table 2, this protocol employs a flow rate of 5 mL/in for all IMAC purification steps. Furthermore, the target protein is eluted at a gradient elution

step resulting in two peaks (blue line). Figure 11B exhibits the elution profile of an IMAC employing protocol detailed in **Table 5** of this section. The IMAC steps were maintained at a constant flow rate of 1 mL/min and the bound fusion proteins were eluted employing a single-step (100% Imidazole) elution process which resulted to a single peak on the chromatogram (blue line).

To confirm the presence of the target protein, fractions from each of the chromatogram peaks were run on a 10% SDS-PAGE (**Figure 13**). Both **Figures 11A and 11B** (corresponding to with chromatograph in **Figure 11C** and **11D**, respectively) show protein bands around the theoretical weight (51 kDa) of the target protein. As observed in **Figure 11C** protein bands are more distinct in the first peak (A9-B7) than in the second peak (C1-D1) implying that most of the target protein was eluted at an Imidazole concentration less than 500 mM. While in **Figure 11D** complete elution of the target protein was achieved at an Imidazole concentration of 250 mM. Additionally, in **Figure 11C** distinct protein bands were observed in both the flow through (F/T) and wash (W) fractions, this implies a possible loss of the target protein during both the sample application and wash step. Conversely at a reduced flow rate (1 mL/min) in **Figure 11D** very little to no protein band is observed around the theoretical weight of the target protein, implying minimum protein loss during the sample application and the wash step. The eluted peak fractions were pooled and concentrated using a 10 kDa Amicon® filter column at 4500 x g for 20 minutes (4^{o}C) and washed in 1x phosphate-buffered saline (pH 7.4). Protein bands (red arrow) around the theoretical weight of the protein of interest are observed in both **Figure 11D** and **11B**, indicating a successful binding and elution of the target protein. The SDS-PAGE analysis demonstrated that while 10 mM has a minimum effect in removing non-specific pre-protein elution (D), 20 mM Imidazole specifically reduced the level of heavy contaminants seen in D**.** On the contrary, protein bands (red rectangle) around the theoretical weight of the target were observed in (E). This is an

indication of possible protein loss in the wash step caused by an increased concentration of Imidazole incorporated in the wash buffer

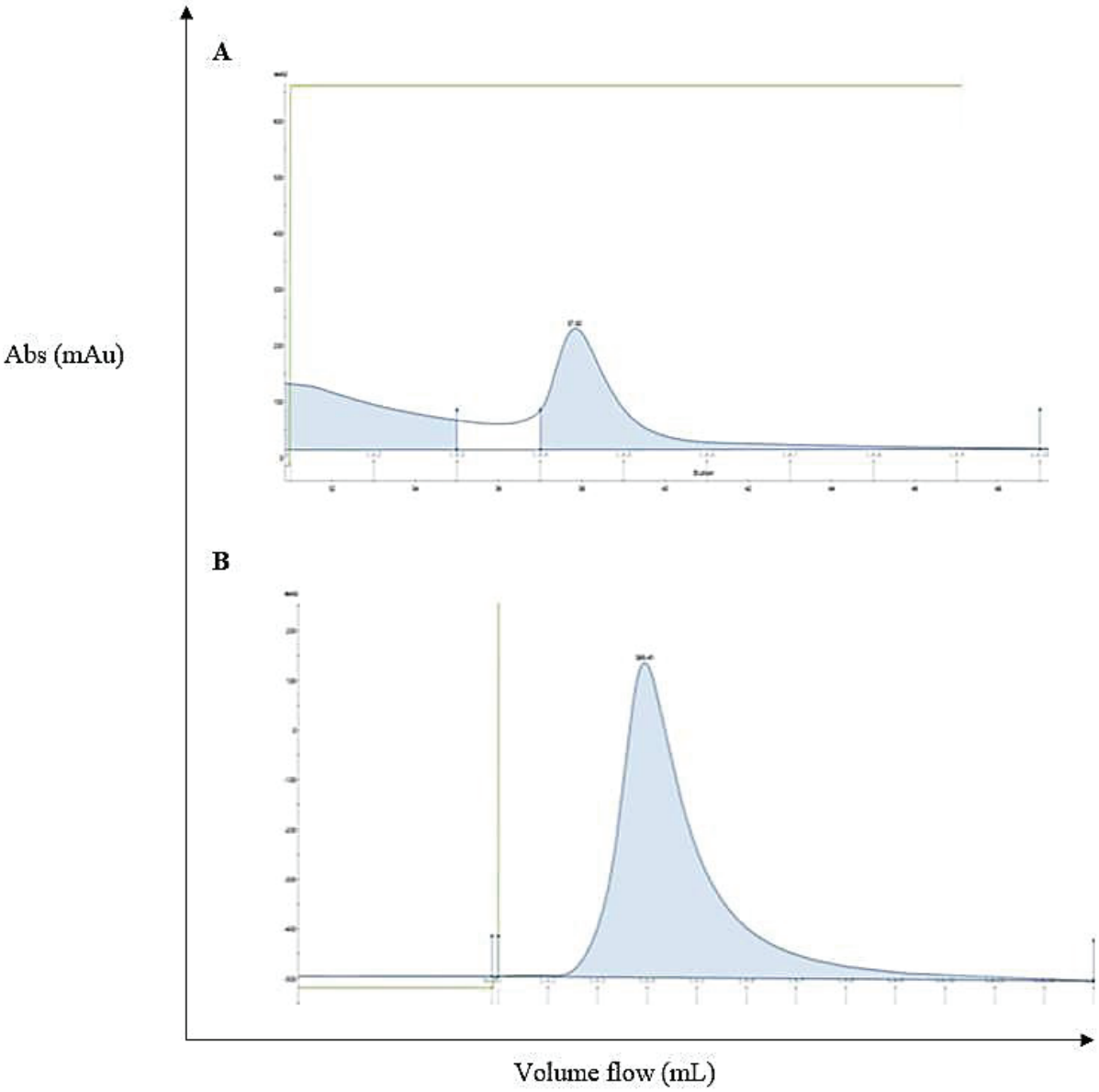

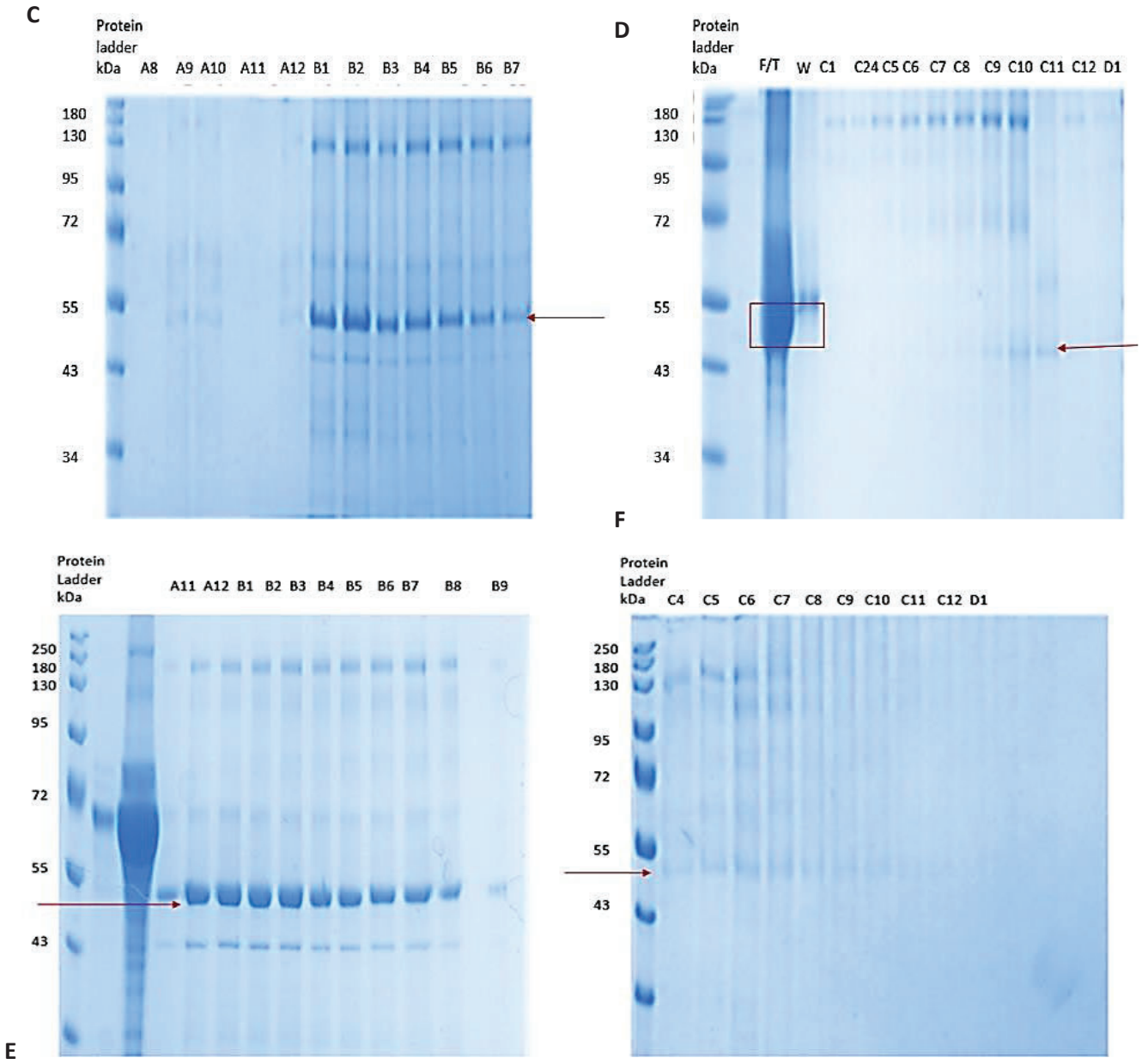

Figure 11: SDS-PAGE analysis for IMAC-purified SNAP fusion protein antibody. (A) elution profile implementing a gradient elution step at a flow rate of 5 mL/min. (B) elution profile implementing a single elution step at a flow rate of 1 mL/min. (C) and (D) represent SDS-PAGE analysis corresponding to elution profiles (A). While (E) and (F) represent SDG-PAGE analysis, corresponding to elution profile (B).

3.3.2 Densitometry Quantification of αASPH(scFv)-SNAP

The BSA curve was generated according to the procedure described in Section 2.3.2. to quantify the SNAP fusion protein purified by immobilized metal Affinity Chromatography (IMAC). purified protein sample using densitometry, gel electrophoresis, gel imaging, and ImageJ analysis software. Using the generated standard curve, the protein was quantified to have an improved purity of 25.7% from 17% previously achieved in the lab, as seen in **Table 4**.

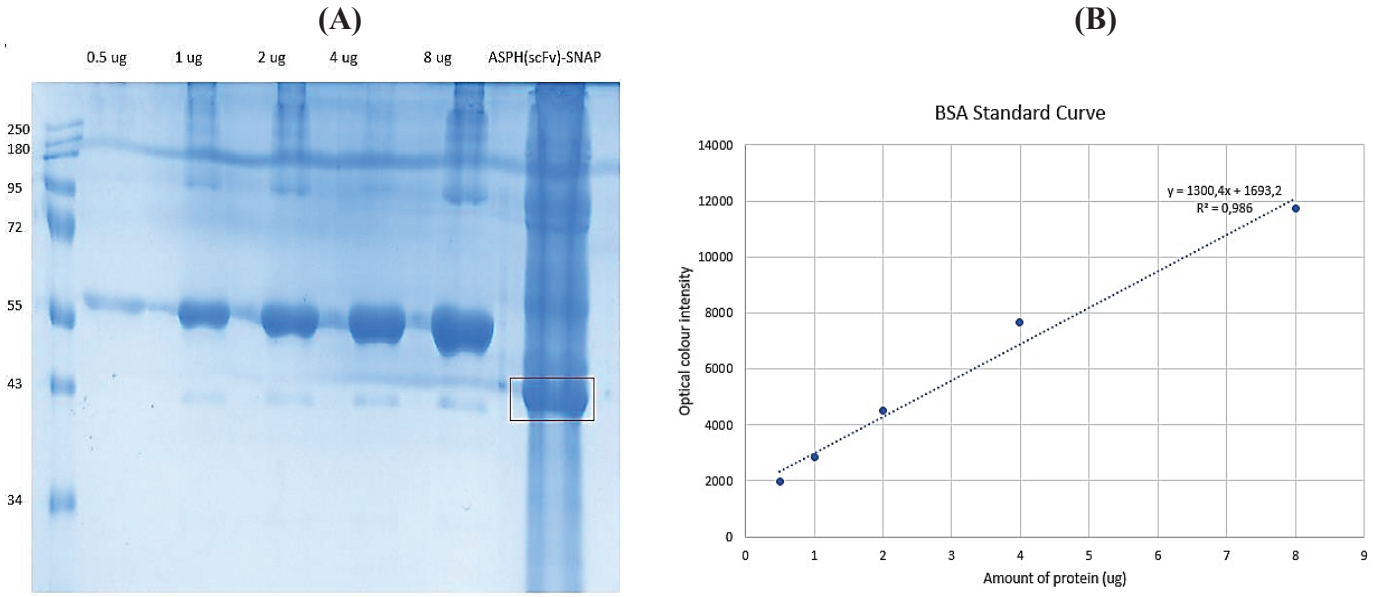

Figure 12: SDS-PAGE analysis of concentrated IMAC elute scFv-SNAP protein fraction with corresponding BSA curve for the determination of αASPH (scFv)-SNAP. (A) SDS-PAGE gel including concentrated αASPH(scFv)-SNAP, Two-fold serially diluted BSA standards for the generation of a standard curve. (B) Standard curve generated by plotting optical density against the amount of BSA protein using ImageJ software.

Table 3: Quantification of αASPH(scFv)-SNAP purified by IMAC

Sample	DeNovix [mg/mL]	Densitometry value [µg/µL]	Relative amount of full-length protein in concentrated fractions [%]	Absolute amount [µg]	Yield [mg/L]
αASPH(scFv)SNAP	10.51	2.70	25.7	1350	1.26

3.4 Optimization of Ion Exchange Chromatography

Ion exchange chromatography (IEX) was employed in combination with IMAC; this combination aims to allow a more comprehensive purification strategy, enhancing the overall purity of the protein of interest. Ion exchange chromatography is a technique that separates proteins by exploiting the differences in their charge properties. For this purification technique, a series of buffer systems with varying pH values and salt concentrations were experimented with for the best resolution and separation of the target molecules through IEX. The physicochemical properties of αASPH(scFv)-SNAP (**Table 4**) were determined using an online Isoelectric point calculator (http://calistry.org/calculate/isoelectric-point-calculator).

In theory, a protein in a buffer solution with a pH above its pI will result in the protein being negatively charged, and the charge of the protein will increase with increasing pH of the buffer solution. In this case, the pI of ASPH (scFv)-SNAP is 6.1, which means that the overall charge of the target protein would be negatively charged in any buffer solution above a pH of 6.1. Therefore, HiTrap Q HP, a strong anion exchange chromatography column, was used to isolate the positively charged protein of interest while negatively charged contaminants were excluded. In addition to pH, factors such as NaCl concentration and flow rate were considered to assess their influence on IEX separation. These variables were optimized for each protein's most effective separation outcome.

The protein sample recovered from the IMAC step was prepared to the composition of the start buffer. This was accomplished by subjecting the sample to high-speed centrifugation at 4,500 rpm for 40 minutes using a 10 kDa Amicon filter. This procedure not only facilitated the removal of salts through buffer exchange but also resulted in an overall imparting of a negative charge to the target protein. The column was initially equilibrated with 25 ml (5 CV) of start buffer. This step was taken to ensure adequate binding of the target protein onto the column. During the initial IEX

round, a mild buffer condition was utilized. Here, 500 µl of αASPH(scFv)-SNAP protein sample at a concentration of 0.9 mg/ml (pH 7.1) was gradually injected into the column via a syringe, maintaining a flow rate of 1 ml/min.

following the sample application, a wash buffer was employed to wash the column with 2 CV while maintaining a consistent flow rate of 1 mL/min. To reverse the binding of αASPH (scFv)-SNAP, an elution buffer with a pH of 7.1 and a NaCl concentration of 1M was introduced into the column. The retrieved protein was then subjected to characterization, quantification, and subsequent storage in 1x PBS at a temperature of -20°C for future use.

Ideally, increasing the charge would enhance the interaction of the negatively charged target protein with the anion exchange column. The ionic strength was further increased by introducing different ranges of NaCl in the start buffer and the wash buffer. **Table 5** displays the different buffer systems and running conditions experimented on while maintaining a flow rate of 1mL/min. The protein collected was concentrated, analyzed, quantified, and stored in 1X PBS at -20 °C until needed for further experiments.

Table 4: Physicochemical properties of ASPH(scFv)-SNAP

Number of amino acids	483
Theoretical weight	51.2 kDa
Theoretical Pi	6.16

Table 5: Buffer system for optimization of Ion Exchange Chromatography

	I	**II**	**III**	**IV**
Protein concentration				
Start buffer				
Tris concentration (mM)	20	40	40	50
NaCl concentration (mM)	0	10	20	40
Wash buffer Tris NaCl	 20 Mm 20 mM	 40mM 20mM	 40mM 20mM	 40mM 50mM

Elution buffer (Start buffer + 1M NaCl Tris NaCl	 20mM 1M	 40mM 1M	 40mM 1M	 50mM 1M
pH	7.1	7.6	8.2	8.2
Flow rate (mL/min)	3	1	1	1

3.4.1 Protein Purification Analysis

The IEX chromatogram reading and SDS-PAGE analysis (**Figure 13**) for each optimized parameter are described in **Table 5**. (A) Two peaks were observed on the chromatogram, showing protein absorbance. The protein band around the theoretical weight (51 kDa) of the protein of interest; however, protein of interest is lost in the wash step (red box), which shows poor binding onto the column. (B) When the flow rate was decreased to 3 mL/min, and 10 mM of NaCl was introduced into the wash buffer, smaller protein bands of the protein of interest were observed in the wash waste as an indication of protein loss. (C) NaCl concentration was increased to 30 mM, while the flow rate was decreased to 1 mL/min, which was aimed to improve the interaction between the positively charged ASPH(scFv)-SNAP with the negatively charged column while excluding heavy contaminants by increasing. As a result, less heavy contamination is observed in Figure 13 (G). while in Figure 13 (H) which represents the SDS-PAGE analysis for elution profile in Figure 13(D), heavy contaminants were still observed. When the NaCl concentration was increased to 40 mM, not much improvement was observed. With each purification round, the pH of the buffer by an interval of 0.5, from 7.1to 8.2was increased from 7.1 to 8.2.

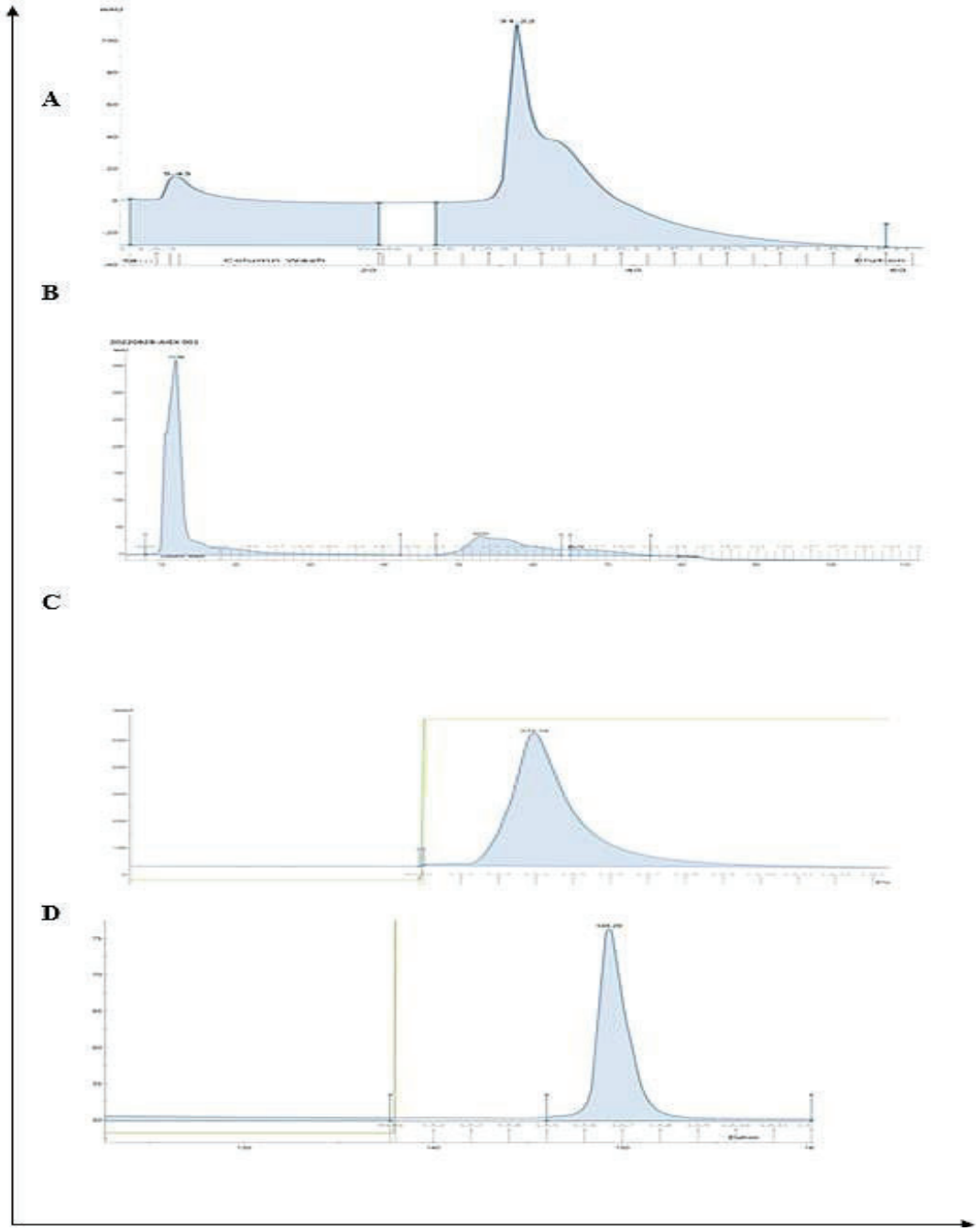
A
B
C
D

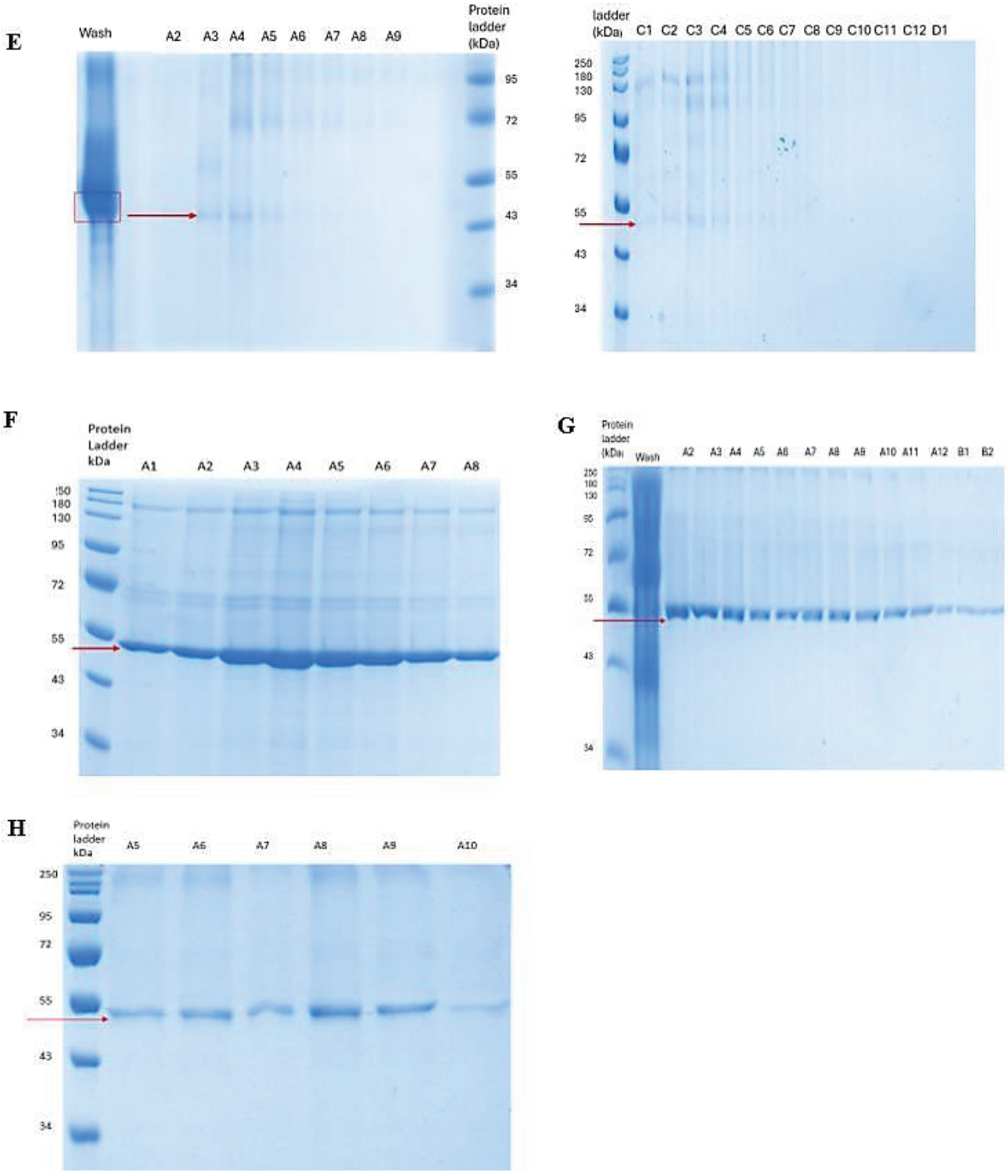

Figure 13: Ion Exchange Chromatography analysis exemplified by αASPH(scFv)SNAP. A-D represents the IEX elution profile under the conditions outlined in Table 5, with a, b, c, and d corresponding to columns A, B, C, and D, respectively. Similarly, E, F, G, and H show the resulting SDS-PAGE analysis for purification conditions in Table 5. The protein of interest is indicated by a red arrow.

Densitometric quantification

The densitometry quantification showed that protein purified employing conditions outlined in Table 6 (column IV) yielded protein with the highest purity (42%) with

minimal protein loss compared to protein purified employing conditions in columns I, II, and III. Under very mild conditions, specifically, low buffer concentration and low pH, running purification at 3 mL/min yielded the lowest protein purification and a significant protein loss in the wash step. This outcome was due to low protein charge and high flow rate, not allowing sufficient protein-column interaction before protein elution. Reducing the flow rate to 1 mL/min improved protein retention before protein elution. Additionally, inclusion of NaCl in the buffer systems along with increased pH significantly enhanced protein retention while minimizing non-specific binding.

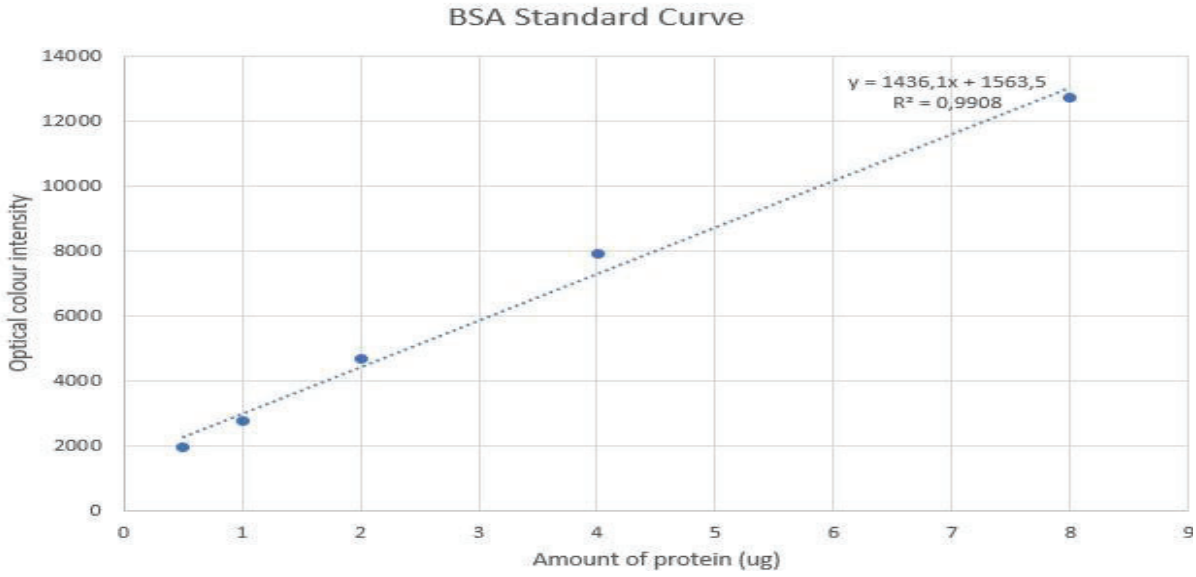

Figure 14: Densitometry analysis for αASPH(scFv)-SNAP purified by IEX. 10% SDS-PAGE gels contain αASPH(scFv)-SNAP purified by IEX employing conditions described in Table 7. (B) represents the BSA curve used to estimate the concentration and purity of the protein. (C) is the summary of the protein quantification.

Table 6: Summary of the protein quantification purified by Ion Exchange Chromatography

Sample	DeNovix (mg/ml)	Densitometry value (µg/µL)		Relative amount of full-length protein in concentrated fraction (%)	Absolute amount	Yield (mg/L)
		Initial	Final			
I	3.9	0.56	-	Negligible	-	-
II	4.4	1.9	1.2	26	480	0.64
III	14.9	6.9	5.7	38	1995	1.33

IV	5.3	3.5	2.2	42	880	1.17

3.4.2 Western blot analysis

A western blot analysis was conducted to confirm the integrity of the purified protein sample (IV). In **Figure 15,** a clear protein band around the theoretical weight of the protein of interest (red box) was observed on both the SDS-PAGE gel and the nitrocellulose membrane. This indicated that the protein was successfully transferred to a nitrocellulose membrane. A very faint protein band (navy box) around 55 kDa was observed, which indicates possible protein yield lost in the wash step.

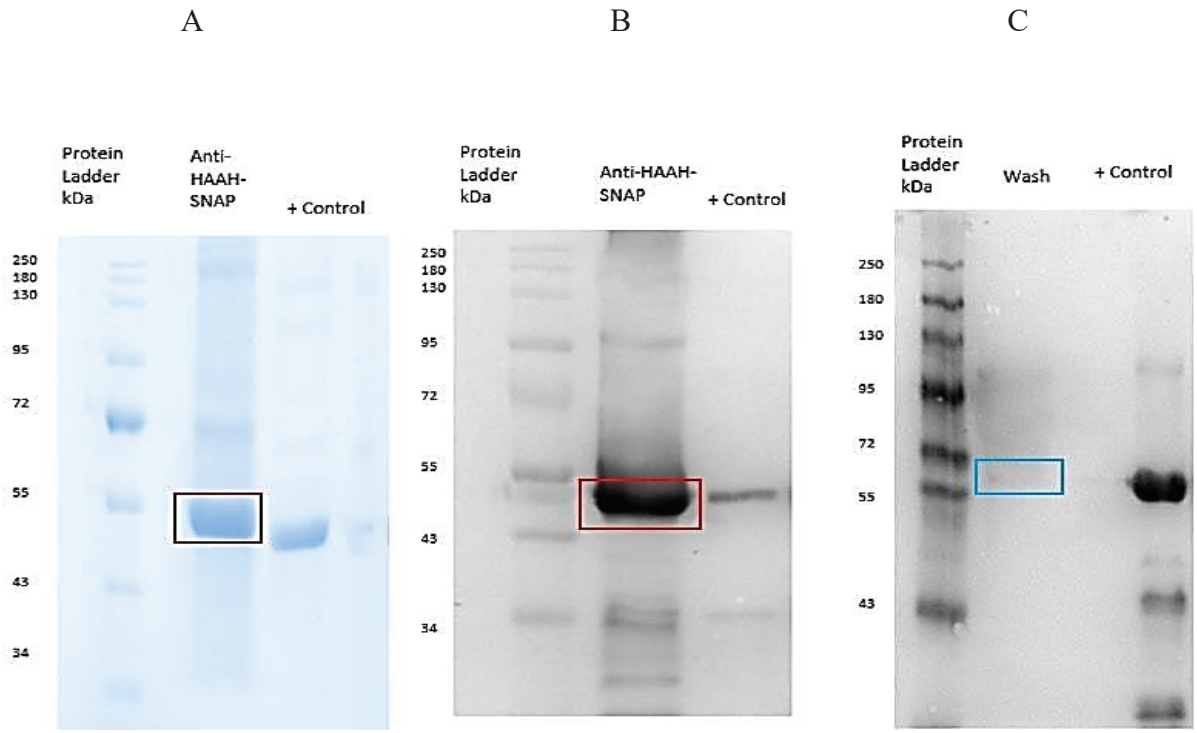

Figure 15: Western blot analysis of αASPH(scFv)-SNAP (51. kDa). Figure 15 (A) represents a 10% SDS-PAGE gel stained with Aqua staining solution. Figure 15 (B) represents an immunoblot of proteins transferred to a nitrocellulose membrane from a duplicate SDS-PAGE gel. Figure 15 (C) is an immunoblot of the wash waste. The SDS-PAGE gel was run at 120 volts for 90 minutes, and the protein of interest was tracked using a protein ladder to confirm the presence of the target protein. In Figure 15A, a distinct protein band (red rectangle) is observed around the target protein size. The presence of the target protein is confirmed by Figure 15 B, where a clear protein band is observed around 51 kDa. Minimum target protein was lost under the purification condition indicated by a very faint band in Figure 15C (blue rectangle).

3.5 Size Exclusion Chromatography

Size exclusion chromatography was the last purification polishing purification step employed. In this section combination SEC was combined with IMAC (IMAC-SEC),

this purification combination was further compared to the combination of IMAC-IEX-SEC. This was done to establish the purification combination that would yield the highest protein purity and maximum protein recovery. A HiLoad® 16/600 Superdex® 200 pg column was used to separate the sample generated from the IMAC and IEX. For each round of purification, a maximum volume of 500 µl of sample of known concentration was loaded onto the column. Prior to the sample application, the column was equilibrated with 3 column volumes of 1x Phosphate-buffered saline concentration (PBS), at a rate of 3 ml/min. Each protein sample was directly loaded onto the column at a flow rate of 2 ml/min through the loop and eluted at 2 ml/min. All the fractions eluted were collected on a 96-well collector for further analysis. In this step, two SEC purification combinations were experimented with: the combination of IMAC-IEX-SEC and IMAC-SEC. Protein from each combinatory purification was characterized by SDS-PAGE, western blot, and quantified. **Table 7** gives details on the purification conditions.

Table 7: Size Exclusion Chromatography running conditions

Purification system	AKTA Avant
Purification column	HiLoad™ Superdex™ 200 pg
Loading buffer	1XPBS
Loading flow rate	3 ml/min
Elution flow rate	2 ml/min

3.5.1. Size exclusion Chromatography analysis

The resulting elution profile for SEC and the corresponding SDS-PAGE analysis are presented in **Figure 16**. Figure 16(A) represents the SEC elution profile for the purification technique combining IMAC with SEC, and Figure 16 (B) represents the

SEC elution profile for the protein purification technique combining IMAC, IEX, and SEC. Figure 16(C) and (D) represent the SDS-PAGE analysis corresponding to (A) and (B), respectively. In Figure 16 (A) three elution peaks were observed, whereas two elution peaks were observed in Figure 16(B). When these peak fractions were run on an SDS-PAGE gel, clear protein bands (red arrow) around the theoretical size of the target protein were observed on the SDS-PAGE gels represented in Figure 16(C) and (D), indicating a successful elution of the target protein. For each combined purification, fractions believed to contain the protein of interest were concentrated and desalted before further characterization.

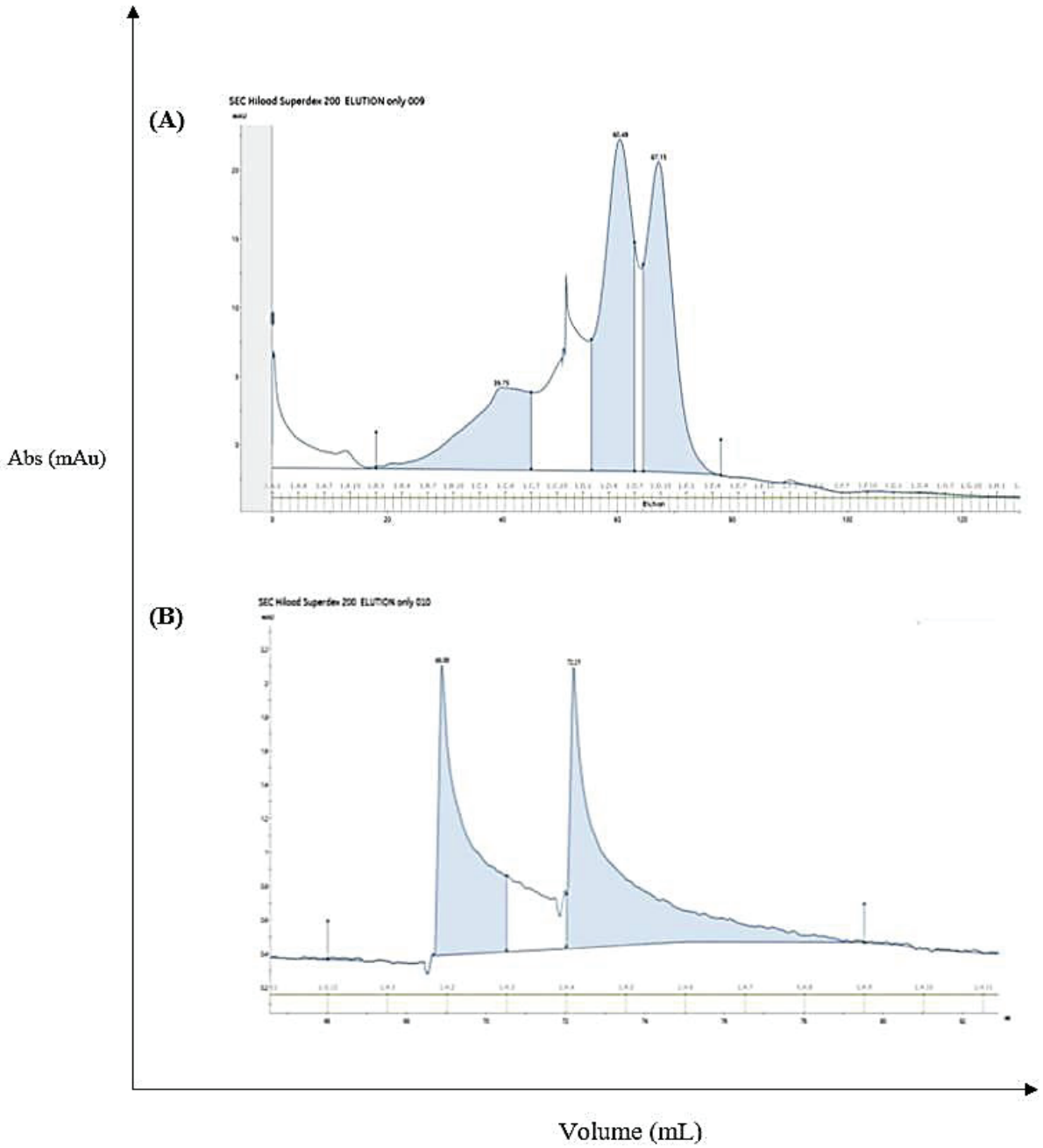
(A)
SEC Hiload Superdex 200 ELUTION only 009
(B)
SEC Hiload Superdex 200 ELUTION only 010
Abs (mAu)
Volume (mL)

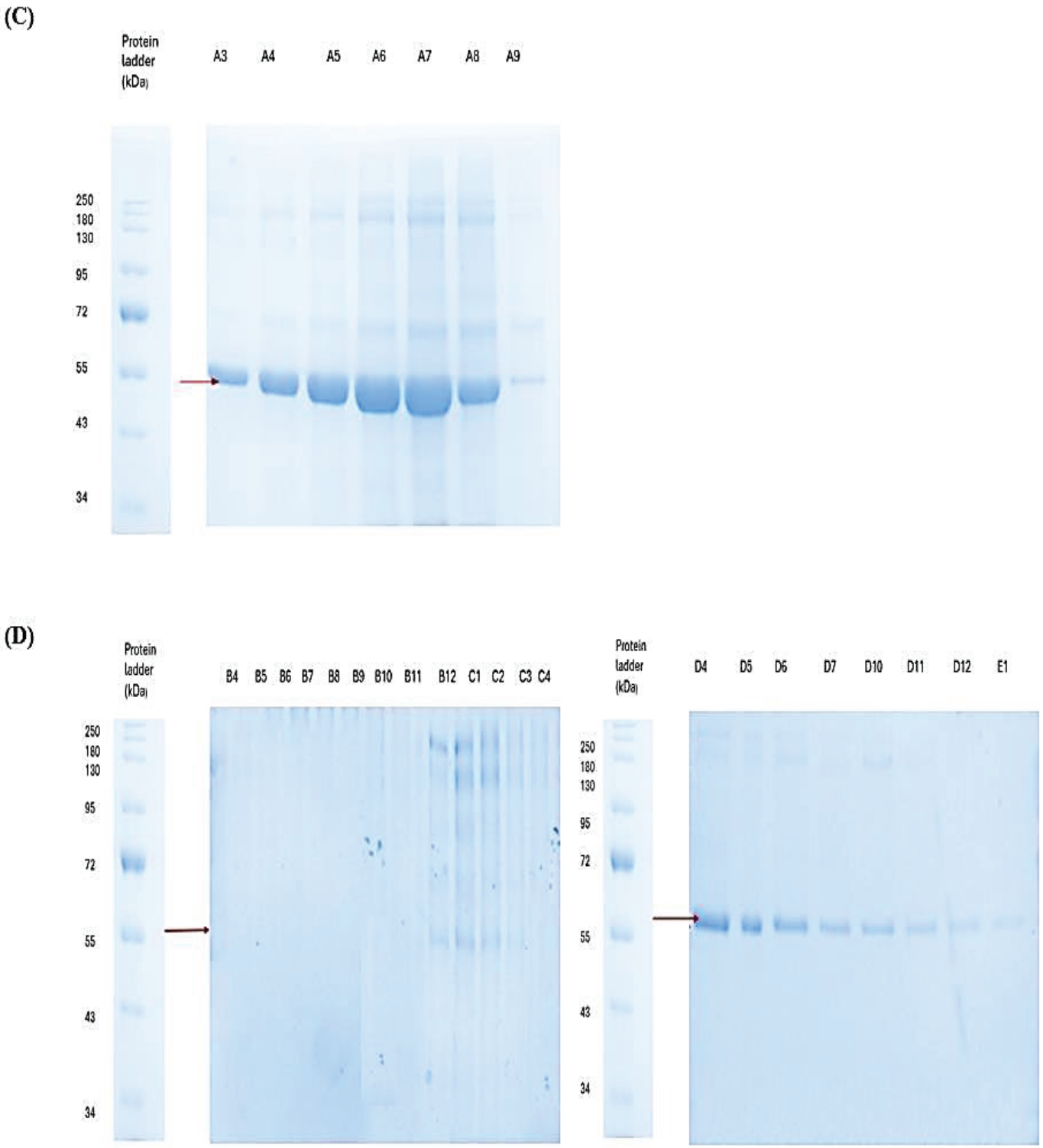

Figure 16: Protein purification analysis of ASPH(scFv)-SNAP purified by Size Exclusion Chromatography analysis. Figures (A) and (B) show the elution profile for SEC. In both elution profiles, multiple peak lines are observed. Figure 16 C and D represent the SDS-PAGE analysis of the peaks corresponding to Figure 16 A and B, respectively. Visible protein bands are indicated by a red arrow on the gels.

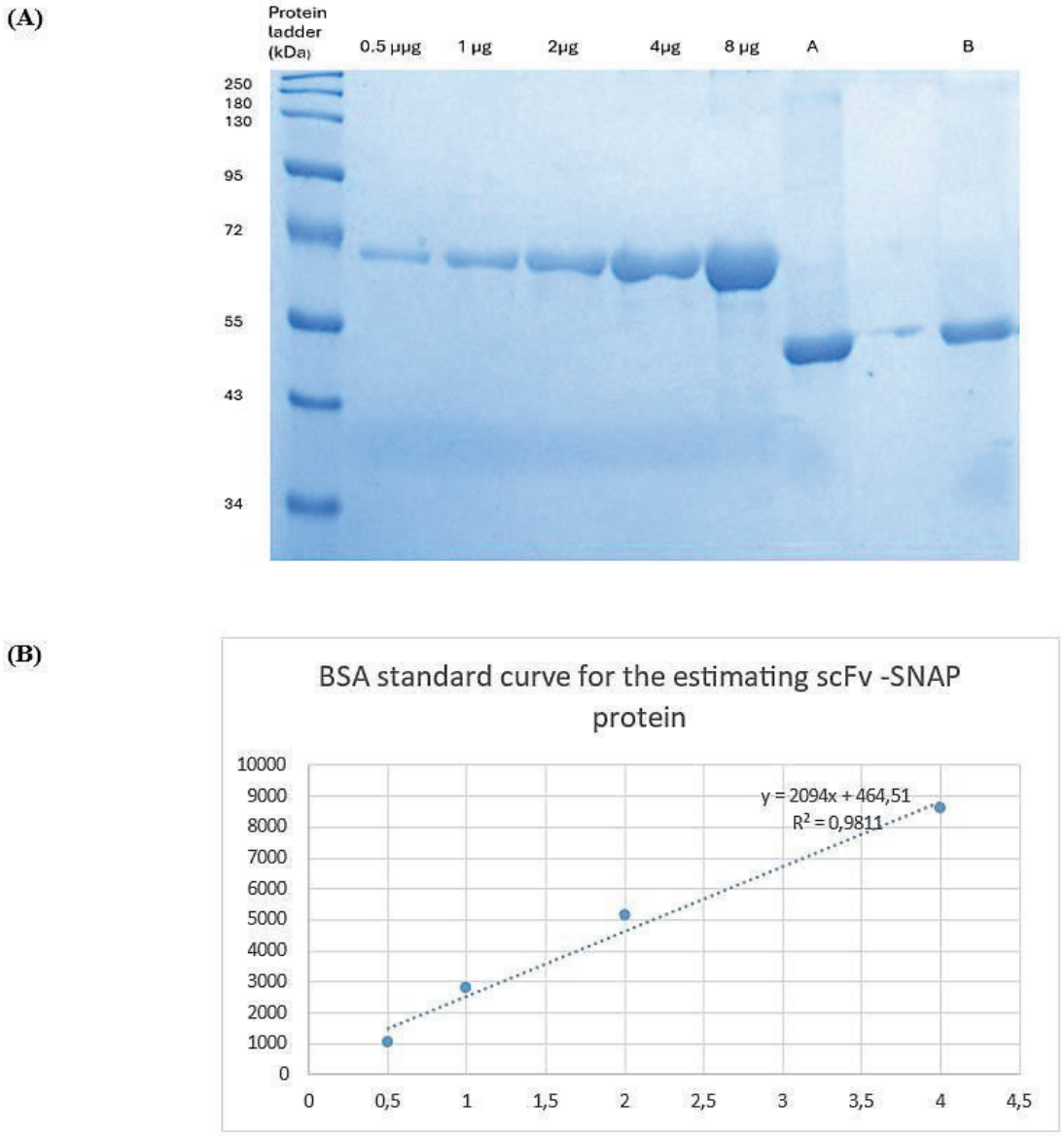

Figure 17: Densitometry analysis of ASPH(scFv)-SNAP purified by SEC. (A) 10% SDS-PAGE gel containing αASPH(scFv)-SNAP and BSA standard dilution (0.5 µg/uL- 8 µg/uL) stained with aquastain. (B) BSA standard curve plotted using band intensities generated by ImageJ.

Table 8: Densitometric quantification of ASPH(scFv)-SNAP purified by Ion Exchange Chromatography

Purification technique	DeNovix (mg/ml)	Densitometry concentration (µg/µL)	Amount of full-length protein in concentrated fraction (%)	Absolute amount (µg)	Yield (mg/L)

A (IMAC-SEC)	5.7	3.5	65	875	1.17
B (IMAC-IEX-SEC)	3.5	2.2	71	550	0.73

3.5.2 Western blot analysis

Following densitometric quantification, the protein sample was characterized for the polyhistidine-tagged C-terminal through western blot analysis following the protocol described in section 2.3.2. The distinct band marked red, corresponding to the theoretical size of (51 kDa) αASPH(scFv)-SNAP on both the 10% SDS-PAGE and on the PVDF membrane (**Figure 18**), ideally indicates the presence of ASPH(scFv)-SNAP sample purified through a combination of both IMAC-IEX-SEC and IMAC-SEC.

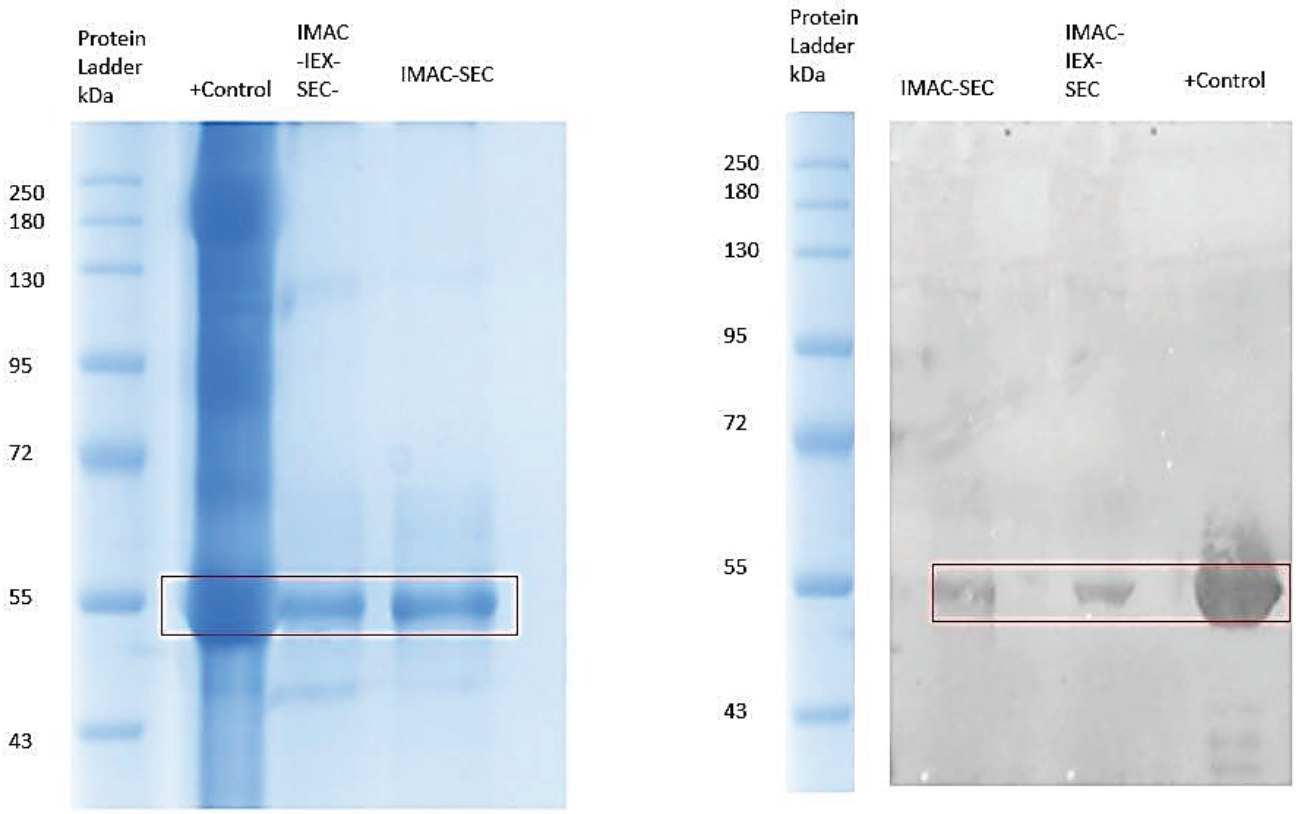

Figure 18: Western blot analysis of SEC purified αASPH(scFv)-SNAP (51 kDa). Left: 10% SDS-PAGE containing protein samples purified by combinatory techniques (IMAC-SEC and IMAC-IEX-SEC), the gel was stained with Aqua staining solution, and on the right is an immunoblot of proteins transferred to a nitrocellulose membrane from a duplicate SDS-PAGE

gel. The SDS-PAGE gel was run at 120 volts for 90 minutes, and the protein of interest was tracked using a protein ladder to confirm the presence of the target protein. An anti-his rabbit antibody (1:1000 primary antibody) and a goat anti-rabbit HRP-conjugate

3.6 Conjugation of SNAP-tag-based fusion proteins to BG-Alexa Fluor 488

The protein sample that was initially subjected to a combination of Immobilized Metal Affinity Chromatography (IMAC) and Ion Exchange Chromatography (IEX) was quantified for purity and further subjected to size exclusion chromatography (SEC) for purification. The recovered protein fraction from the IMAC-IEX combination was further separated by SEC again to achieve further purification. The purification combination of IMAC-SEC was also experimented with and further compared against the combination of IMAC-IEX-SEC (Figure 18). To determine the integrity of the N-terminal, the purified protein was conjugated with BG-Alexa Fluor 488 following the protocol discussed earlier. Conjugation analysis of SNAP-tag-based protein fused to BG-Alexa Fluor 488 showed positive results, as seen in **Figure 19**, where a bright green colour (right panel) was observed around the theoretical size of the protein of interest. Indicating the functionality of the N-terminal of the fusion protein.

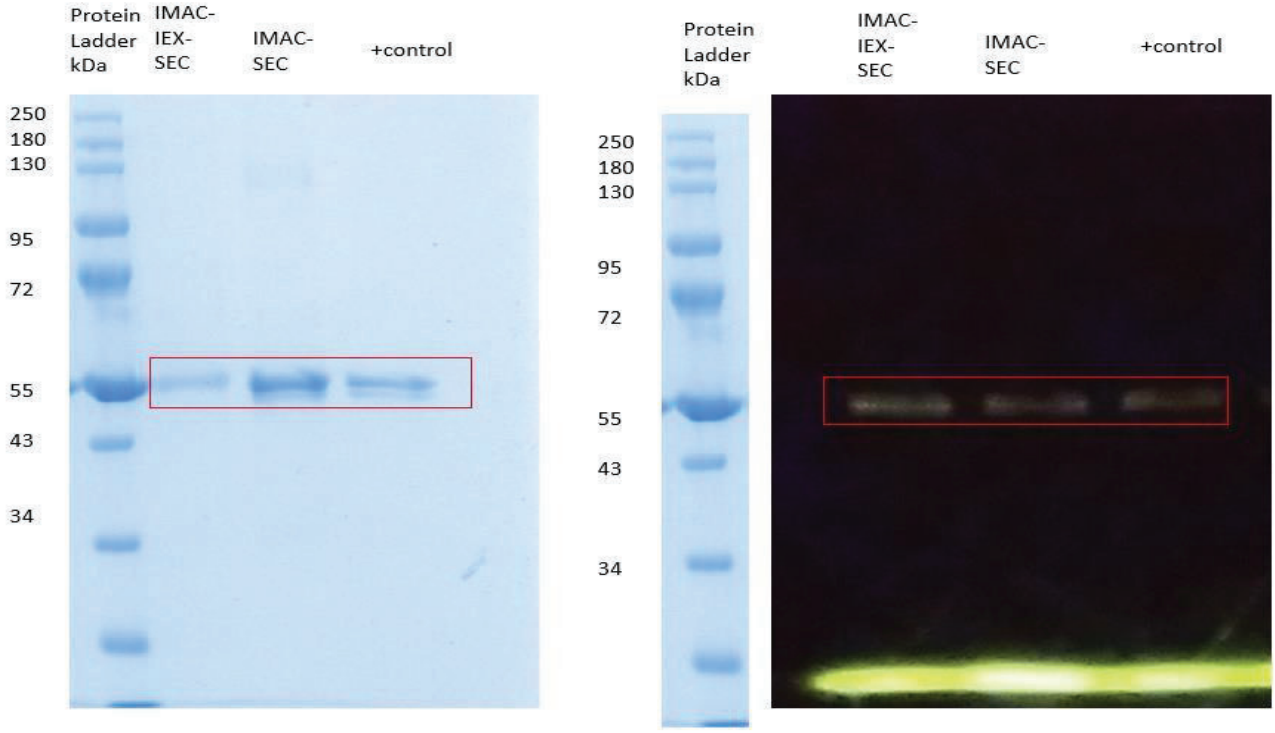

Figure 19: Assessing the binding activity of scFv-SNAP to BG-Alexa Fluor 488. A ratio of 1:2 of protein to BG-Alexa Fluor 488 was used in the conjugation reaction (5 µM to 10 µM). αASPH(scFv)SNAP (~51.kDa). Left panel: SDS-PAGE gel visualized under blue light for potential fluorescence, run on a 10% SDS-PAGE gel stained with Aqua staining solution. On the right panel, Alexa488-conjugated protein ran on a 10% SDS-PAGE gel, visualized under blue light for potential fluorescence

3.7. Validation of surface binding by confocal microscopy

Imaging analysis was performed to confirm the biological activity of the recombinant SNAP fusion protein (scFv-SNAP-Alexa Fluor 488). This analysis allowed for the visualization of the specific binding ability of the scFv-SNAP-Alexa Fluor 488 to target cells expressing HAAH. The scFv-SNAP-Alexa Fluor 488 was designed to incorporate a small peptide tag (SNAP-tag) that enables the specific labelling of the protein with a fluorophore or other imaging probes. This tagging system facilitates the visualization and tracking of the protein of interest, in this case, the scFv binding to αASPH(scFv)-SNAP. Based on the observations made during the confocal microscopy imaging (**Figure 20**), the results indicated minimum and infrequent binding of the targeted proteins on MDA-MB-468 cells (red arrow). Very minimal binding was detected on HEK 293T served as the negative control since they do not

exhibit the expression of HAAH. This confirms the functionality of the protein purified.

(A) **(B)**

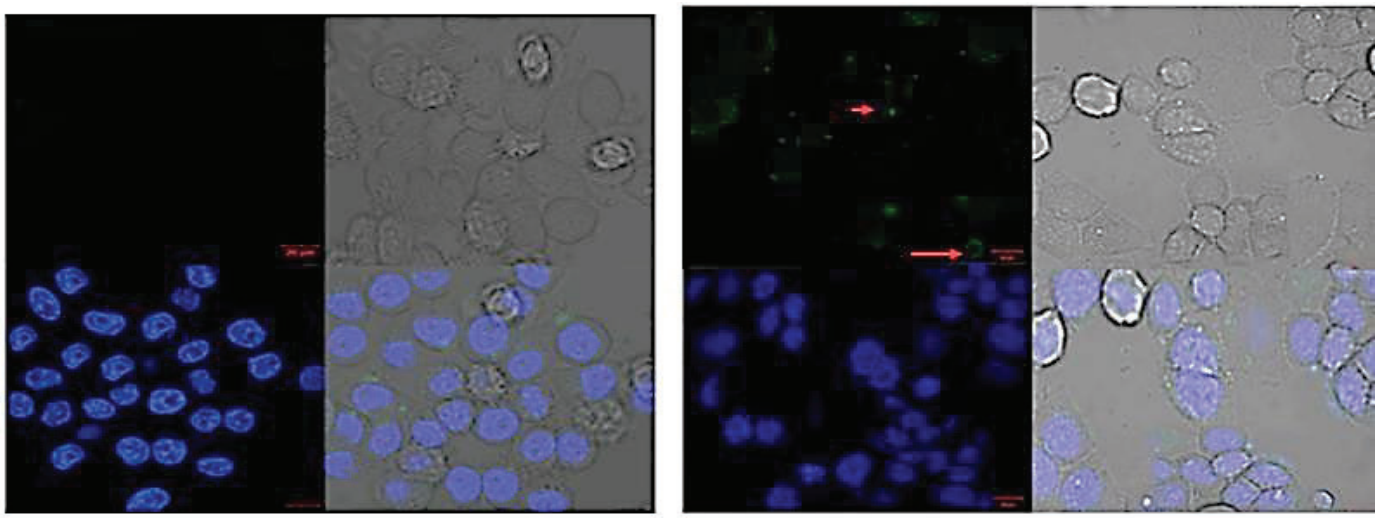

Figure 20: Binding activity analysis of ASPH(scFv)-SNAP-Alexa488. Functionality of the expressed and purified protein was determined through confocal analysis, to determine if Aasph(scFv)-SNAP would bind to the target cell expressing ASPH (A) HEK 293 cells and (B) MDA-MB-468. Cell lines were incubated with 15 µM of conjugated protein (green signal) for 15-20 minutes at 37 ºC. Hoechst (1:5000 dilution in media) was used as a stain for the nuclei (blue signal). Washes were performed 3 times with 1x PBS, before fixing with 4% PFA and mounting the coverslips on a microscope slide. Images were captured using a Zeiss confocal scanner microscope (LSM880) with Airyscan at 20 µm magnification.

3.8 Application of established protocol to other αL243(scFv)-SNAP

The optimal buffer system and running conditions for achieving maximum protein purification with minimal yield loss for αASPH(SNAP) are detailed in Tables 19, 20, and 21 below. Subsequently, this methodology was extended to assess its applicability to other scFv(SNAP) fusion proteins produced within the MB&I unit, including αL243(SNAP).

3.8.1 Purification analysis: SDS-PAGE analysis

The outcomes obtained from αASPH(scFv)-SNAP purification experiments revealed that, during IMAC purification, lowering the flow rate during the sample application stage led to reduced loss of the target protein during the washing process and enabled more efficient protein elution. Additionally, the inclusion of 30 mM imidazole in the wash buffer effectively removed contaminating proteins. Furthermore, it was observed

that most of the target protein was eluted when the imidazole concentration reached a maximum of 250 mM. Consequently, it was concluded that the integration of IMAC with IEX and SEC techniques enhanced

protein purity.

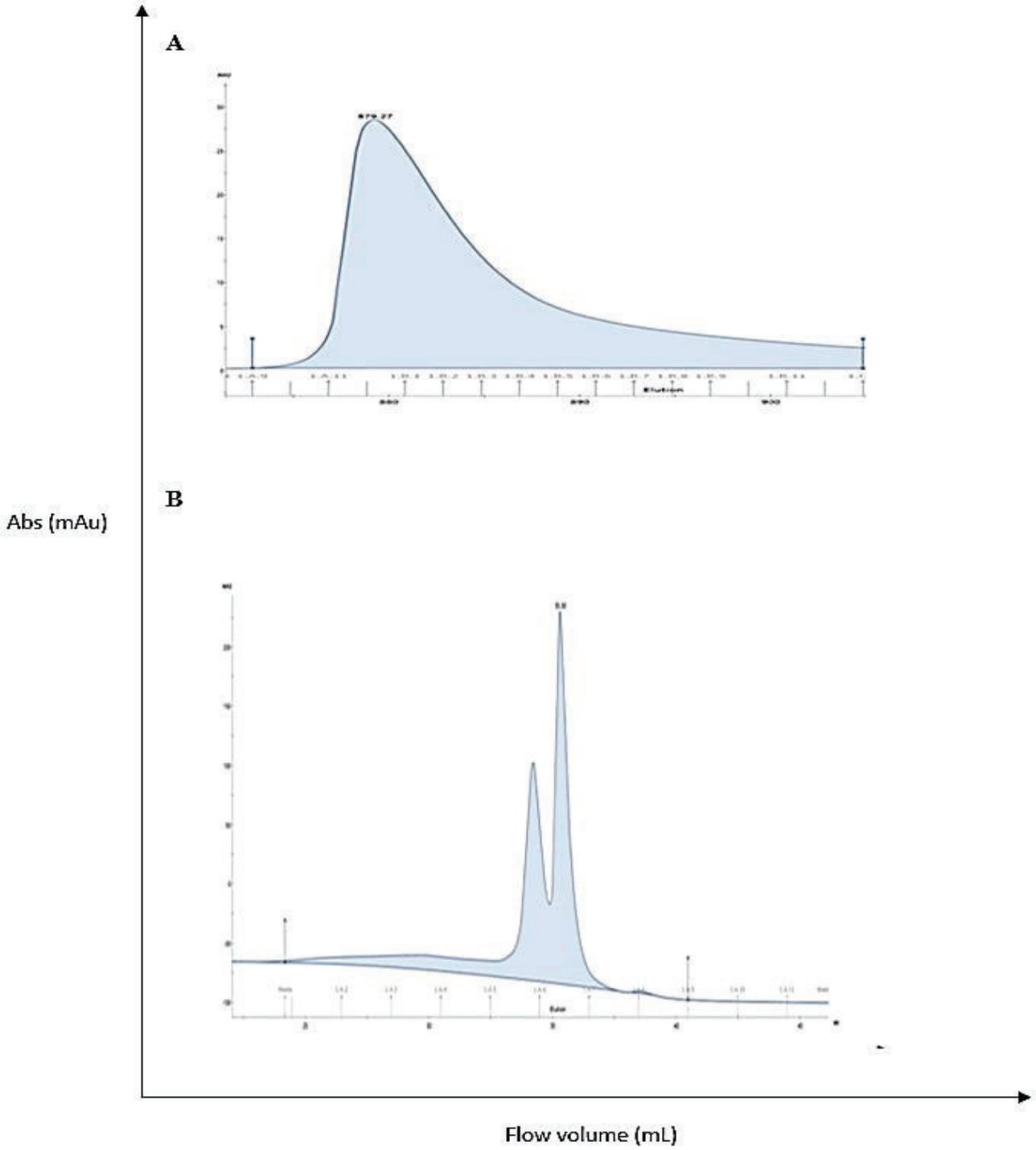

C

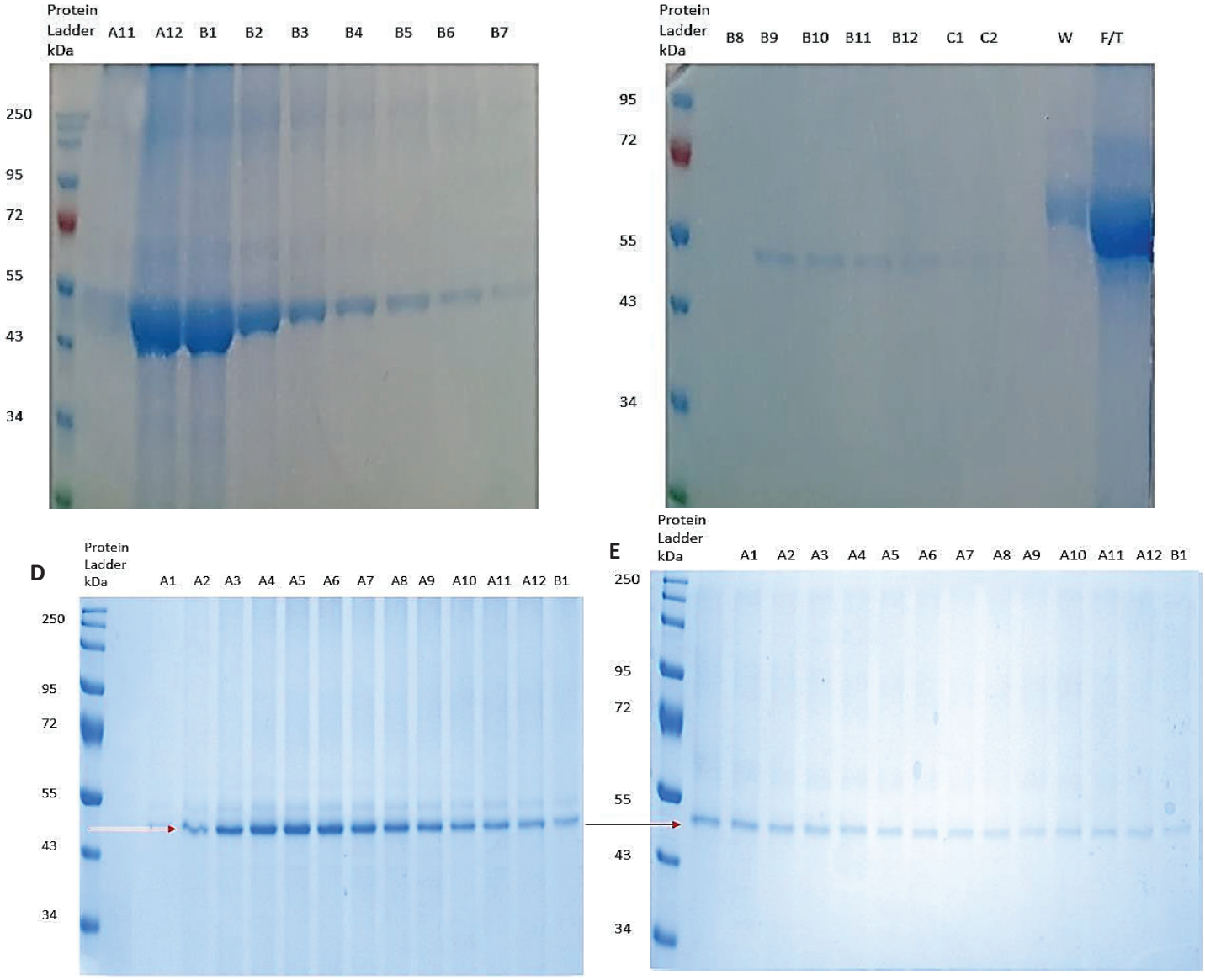

Figure 21: Analysis of αL243(scFv)-SNAP purified employing a combinatory purification technique. (A) and (B) represent the chromatograms for IMAC and IEX, respectively. Figures 21 (C), (D), and (E) represent SDS-PAGE gel analysis for IMAC, IEX, and SEC, respectively. The protein sizes were determined using a pre-stained protein marker

(A)

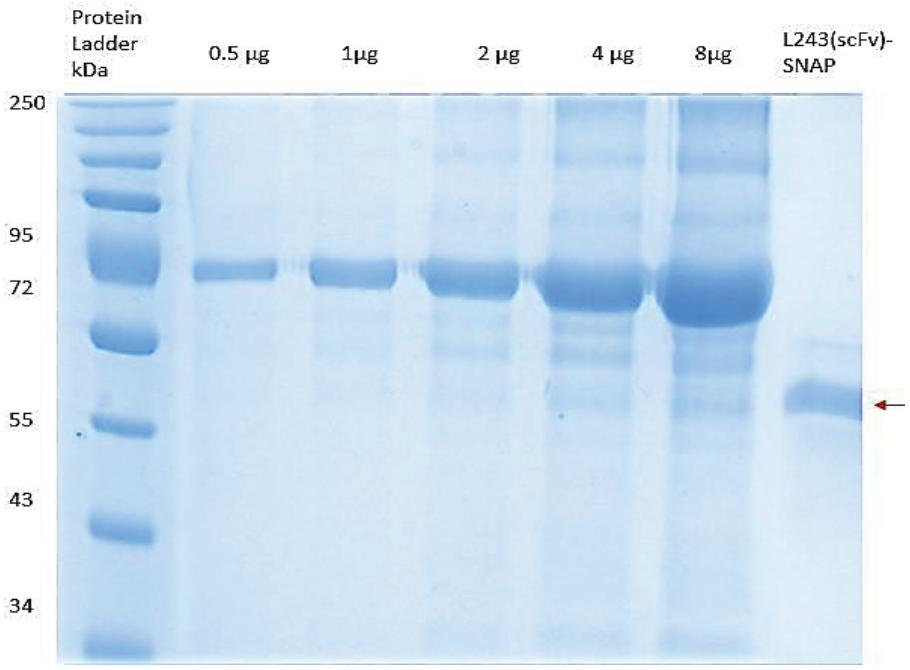

(B)

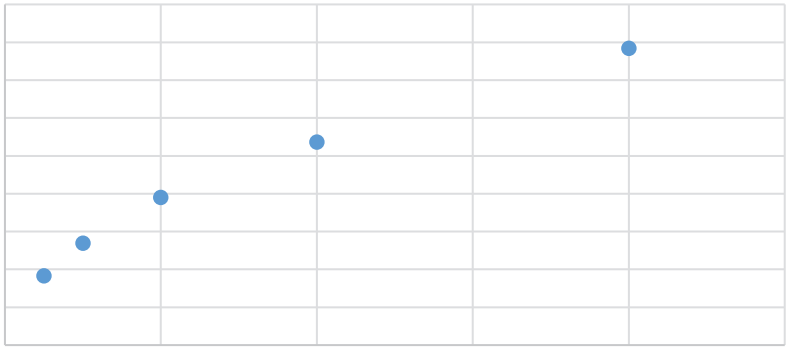

(C)

Table 9: Densitometric quantification of L243(scFv)-SNAP

Sample	DeNovix value (mg/mL)	Densitometry value (µg/µL)	Relative amount of full-length protein in concentrated fraction (%)	Absolute amount	Yield (mg/L)
αL243(scFv)SNAP	2.32	1.92	82.8	768	1.54

Figure 22: Quantification analysis of L234(scFv)-SNAP. (A) SDS-PAGE gel analysis for concentrated L243-SNAP recovered from SEC. (B) A standard BSA curve corresponding to the SDS-PAGE gel in (A), and (C) represents a summary of the protein concentration and purity. .

BG-Alexa 488 conjugation to αL243(scFv)-SNAP

The functionality of the SNAP-tag positioned at the N-terminal was also determined by conjugating the protein sample with BG-modified fluorophores, Alexa 488, at a

ratio of 1:1. A stained SDS-PAGE gel (left panel) containing unconjugated protein was also prepared, along the gel containing conjugated protein (right panel) to serve as a control. When conjugated proteins were viewed under a Dark Reader Transilluminator, distinct bright green bands were observed around the theoretical weight of the target protein, which confirmed that the SNAP-tagged N-terminal was functional and successfully conjugated to BG Alexa 488. Furthermore, the unconjugated fluorophore was seen at the lower bottom of the gel, which confirmed that the target protein was fully saturated; thus, the access fluorophore is observed. Following the determination of full-length protein by SDS-PAGE analysis and functionality of both N and C termini by western blot analysis and fluorophore conjugation, respectively.

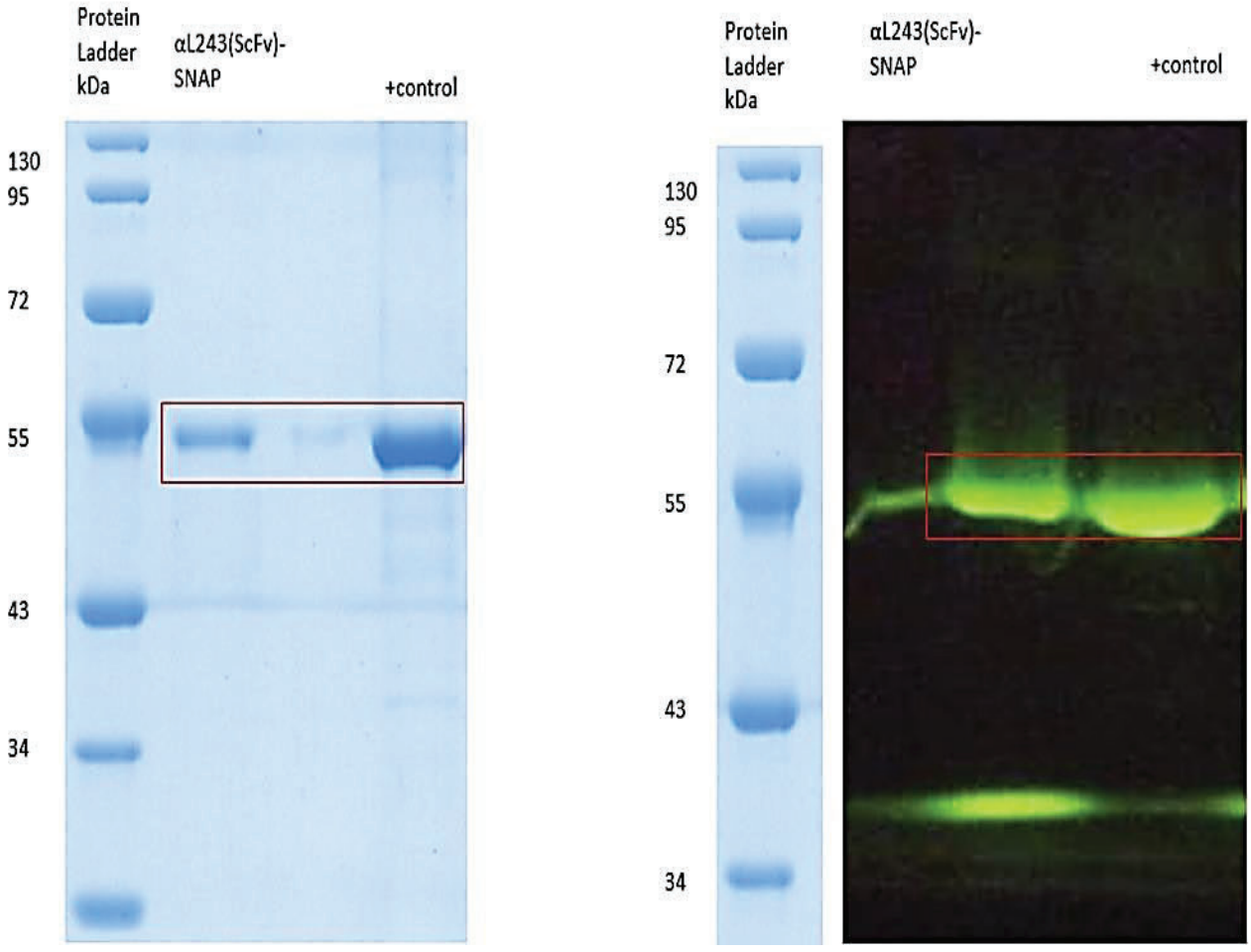

Figure 23: Conjugation analysis of L243(scFv)-SNAP with Alexa 488. αL243(scFv)SNAP was conjugated with Alexa 488 at a ratio of 1:1. On the left panel is the 10% SDS-PAGE gel used as the control corresponding to the unstained conjugation gel on the right panel viewed on Dark Reader Transilluminator for the visualization of fluorescent signal.

3.9 Expression and Production of H22(scFv)-ETA

H22(scFv)-ETA was successfully expressed in BL21 in the presence of compatible solutes under osmotic pressure. The rITs are produced in the periplasmic space, which enhances proper folding and stability of the rIT. A total of 17g cell mass was collected. The cells were harvested as described in **section 2.1.2** and prepared for purification.

3.9.1 Re-establishment of protocol: IMAC purification of bacterially expressed protein

The initial IMAC purification protocol for bacterially expressed proteins involved a single IMAC purification that included three main purification steps in the order of sample application, wash, and elution step. This technique employed a high flow rate under mild buffer conditions, summarized in **Table 10**. Poor protein recovery and purity were some of the major challenges experienced when employing this protocol. Therefore, to address these challenges, an IMAC technique was improved by implementing two IMAC steps (IMAC I and IMAC II). The first IMAC step, which serves as a rapid wash and elution step will allow the washing of weakly bound contaminants without compromising the target protein. In addition, the HiTrap ff Crude HP column was employed for the first IMAC (IMAC I), which allows for fast flow, intended for this step, making it a good choice for protease-sensitive proteins. However, HiTrap chelating was used for IMAC II. Other measures, such as reduced viscosity of the lysate or high viscosity, may lead to increased back pressure and clog the column. The flow rate employed in IMAC II was further reduced to 1 ml/min for the sample application wash step and the elution step. Furthermore, imidazole concentrations in the wash buffer were also optimized for higher protein purity. The buffer system and running conditions employed in IMAC I and IMAC II are detailed in **Tables 10** and **11,** respectively.

Table 10: Buffer system employed in IMAC I and IMAC II

Buffers	**Buffer composition**		
	Initial IMAC	IMAC I	IMAC II
Load buffer	Tris-base, 50 Mm, NaCl, 500 mM Imidazole 10 mM pH 7.4	Tris-base, 100mM NaCl, 1 M pH 8.0	Tris-HCl, 20mM NaCl, 500mM Imidazole, 10mM pH 8.0
Wash buffer	Tris-base, 50 mM, NaCl, 500 mM pH 7.4	Tris-base, 100mM NaCl, 1M pH 8.0	Tris-base, 20mM NaCl, 500mM Imidazole, 30mM pH 8.0
Elution	Tris-base, 50 Mm, NaCl, 500 Mm, Imidazole 500 mM pH 7.4	Tris-base, 100 mM NaCl, 1 M Imidazole, 250 Mm pH 8.0	Tris-base, 20 mM NaCl, 500 mM Imidazole, 500 mM pH 8.0

Table 11: Running conditions for IMAC I and IMAC II

Purification steps	**Flow rate, CV**		
	Initial IMAC	IMAC I	IMAC II
Column Equilibration	7 mL/min	5 ml/min, 5CV	5 mL/min, 5 CV
Sample Application	5 mL/min	4 mL/min	1 mL/ min
Column Wash	5 mL/min, 10 CV	5mL/min, 5CV	1 mL/min, 10 CV
Elution step	5 mL/min, 7CV	2 mL/min, 5 CV	1mL/min, 10 CV

3.9.1.1. IMAC analysis

In preparation for IMAC I, the HiTrap ff crude HP column was equilibrated with 5 CV of equilibration buffer at a 5 mL/min flow rate. A total of 35 mL of lysate recovered was loaded onto the column at a 4 mL/min flow rate. The column was subsequently

washed with 5 CV of the wash buffer containing 10 mM Imidazole. Following column wash, the target protein was recovered by a single-step elution method with a maximum Imidazole concentration (250 mM). The elution step maintained the flow rate at 2 mL/min. **Figure 24** (A) and (C) show the absorbance (UV 280 nm) of eluate from IMAC-purified lysate. In preparations for IMAC II, elutes from IMAC I, believed to contain H22(scFv)-ETA (72 kDa), were collected, concentrated down to 500 uL, and further exchanged with loading buffer (Tris-base 20 mM, NaCl, 500 mM, pH 8) using a 10 kDa Amicon. The collected protein sample was subjected to a second IMAC. Compared to the first IMAC, IMAC II had a lower flow rate, and extended column wash was implemented. The collected sample was loaded onto the column at a flow rate of 1 mL/min Once all the protein sample was loaded, the column was washed with 10 CV wash with a gradient wash step (4%-12% Imidazole concentration). Finally, the protein was eluted with 10 CV elution buffer at 100% Imidazole concentration. The eluted fraction from the single elution peak displayed in **Figure 24B** (blue line) was run at a 10% SDS-PAGE. The observation of bands (red arrow) corresponding to the theoretical weight of H22(scFv)-ETA (**Figure 24D**) was an indication of the possible presence of the protein of interest.

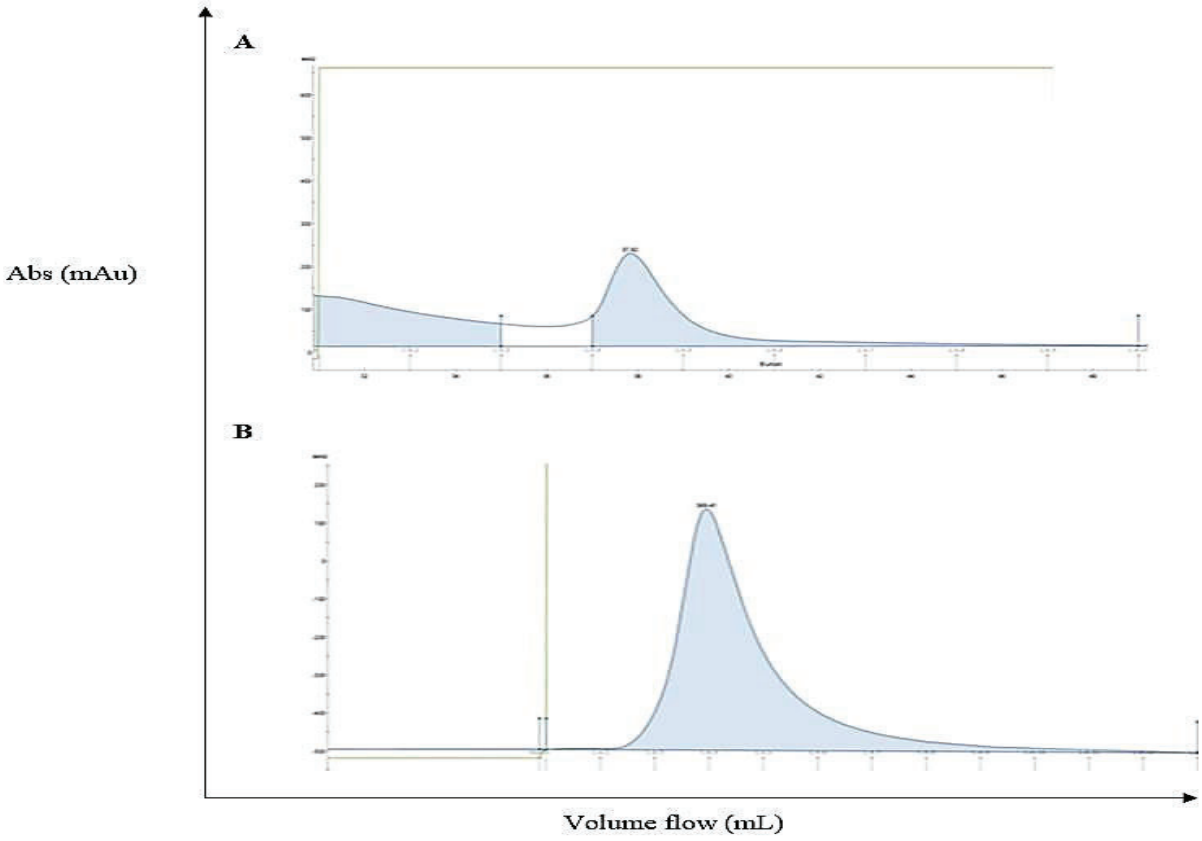
A
B
Abs (mAu)
Volume flow (mL)

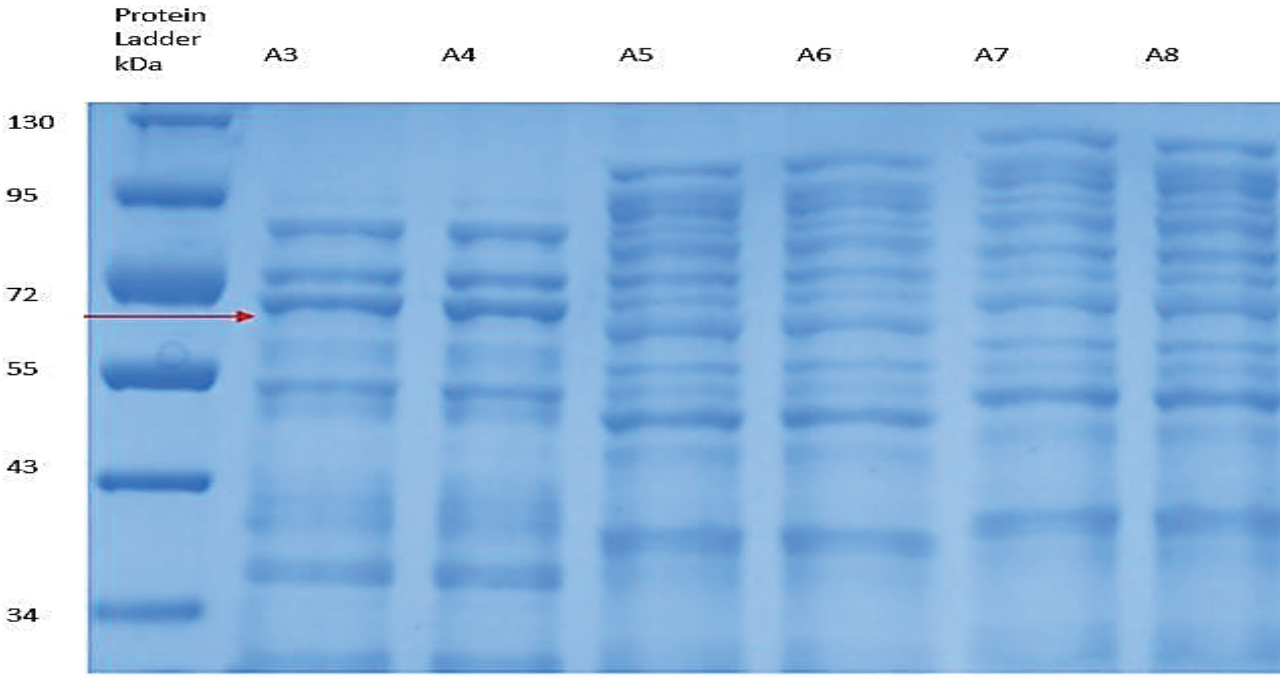
Protein Ladder kDa
A3
A4
A5
A6
A7
A8
130
95
72
55
43
34

(C)

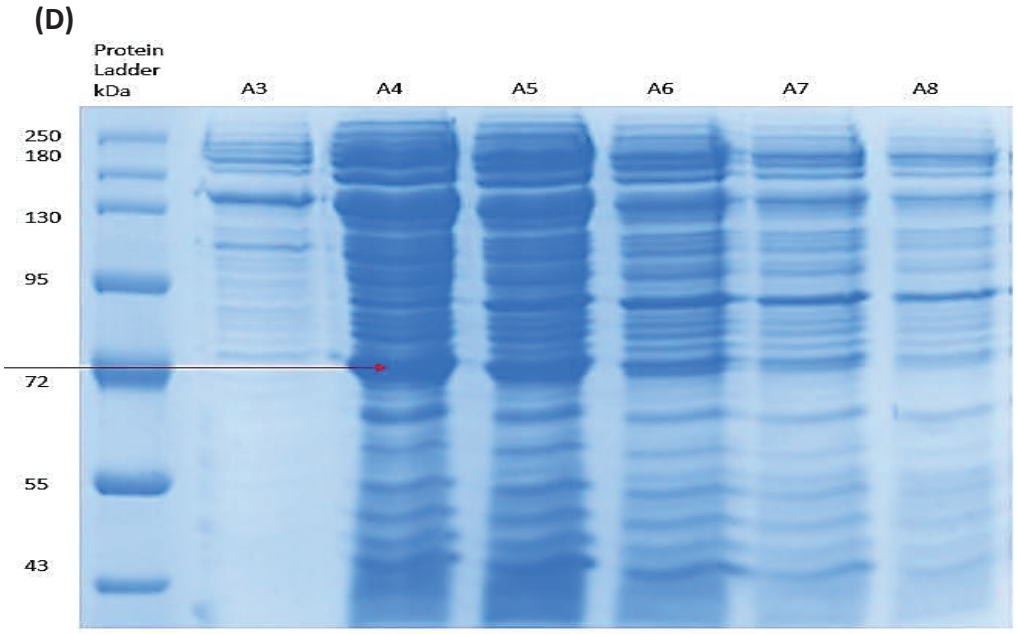

Figure 24: IMAC purification analysis of H22-ETA. (A) and (B) represents the absorbance profile (UV 280 nm). Of elute for IMAC I and IMAC II, respectively. (C) and (D) are corresponding 10% SDS PAGE analysis showing the presence of the target protein indicated by a red arrow.

3.9.2 Combination of IMAC-IEX

The H22(scFv)-ETA sample protein recovered from the IMAC II was further purified using a combinatory purification approach. Before IEX, H22(scFv)-ETA sample was exchanged with start buffer (50 mM Tris, 10 mM NaCl, pH 8), the column was equilibrated with 5 CV of the start buffer at a flow rate of 5 mL/min followed by sample application onto the column (HiTrapQ HP) at a flow rate of 1 ml/min. After the sample application, the column was washed with 5 CV wash buffers (50 mM Tris, 100 mM NaCl, pH 8) at a flow rate of 1 mL/min. After that, the protein sample was eluted from the column with 10 CV elution buffers (20 mM Tris, 1 M NaCl, pH 8) at a 1 ml/min flow rate. Protein elutes recovered from IMAC (5.53 ug/uL) and IEX (3.2 ug/uL) were separately concentrated and exchanged with 1X PBS using a 10 kDa Amicon before being subjected to Size Exclusion Chromatography

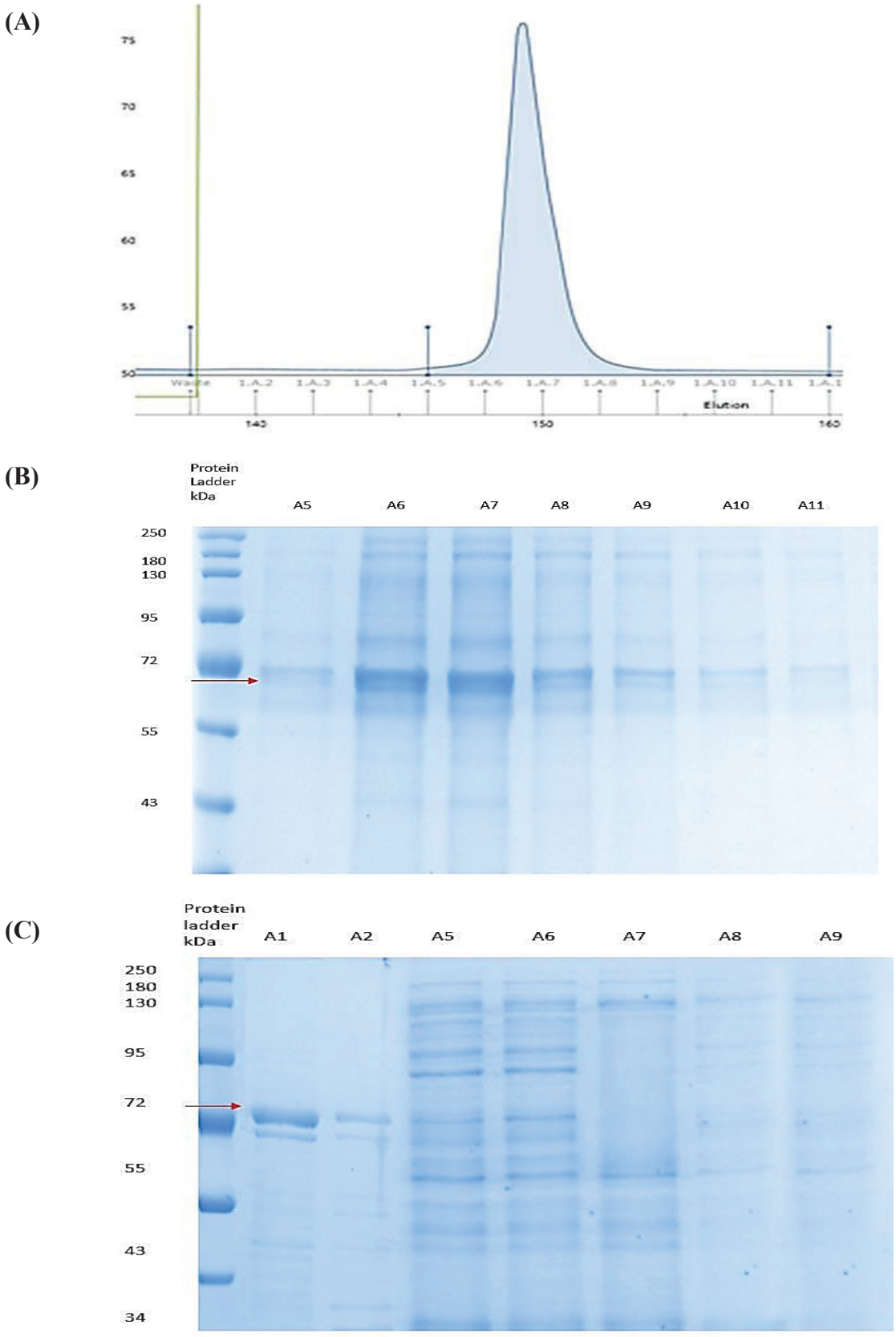

Figure 25: combinatory purification analysis of H22(scFv)-ETA. Figure (A) represents the absorbance profile (UV 280 nm) for IMAC purification of H22(scFv)-ETA . Figures (B) and (C) represent the SDS-PAGE gels of the peak fractions collected from IMAC and IEX, respectively. Protein bands (red arrow) are observed around the theoretical size of H22(scFv)-ETA for IMAC and IEX.

3.9.3 Quantification of purified H22(scFv)-ETA protein

Proteins recovered from each combination purification technique were concentrated and run on a 10% SDS-PAGE against a two-fold BSA standard serial dilution. Distinct protein bands were observed on the gel around the expected target protein molecular weight (marked red). Heavy bands (>72 kDa) of contamination were observed on protein purified through the technique combining both the IMAC-IEX and IMAC-IEX-SEC. Non-specific binding was also observed in protein samples purified through IMAC. **Figure 26** below represents the BSA standard SDS PAGE used to quantify. The protein yield calculated by densitometry **(Table 12**) was 24%, 31%, and 64% for the purification technique employing IMAC.IMAC-IEX and IMAC-IEX-SEC, respectively.

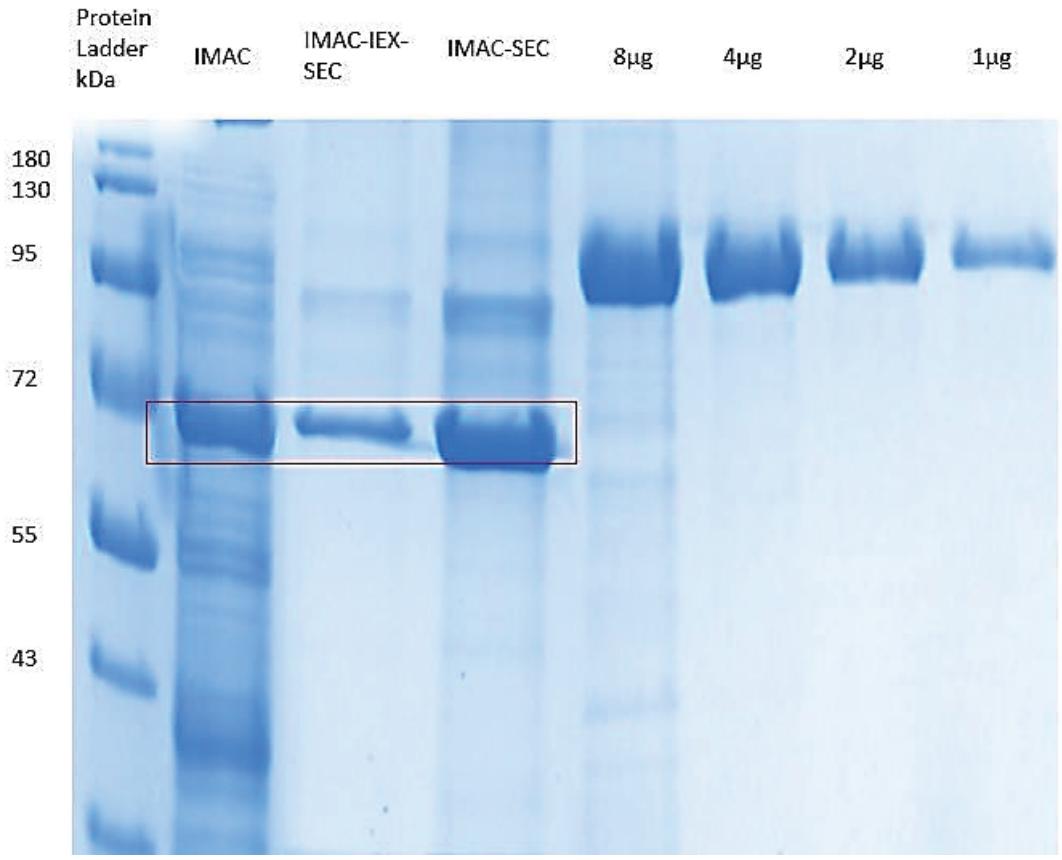

Figure 26: SDS-PAGE analysis of concentrated H22(scFv)-ETA against BSA standard for densitometry quantification. . Protein purified by IMAC, IMAC-IEX-SEC, and IMAC-SEC was loaded on lanes 1,2, and 3, respectively, along with BSA standards for quantification. A pre-stained protein ladder was added to the first lane to track protein by size

Table 12: Densitometric quantification of HEE(scFv)-ETA purified by combinatory purification

Sample	DeNovix (mg/µL)	Densitometry value (µg/µl)	Amount of full-length protein in concentrated fraction (%)	Absolute amount	Yield mg/L
A(IMAC)	18.43	5.53	24	2765	2.77
B(IMAC-IEX-SEC)	1.1	0.7	64	350	1
C(IMAC-SEC)	14.73	3.8	31	1710	1.71

3.9.4 Western blot analysis

Western blot analysis was carried out to validate the integrity of purified H22(scFv)-ETA recovered from **section 3.3.2**. The samples were run on an SDS-PAGE gel and successfully transferred to a PVDF membrane as seen in **Figure 27**. The PVDF membrane was further incubated in an anti-His primary antibody that binds to the poly-His tag at the C-terminal of the target protein. A secondary antibody (goat anti-rabbit HRP-conjugate antibody), which further binds to the anti-His primary antibody, allowed the visualization of the His-tagged fusion proteins. Thick bands corresponding to the theoretical size (71 kDa) of the protein of interest are observed in Figure 32 (marked red) this indicating the presence of the target protein. Smaller size bands (<55 kDa) are also observed on the PVDF membrane, which is an indication of protein degradation.

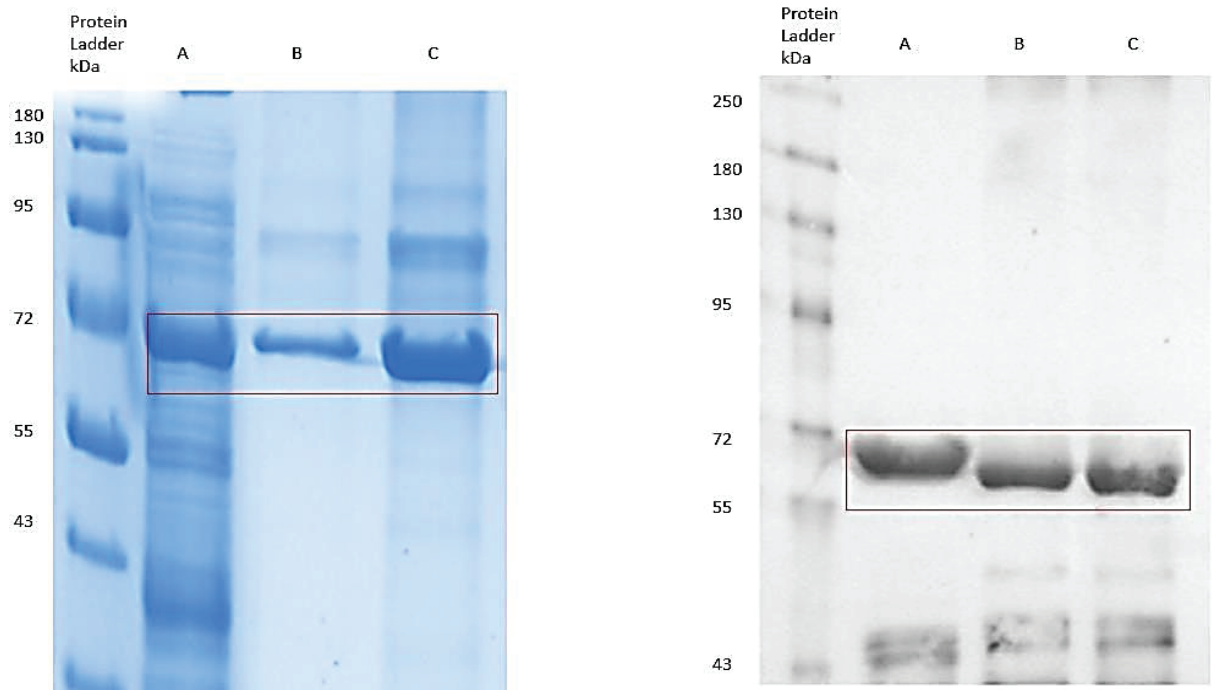

Figure 27: Western blot analysis of concentrated H22(scFv)-ETA protein fraction generated from the combinatory purification technique. On the left panel is an SDS-PAGE gel, which is a control for the western blot membrane. (A) Protein from IMAC II, (B) protein after IMAC-IEX-SEC, and (C) protein after IMAC-SEC

3.9.5 Validation of binding by flow cytometry for H22(scFv)-ETA

Following confirmation of full length by SDS-PAGE characterization,30 µg of H22(scFv)ETA was labelled with an anti-His PE antibody conjugated to BG-Alexa Fluor 647. This labelling process allowed the fusion protein to be visualized and quantified during flow cytometry analysis. The target cells used in this experiment are IFN-Y (Interferon-Y) stimulated U937 cells engineered to express CD64, which is the target of the CD64-targeting fusion protein. The labelled H22(scFv)-ETA fusion protein was then incubated with the IFNγ-stimulated U937 cells. Of which the fusion protein is expected to efficiently bind to CD64 receptors on the cell surface due to the targeting ability of the scFv (single-chain variable fragment) portion. **Table 14** shows the precise steps for this experiment.

To enable detection in flow cytometry, 30 µg of H22(scFv)-ETA is labelled with an anti-His PE antibody that is conjugated to BG-Alexa Fluor 647. This labelling process allows the fusion protein to be visualized and quantified during flow cytometry analysis. As observed in **Figure 28**, in the context where baseline and CD64 antibody

controls are both present, each of the CD64-targeting fusion proteins exhibits notable binding to IFN-γ-stimulated U937 cells. This demonstrates good binding of the final recovered protein from the purification technique combining IMAC-IEX and SEC.

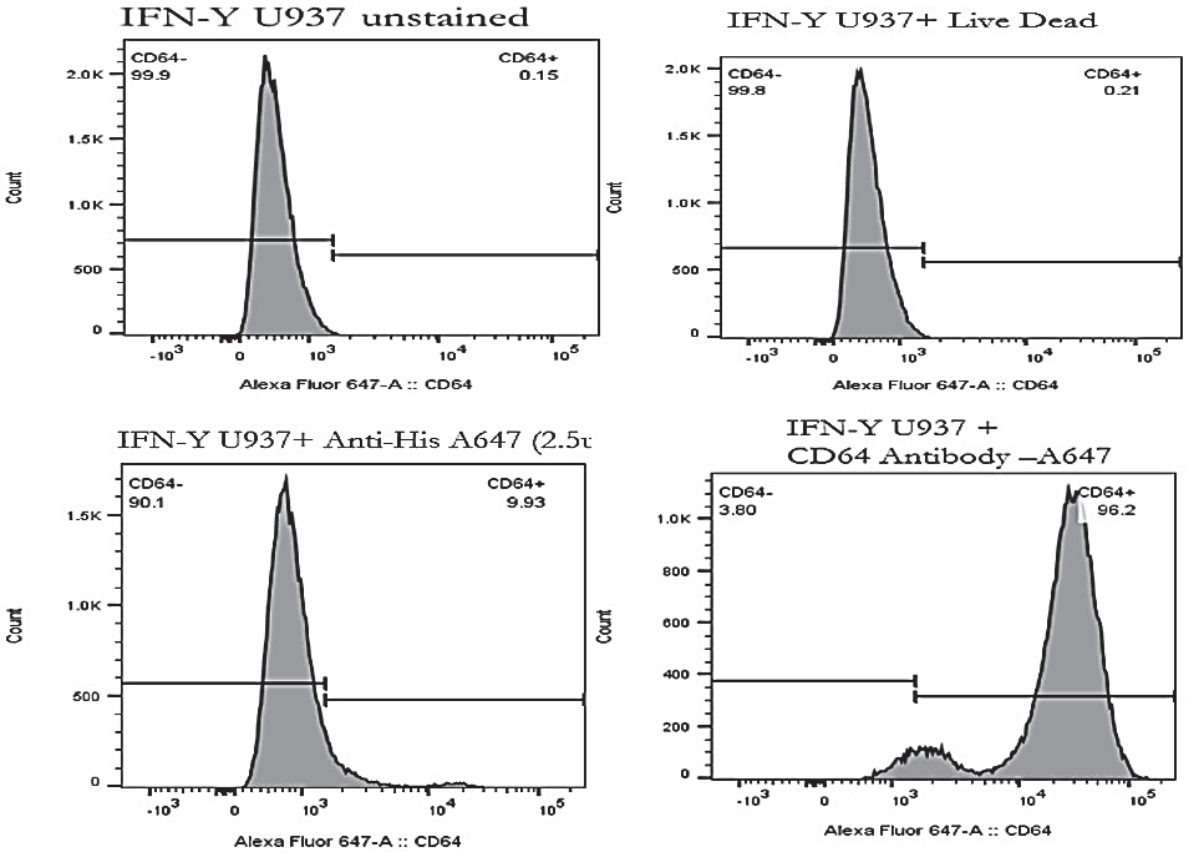

Figure 28: Validation of binding of CD64 fusion protein to to IFN-Y stimulated U937 cells by flow cytometry. The functional activities of CD64-targeting cells, H22(scFv)-ETA on CD64+ cells (IFNY stimulated U937) using flow cytometry, and a standard protocol described in section 3.3.4 (Table 16). 30 µg of H22(scFv)-ETA was labelled with an anti-His PE antibody conjugated to BG-Alexa Fluor 647 on ice for 1 hour. Following this, the conjugated cells underwent washing, resuspended in FASC buffer, and were analyzed using a BD LSR-II flow cytometry system from BD Biosciences In the presence of both baseline and CD64 antibody controls, each of the CD64-targeting fusion proteins demonstrates significant binding to IFN-γ stimulated U937 cells.

Chapter 4: DISCUSSION

4.1 Development of cancer therapeutics

Despite the development of major advances, difficulty in treating certain cancers remains a major challenge in public health worldwide (110,111). Because cancer is a heterogeneous disease various factors influence its molecular characteristics and response to treatment. Some of the major unmet needs in current therapeutic

approaches include the development of drug resistance, delayed detection of some cancer types, toxicity, and side effects of some therapies (112,113). Increasing knowledge of molecular and tumor biology through research can circumvent these challenges. Preclinical studies using well-characterized and high-quality proteins play a pivotal role in the reliability of research findings. This data is also used as a tool to guide the efficacy of promising therapeutic candidates to clinical trials, accelerating the drug development process. Developing novel cancer therapies is complex and finding a balance between effective treatment and cost consideration is a multifaceted challenge involving intensive research, clinical trials, and regulatory approvals.

The production process of therapeutic protein includes both the downstream application and the upstream processing. The upstream processing involves the generation of the cell line for adequate expression of the protein of interest and the downstream processing encompasses all process steps from cell harvest to the final purified product (114). Expression of recombinant protein-based biopharmaceuticals can be achieved using eukaryotic and prokaryotic microorganisms (61). The majority of the approved recombinant protein-based biopharmaceuticals are expressed in the mammalian expression system. This is due to the capacity to express large and complex recombinant proteins. The extended duration of protein expression, inadequate protein yield, and high cost of media requirements necessitate consideration of alternative expression systems(61,115). Though the *E. coli* provides a much lower cost, rapid growth, and good productivity, its major limitation is a lack of proper post-translational modifications. Another major challenge is that rIT is their toxicity to the expressing host itself. To limit the toxicity to productive cells while obtaining an adequate yield, genetic engineered bacterial hosts enable the selection of appropriate strains to tolerate high amounts of ITs, without being intoxicated (115). This study focused on establishing an integrated approach that combined advanced chromatography techniques to streamline the enhanced purification of recombinant

proteins while maintaining low cost and high protein quality. Additionally, this establishment will allow for a versatile application to a broader range of proteins expressed by mammalian and bacterial expression systems. The upstream process (protein expression) employed already existing protocols developed at the MB&I research group, confirmed to produce functional full-length fusion proteins.

4.2 Expression of protein-based pharmaceuticals

Recombinant immunotoxins and antibody-drug conjugates are protein-based pharmaceuticals representing target therapy (116). Antibody-drug conjugates primarily deliver synthetic small-molecule drugs or toxins using stable linkers to target cells where the antibody component recognizes specific antigens on the surface of target cells, facilitating targeted delivery of the cytotoxic payload (29,40,117). While recombinant immunotoxins (rITs), which are proteins composed of fragments of monoclonal antibodies fused to truncated protein toxins, deliver apoptosis-inducing protein toxins without the need for such linkers (116,118,119). Advancements in the application of recombinant immunotoxins have significantly expanded therapeutic potential, however, there is still a need to improve specificity, reduce side effects, and further expand therapeutic applicability.

Therapeutic recombinant proteins can be expressed in both mammalian and bacterial expression systems (120). The choice of expression host depends on the ability of the expression host to produce a sufficient yield of functional protein of interest, ease of protein extraction, and relative protein purity (61). Hence, the accurate design of the protein chimera and the host of expression play a crucial role in producing functional full-length recombinant proteins (78). This study employed pre-existing protocols developed by the MB&I research group. These protocols have been confirmed to produce functional full-length proteins, proving suitable to support laboratory-scale research. However, the focus was on improving protein quality by establishing an

improved standard purification protocol yielding high protein quality. This establishment allows for a versatile application to a broader range of proteins expressed by mammalian and bacterial expression systems (134). On the contrary, bacterial expression systems, such as *Escherichia coli* are often used for producing recombinant proteins that do not require extensive post-translational modifications. *E. coli* is a well-characterized and easily manipulated organism, making it a popular choice for recombinant protein production due to its fast growth rate and high protein expression yields (120). In this case, the SNAP fusion protein was expressed in HEK 293T cells, this is because the bacterial expression system may lack the ability to perform certain post-translational modifications found in mammalian cells. while immunotoxins were successfully expressed in the bacterial system. SNAP-tagged antibody fusion proteins were expressed in the mammalian expression system. Toxins were expressed in bacterial expression systems because many toxins do not require complex post-translational modifications, such as glycosylation or disulfide bond formation, which are often essential for proper folding and function in mammalian proteins (121). This simplifies the expression process for toxins, allowing high expression levels at a low cost (61).

4.2.1 Mammalian expression of SNAP tag-based ADC

A mammalian expression system was used for the expression of complex scFv-(SNAP) This was because the mammalian cells have the machinery to perform post-translational modifications, which are crucial for the stability, function, and immunogenicity (122). SNAP-tagged fusion antibodies consist of multiple domains, maintaining the integrity and functionality of all domains throughout the downstream and upstream production can be challenging. The monoclonal component of the ADC is responsible for the specific selection of the target antigen on the cell, along with other structural features such as the Fc region, which allow internalization and trafficking of the ADC-antigen complex. The stability of the linker connecting the

cytotoxic payload to the antibody in circulation and the ability to cleave upon reaching the target are important factors (39,41). Additionally, the capacity of SNAPtag to efficiently and specifically undergo covalent labelling with benzylguanine derivatives is dependent on the modified active site, substrate-binding pocket, and overall protein structure. Each component of the complete ADC fusion protein plays an important role in its overall function. It is then crucial to ensure that the choice of expression system supports the production of biologically active therapeutic proteins.

The production of functional therapeutic SNAP-tagged fusion antibody proteins may present several challenges. This is due to the complexity of these molecules and the need for high purity and biological activity. Some of the challenges experienced in this study included the expression of highly contaminated proteins, attributable to the expression of Host Cell Proteins (HCPs) and Impurities, possible aggregation, and protein degradation (123). The outcomes of this study demonstrated that implementing similar protocols previously employed at the MB&I research unit led to the successful production of the SNAP-tag fusion antibody fusion protein. However, persistent contaminants of small and larger sizes were observed following IMAC on the SDS gel and the western blot membrane seen in Figure 12 (109,124,125). As a result, the protein quality remained compromised, with a purity of 25%

4.2.2 Bacterial expression of recombinant immunotoxins

In contrast to mammalian expression systems, bacterial expression systems, employing *Escherichia coli*, are often used for producing recombinant proteins that do not require extensive post-translational modifications. *E. coli* is a well-characterized and easily manipulated organism, making it a popular choice for recombinant protein production due to its fast growth rate and high protein expression yields (120). Because many toxins do not require complex post-translational modifications, such as glycosylation or disulfide bond formation, which are often essential for proper folding and function in mammalian proteins (121). This simplifies

the expression, allowing high expression levels at a low cost. It is worth mentioning that the stability of any potential therapeutic protein is vital to ensure its structural integrity and functional activity. Proteins that undergo degradation or denaturation may lose their ability to bind to the target protein effectively, reducing their therapeutic efficacy. Maintaining the stability of therapeutic proteins ensures their proper folding and retention of critical binding sites necessary for target engagement and therapeutic activity (126). Furthermore, protein stability and purity are essential for reliable and reproducible results in further studies, moreover, the consistency of antibody quality is critical for conducting preclinical experiments, such as in vitro assays, animal models, and toxicity studies. For this reason, both the upstream and downstream processes in the production of therapeutic antibodies play a critical role in successful product development (123).

In this study, rIT H22(scFv)-ETA was expressed under the control of the IPTG-inducible

T7 lac promoter in E. coli BL21(DE3). The lac promoter is a special feature of the BL21 cell. The lac promoter is activated upon the addition of IPTG into the growth medium, initiating transcription and expression of the target genes. However, the downside is that the folding machinery of prokaryotic cells is likely not proficient in producing fully functional folded proteins of heterologous origin. To overcome the foreseen challenge, functional H22(scFv)ETA was efficiently expressed by employing the periplasmic expression under osmotic pressure in the presence of compatible solutes established by Barth *et al*., 2000. This process of expression makes use of *E. coli's* natural ability to accumulate the newly expressed protein into the periplasmic space in response to osmotic stress. The compatible solutes allow *E. coli* to protect proteins at high salt concentrations. Furthermore, incorporating glycine betaine allows the bacteria to survive in such harsh conditions. It also has the additional advantage of producing a conducive environment for proper protein folding and disulfide bond formation, which are essential for the functionality of the proteins

(127,128). A total yield of 2.77 mg/L for full-length H22(scFv)-ETA validated through western blot analysis was recovered from IMAC purification from a 2L, as seen in the result section (section 3). This affirms the efficiency of the *E.coli* in expressing recombinant immunotoxin H22(scFv)-ETA under osmotic stress.

4.3 Purification approach overview exemplified by αASPH(scFv)-SNAP

Previous protein purification approaches implemented by the MB&I involve Immobilized Metal Affinity Chromatography as the main purification strategy to purify both bacterial and mammalian expressed recombinant proteins. Although this strategy successfully recovered expressed protein, the recovered protein had low purity. To address this challenge, two additional chromatographic steps in sequence were added to complement IMAC. Specifically, the Ion Exchange Chromatography and Size Exclusion Chromatography. Each purification strategy was independently explored and optimized to establish an adaptable single workflow protocol suitable for the purification of a variety of recombinant fusion proteins.

4.3.1 Improved IMAC Protein Purification

Protein purification plays a critical role in the production of biologically active and pure proteins. during the expression of proteins in biological systems, various impurities such as the host proteins, may be co-expressed with the target protein. It is estimated that separation and purification procedures may account for as much as 60–80% of the total production cost (129). Moreover, the level of contamination varies depending on the choice of host and other factors. Protein analysis through SDS-PAGE and protein quantification post-IMAC purification shows high levels of contamination for both bacterial and mammalian expressed proteins. This observation indicated that employing IMAC as the sole purification strategy does not efficiently separate the target protein from other cell culture by-products. Achieving an optimal a good balance between protein quality and yield can be challenging. Because proteins

are sensitive, changes to their environment, such as NaCl concentrations, pH, and temperature, may lead to protein degradation and yield loss (130-131). Therefore, strategies to optimize purification conditions, including buffer composition, chromatography parameters, and protein handling techniques, need to be carefully considered for maintaining the native structure and function of the protein (132).

4.3.1.1 Improving Binding Conditions

To address the above-mentioned challenge IMAC optimization technique was focused on improving the interaction of the target protein and the Nickle (Ni^{2+}) column prior elution step while reducing non-specific binding. The system flow rate was decreased from 5 mL/min to 1 mL/min specifically for the sample application step, the column wash step, and the elution step. This initiative allowed stronger interaction of the His-tagged proteins with the immobilized metal ions (Ni^{2+}) in the column (133). Minimum to no target protein was eluted in the sample application and the wash step.

4.3.1.2 Improving resolution

As discussed earlier, non-specific binding was one of the major challenges resulting in poor protein purity. In this study, a series of wash buffers were experimented with to reduce nonspecific binding without compromising the protein of interest bound onto the column. Following this action, it was observed that adding moderate imidazole concentration in the wash buffer decreased the level of non-specific binding by washing out weakly bound contaminants while maintaining the binding of the His-tagged target protein to the nickel resin. This was efficiently achieved while maintaining a flow rate of 1 mL/min for the wash step

4.3.1.3 Improving in Elution Strategy

The elution step was improved along with a reduced flow rate (1 mL/min). A single-step elution with 250 mM imidazole was further implemented; this was based on the rationale that an extensive column wash step was implemented before the elution step. This action reduced non-specific interaction and allowed for a more specific protein

recovery using lower Imidazole concentration when compared to the gradient elution step, coupled with a wash step without imidazole (As previously implemented in the MB&I group).

4.3.1.4 Improved IMAC for mammalian-expressed SNAP-tagged fusion protein

Immobilized Metal Affinity Chromatography is a powerful and widely employed purification technique used to separate and purify target proteins based on their affinity for specific metal ions immobilized onto a solid support(89). This strategy takes advantage of the specific metal affinity tagged to the protein of interest. In the case of this research, all target proteins were tagged to a poly-histidine (His-tag) at the C-terminal. His-tag is widely utilized due to its strong binding affinity to metal ions immobilized on the resin. As it is observed in this study (**section 3.2**), in some cases, the His-tag may not provide sufficient specificity, leading to the copurification of impurities. This could be due to several reasons, including that cellular proteins expressed by the host may contain high amounts of histidine, which leads to non-specific binding. Another challenge observed in previous studies is poor interaction between the polyhistidine affinity tag and the metal ions on the column, leading to protein loss during the sample application step and column wash step. This observation may be due to the folding of the purified poly-his protein, which might embed the affinity tag, thus leading to inefficient binding onto the nickel ion column, or due to the high flow rate, which does not allow transient interaction between the target protein and the purification column. Other factors may involve the purification itself, that is, the column may need to be charged or replaced.

4.3.1.5 Improved IMAC for bacterially expressed protein

In the case of bacterial expression systems, implementing Immobilized Metal Affinity Chromatography (IMAC) optimized for the purification of mammalian expressed protein made it possible to purify the target protein by reducing non-specific binding and removing impurities. However, the purification of recombinant proteins was more

challenging and less enhanced compared to that of mammalian-expressed proteins. This could be due to the presence of increased host cell proteins and contaminants. As a result, implementing IEX and SEC may be challenging due to very high levels of impurities. Incorporating two IMAC steps in the purification process before the implementation of IEX and SEC allowed enhancement of protein purity of the target protein by reducing non-specific binding and removing impurities. The first IMAC step serves as an initial purification step, removing most of the host cell proteins and contaminants. By utilizing a specific His-tag, the target protein can be selectively bound to the IMAC resin, while impurities are washed away. The second IMAC step acts as a polishing step, further eliminating any remaining contaminants or residual nonspecifically bound proteins. This dual-step approach significantly enhanced the selectivity of the purification process, resulting in improved protein purity. In previous studies where only one IMAC purification was employed at higher flow rates (5 mL/min- 7 mL/min) target protein was displaced prior elution step, leading to yield loss. As also observed in IMAC purification of mammalian expressed proteins, including a moderate amount of imidazole in the 2^{nd} IMAC wash buffer, at a reduced flow rate (1 mL/min) enhanced the removal of non-specific binding.

4.3.2 Ion Exchange Chromatography

To achieve improved separation of the target protein from contaminants IEX technique was used as the second purification step. IEX is a technique that can selectively separate and purify target proteins based on their charge properties (97). A range of buffers with different ionic strengths to isolate proteins of interest selectively. Furthermore, this study focused on maximizing the efficiency of Ion Exchange Chromatography (IEX) by exploring the pH and the ionic strength of the buffer system. while maintaining a constant temperature and flow

rate.

4.3.2.1 Buffer pH

Based on the principle that the charge of a protein depends on the pH of the solution relative to the protein's pI, adjustment of the buffer pH determined the net charge of the protein of the target protein (134). In this study, the buffer system was adjusted to a pH above the pI of the target protein, which resulted in a negatively charged protein. The column used for selecting the negatively charged protein of interest would be the positively charged column; in this case, the anion exchange (HiTrap Q HP) column was used. The results generated in **section 3,** as expected, demonstrated that increasing the buffer pH improved binding efficiency. Whereas at a lower pH, poor protein retention was observed, leading to the protein being eluted prematurely.

4.3.2.2 Ionic Strength (Salt Concentration)

The ionic strength of the buffer system highly influences the interaction between the ions and the stationary. While a moderate amount of NaCl can improve resolution by displacing nonspecific binding, slight access can significantly reduce the interaction of the ions to the stationary phase. A buffer system of varying ionic strength (NaCl concentrations) was evaluated. The results in **section 3.3.1** demonstrated that incorporating a controlled concentration of NaCl complemented by a strongly charged protein can effectively improve the resolution by up to 42% with minimal protein loss. Whereas lower protein charge demonstrated lower protein purity (26%-38%) and high loss protein lost during the sample application step and the wash step (**Figure 14 E**). Moreover, 1 M NaCl included in the elution buffer was efficient to recover the rest of the target protein.

4.3.3 Size Exclusion Chromatography

Implementation of Size Exclusion Chromatography enhanced the protein purity up to 71% and 83% for mammalian expressed protein and for bacterially expressed protein up to 31 % from 24%. This means there are some limitations associated with the SEC. Because Size Exclusion Chromatography relies on does not account much for the

conformation of the protein and relies more on the assumption that the protein size correlates to molecular weight, discrimination of protein based on size may be challenging, as observed in **Figure 17**. The SDS-PAGE gel shows little to no separation by say for some proteins. This makes the SEC an unreliable purification technique. Rather, proteins may elute differently, not just on their size but their conformation.

4.4 Implications of Integrated Chromatographic Purification

The results generated in this study demonstrated that an integrated purification technique yields high protein production. In comparison to traditional chromatography, which involves one purification step. Each of the purification techniques adds a unique advantage depending on the nature of the target protein. Immobilized Metal Affinity Chromatography takes advantage of the affinity tag linked to the target protein, in this case, the poly-histidine tag, to isolate the protein of interest. While Ion Exchange Chromatography isolates the protein of interest based on charge. Lastly, Size Exclusion Chromatography acts as the last purification step and resolves protein-based size separation. Integrating these purification techniques in a single workflow improves protein purity and has the added advantage of being optimized to accommodate a range of protein products under mild conditions, sustaining protein quality and bioactivity (135). On the contrary, despite the optimization and integration of different purification techniques, the established integrated technique may not be compatible with certain protein products. This is due to the nature of different proteins. Factors such as the protein affinity tag, pI, and the expression host influence the type of purification technique and running conditions. This means further optimization steps may be required, tailored to the needs of individual proteins. A good example is the difference in the optimization of IMAC for bacterially expressed protein and mammalian expressed protein. Bacterial-expressed proteins

tend to contain more contaminants compared to those expressed in the mammalian expression system. To achieve desired purity levels, it may be necessary to implement more rigorous and extended purification steps. As demonstrated in **section 3.8.1**.

CHAPTER 5: CONCLUSION

In summary, it has been proven through this research that the strategic combination of Immobilized Metal Affinity Chromatography (IMAC), Ion Exchange Chromatography (IEX), and Size Exclusion Chromatography (SEC) is a highly effective and robust approach. This integrated purification strategy it is worth noting that this integrated purification approach addresses the diverse physicochemical properties of the target proteins, ensuring a comprehensive purification process. subsequently, it is important to consider the unique physicochemical properties of each protein to be purified.

In this research, IMAC was demonstrated as a good initial purification step, selectively capturing the Histidine-tagged target fusion protein based on its strong affinity for the Nickel ions embedded in the purification column. Whereas, IEX served as a subsequent purification, to further separate the protein of interest from contaminants by exploiting the difference in charge. Lastly, SEC was incorporated as the last polishing step that isolated the target protein from contaminants based on the difference in size. It was further demonstrated that for both mammalian-expressed proteins and bacterially expressed proteins, the combination of IMAC-IEX-SEC had a higher purity outcome, but less yield recovery compared to the purification combination of IMAC-IEX and IMAC-SEC. Higher purity and lower yield loss were observed for the purification combination IMAC-IEX compared to that of IMAC-SEC. furthermore purification combination of IMAC-SEC took much longer compared to that of IMAC-IEX. Moreover, this can impact overall yield and efficiency

as there is yield loss with every purification step, necessitating careful consideration of the trade-off between purity and recovery.

In addition to the enhanced purity of recombinant antibodies synergistic use of these three chromatography techniques further provides flexibility, which allows for the customization and adaptation to specific characteristics of different antibody fusion proteins. This applies to a much wider range of pharmaceutical development projects. On the contrary, isolating the protein of interest from closely related contaminants can be a challenge. The established protocol, as illustrated by αASPH(scFv)-SNAP, has been developing; however, extending this method to purify a broader range of antibody fusion proteins with diverse physicochemical properties may necessitate additional optimization steps. However, the established protocol serves as a solid foundation, requiring minimal validation of efficiency to determine the most suitable purification strategy for their specific needs and thereby streamlining the production timeline and reducing costs significantly.

CHAPTER 6. REFERENCES

1. Deo SVS, Sharma J, Kumar S. GLOBOCAN 2020 Report on Global Cancer Burden: Challenges and Opportunities for Surgical Oncologists. Ann Surg Oncol. 2022;
2. Sitaram Hole A, Anita Suresh R, Ade A V, Amol KN, Sujata VU. REVIEW ON CURRENT STATUS
   OF CANCER IN WORLD [Internet]. International Research Journal of Modernization in Engineering Technology and Science. Available from: www.irjmets.com
3. Hofmarcher T, Manzano García A, Wilking N, Lindgren P. The Disease Burden and Economic Burden of Cancer in 9 Countries in the Middle East and Africa. Value Health Reg Issues. 2023 Sep 1;37:81–7.
4. Franceschi S, Wild CP. Meeting the global demands of epidemiologic transition - The indispensable role of cancer prevention. Vol. 7, Molecular Oncology. John Wiley and Sons Ltd; 2013. p. 1–13.
5. Thun MJ, DeLancey JO, Center MM, Jemal A, Ward EM. The global burden of cancer: Priorities for prevention. Carcinogenesis. 2009 Nov 24;31(1):100–10.

6. Saini A, Kumar M, Bhatt S, Saini V, Malik A. CANCER CAUSES AND TREATMENTS. Int J Pharm Sci Res [Internet]. 2020;11(7):3121. Available from: http://dx.doi.org/10.13040/IJPSR.09758232.11

7. Sina Taefehshokr, Aram Parhizkar, Shima Hayati, Morteza Mousapour, Amin Mahmoudpour, Liliane Eleid, et al. Cancer immunotherapy: Challenges and limitations . Science direct. 2022 Jan;229.

8. Dobosz P, Stępień M, Golke A, Dzieciątkowski T. Challenges of the Immunotherapy: Perspectives and Limitations of the Immune Checkpoint Inhibitor Treatment. Vol. 23, International Journal of Molecular Sciences. MDPI; 2022.

9. Obafemi FA. A Review of Global Cancer Prevalence and Therapy. Journal of Cancer Research, Treatment & Prevention [Internet]. 2023 Apr 30; Available from: https://maplespub.com/article/a-review-of-global-cancer-prevalence-and-therapy

10. Soerjomataram I, Bray F. Planning for tomorrow: global cancer incidence and the role of prevention 2020–2070. Nat Rev Clin Oncol [Internet]. 2021;18(10):663–72. Available from: https://doi.org/10.1038/s41571-021-00514-z

11. Deo SVS, Sharma J, Kumar S. GLOBOCAN 2020 Report on Global Cancer Burden: Challenges and Opportunities for Surgical Oncologists. Ann Surg Oncol. 2022;

12. Di Cristina M, Minenkova O, Pavoni E, Beghetto E, Spadoni A, Felici F, et al. A novel approach for identification of tumor-associated antigens expressed on the surface of tumor cells. Int J Cancer. 2007 Mar 15;120(6):1293–303.

13. Bagnyukova T, Serebriiskii IG, Zhou Y, Hopper-Borge EA, Golemis EA, Astsaturov I. Chemotherapy and signaling: How can targeted therapies supercharge cytotoxic agents? Vol. 10, Cancer Biology and Therapy. 2010. p. 839–53.

14. Donlon NE, Power R, Hayes C, Reynolds J V., Lysaght J. Radiotherapy, immunotherapy, and the tumour microenvironment: Turning an immunosuppressive milieu into a therapeutic opportunity. Vol. 502, Cancer Letters. Elsevier Ireland Ltd; 2021. p. 84–96.

15. Bruheim K, Guren MG, Skovlund E, Hjermstad MJ, Dahl O, Frykholm G, et al. Late Side Effects and Quality of Life After Radiotherapy for Rectal Cancer. Int J Radiat Oncol Biol Phys. 2010 Mar 15;76(4):1005–11.

16. Payandeh Z, Khalili S, Somi MH, Mard-Soltani M, Baghbanzadeh A, Hajiasgharzadeh K, et al. PD-1/PD-L1-dependent immune response in colorectal cancer. Vol. 235, Journal of Cellular Physiology. Wiley-Liss Inc.; 2020. p. 5461–75.

17. Zahavi D, Weiner L. Monoclonal antibodies in cancer therapy. Vol. 9, Antibodies. MDPI; 2020. p. 1–20.

18. Scott AM, Allison JP, Wolchok JD. Monoclonal antibodies in cancer therapy. 2012;12:14. Available from: www.cancerimmunity.org

19. Liu S, Nguyen K, Park D, Wong N, Wang A, Zhou Y. Harnessing natural killer cells to develop next-generation cellular immunotherapy. Vol. 8, Chronic Diseases and Translational Medicine. John Wiley and Sons Inc; 2022. p. 245–55.

20. Shah MA, Schwartz GK. Cell Cycle-mediated Drug Resistance: An Emerging Concept in Cancer Therapy 1.

21. Fu Z, Li S, Han S, Shi C, Zhang Y. Antibody drug conjugate: the “biological missile” for targeted cancer therapy. Vol. 7, Signal Transduction and Targeted Therapy. Springer Nature; 2022.

22. Nelson PN, Reynolds GM, Waldron EE, Ward E, Giannopoulos K, Murray PG. Demystified. .. Monoclonal antibodies. Vol. 53, J Clin Pathol: Mol Pathol. 2000.

23. Rodrigues ME, Costa AR, Henriques M, Azeredo J, Oliveira R. Technological progresses in monoclonal antibody production systems. Vol. 26, Biotechnology Progress. 2010. p. 332–51.

24. Senter PD. Potent antibody drug conjugates for cancer therapy. Vol. 13, Current Opinion in Chemical Biology. 2009. p. 235–44.

25. Tsuchikama K, An Z. Antibody-drug conjugates: recent advances in conjugation and linker chemistries. Vol. 9, Protein and Cell. Higher Education Press; 2018. p. 33–46.

26. An Z. Monoclonal antibodies - a proven and rapidly expanding therapeutic modality for human diseases. Vol. 1, Protein and Cell. Higher Education Press; 2010. p. 319–30.

27. Nagayama A, Vidula N, Ellisen L, Bardia A. Novel antibody–drug conjugates for triple negative breast cancer. Vol. 12, Therapeutic Advances in Medical Oncology. SAGE Publications Inc.; 2020.

28. Chalouni C, Doll S. Fate of Antibody-Drug Conjugates in Cancer Cells. Vol. 37, Journal of Experimental and Clinical Cancer Research. BioMed Central Ltd.; 2018.

29. Flygare JA, Pillow TH, Aristoff P. Antibody-Drug Conjugates for the Treatment of Cancer. Chem Biol Drug Des. 2013 Jan;81(1):113–21.

30. Xenaki KT, Oliveira S, van Bergen en Henegouwen PMP. Antibody or antibody fragments:
Implications for molecular imaging and targeted therapy of solid tumors. Front Immunol. 2017 Oct 12;8(OCT).

31. Jeffrey SC, Burke PJ, Lyon RP, Meyer DW, Sussman D, Anderson M, et al. A potent anti-CD70 antibody-drug conjugate combining a dimeric pyrrolobenzodiazepine drug with site-specific conjugation technology. Bioconjug Chem. 2013 Jul 17;24(7):1256–63.

32. Hussain AF, Amoury M, Barth S. Send Orders for Reprints to reprints@benthamscience.net SNAP-Tag Technology: A Powerful Tool for Site Specific Conjugation of Therapeutic and Imaging Agents. Vol. 19, Current Pharmaceutical Design. 2013.

33. Chudasama V, Maruani A, Caddick S. Recent advances in the construction of antibody-drug conjugates. Vol. 8, Nature Chemistry. Nature Publishing Group; 2016. p. 114–9.

34. Aron L Nelson, Janice N Reichert. Development trends for therapeutic antibody fragments. Nat Biotechnol. 2009 Apr;27:331–7.

35. Ahmad Fawzi HHPKFMHIBS. one-step site-specific antibody fragment auto-conjugation using SNAP-tag technology. Nature protocols . 2019;14(11):3101–25.

36. Ma Z, Zhao Y, Lv J, Pan L. Development and application of classical swine fever virus monoclonal antibodies derived from single B cells. Vet Res. 2023 Oct 16;54(1):90.

37. Reichert VA. Development trends for monoclonal antibody cancer therapeutics. Nature Reviews Drug Discovery.

38. Erickson HK, Lewis Phillips GD, Leipold DD, Provenzano CA, Mai E, Johnson HA, et al. The effect of different linkers on target cell catabolism and pharmacokinetics/pharmacodynamics of trastuzumab maytansinoid conjugates. Mol Cancer Ther. 2012;11(5):1133–42.

39. Nguyen TD, Bordeau BM, Balthasar JP. Mechanisms of ADC Toxicity and Strategies to Increase ADC Tolerability. Vol. 15, Cancers. MDPI; 2023.

40. Cindy H Chau, Patricia S Steeg, William D Figg. Antibody-drug conjugate for cancer . The Lancet . 2019 Sep 31;398(10200):793–804.

41. Jain N, Smith SW, Ghone S, Tomczuk B. Current ADC Linker Chemistry. Vol. 32, Pharmaceutical Research. Springer New York LLC; 2015. p. 3526–40.

42. Hussain AF, Heppenstall PA, Kampmeier F, Meinhold-Heerlein I, Barth S. One-step sitespecific antibody fragment auto-conjugation using SNAP-tag technology. Nat Protoc. 2019 Nov 1;14(11):3101–25.

43. Fu Z, Zhang X, Gao Y, Fan J, Gao Q. Enhancing the anticancer immune response with the assistance of drug repurposing and delivery systems. Clin Transl Med. 2023 Jul;13(7).

44. Woitok M, Klose D, Di Fiore S, Richter W, Stein C, Gresch G, et al. Comparison of a mouse and a novel human scFv-SNAP-auristatin F drug conjugate with potent activity against EGFRoverexpressing human solid tumor cells. Onco Targets Ther. 2017 Jul 6;10:3313–27.

45. Zhao J, Xu Z, Liu Y, Wang X, Liu X, Gao Y, et al. The expression of cancer-testis antigen in ovarian cancer and the development of immunotherapy [Internet]. Vol. 12, Am J Cancer Res. 2022. Available from: www.ajcr.us/

46. Coukos G, Tanyi J, Kandalaft LE. Opportunities in immunotherapy of ovarian cancer. Annals of Oncology. 2016 Apr 1;27:i11–5.

47. Edgardo D Carossella, Guiliaume Plourssard, Joel Lemaoult, Francios Desgrandchamps. A Systematic Review of Immunotherapy in urologic Cancer: involving roles of targeting of CTL 4, PD-1/PD L1and HLA DA. PubMed. 2015 Sep;63(2):267–79.

48. Tan EM, Zhang J. Autoantibodies to tumor-associated antigens: Reporters from the immune system. Vol. 222, Immunological Reviews. 2008. p. 328–40.

49. Criscitiello C. Tumor-associated antigens in breast cancer. Vol. 7, Breast Care. 2012. p. 262–6.

50. López de Sá A, Díaz-Tejeiro C, Poyatos-Racionero E, Nieto-Jiménez C, Paniagua-Herranz L, Sanvicente A, et al. Considerations for the design of antibody drug conjugates (ADCs) for clinical development: lessons learned. Vol. 16, Journal of Hematology and Oncology. BioMed Central Ltd; 2023.

51. Kanwal M, Smahel M, Olsen M, Smahelova J, Tachezy R. Aspartate ß-hydroxylase as a target for cancer therapy. Vol. 39, Journal of Experimental and Clinical Cancer Research. BioMed Central; 2020.

52. Shimoda M, Tomimaru Y, Charpentier KP, Safran H, Carlson RI, Wands J. Tumor progressionrelated transmembrane protein aspartate-b-hydroxylase is a target for immunotherapy of hepatocellular carcinoma.

53. Tomimaru Y, Mishra S, Safran H, Charpentier KP, Martin W, De Groot AS, et al. Aspartate-βhydroxylase induces epitope-specific T cell responses in hepatocellular carcinoma. Vaccine. 2015 Mar 3;33(10):1256–66.

54. Aihara A, Huang CK, Olsen MJ, Lin Q, Chung W, Tang Q, et al. A cell-surface β-hydroxylase is a biomarker and therapeutic target for hepatocellular carcinoma. Hepatology. 2014 Oct 1;60(4):1302–13.

55. Kreitman RJ. Recombinant Immunotoxins Containing Truncated Bacterial Toxins for the Treatment of Hematologic Malignancies.

56. Grossbard ML, Gribben JG, Freedman AS, Lambert JM, Kinsella J, Rabinowe SN, et al. Adjuvant
Immunotoxin Therapy With Anti-B4-Blocked Ricin After Autologous Bone Marrow Transplantation for Patients With B-Cell Non-Hodgkin's Lymphoma [Internet]. Available from: http://ashpublications.org/blood/article-pdf/81/9/2263/610368/2263.pdf

57. Baluna R, Rizo J, Gordon BE, Ghetie V, Vitetta ES. Evidence for a structural motif in toxins and interleukin-2 that may be responsible for binding to endothelial cells and initiating vascular leak syndrome (immunotoxinintegrinsdisintegrincytokine) [Internet]. Vol. 96, Medical Sciences. 1999. Available from: www.pnas.org.

58. Tur MK, Huhn M, Jost E, Thepen T, Brümmendorf TH, Barth S. In vivo efficacy of the recombinant anti-CD64 immunotoxin H22(scFv)-ETA' in a human acute myeloid leukemia xenograft tumor model. Int J Cancer. 2011 Sep 1;129(5):1277–82.

59. Tur MK, Huhn M, Thepen T, Stöcker M, Krohn R, Vogel S, et al. Recombinant CD64-Specific Single Chain Immunotoxin Exhibits Specific Cytotoxicity against Acute Myeloid Leukemia Cells [Internet]. Vol. 63, CANCER RESEARCH. 2003. Available from: http://aacrjournals.org/cancerres/article-pdf/63/23/8414/2510954/zch02303008414.pdf

60. Tur MK, Huhn M, Jost E, Thepen T, Brümmendorf TH, Barth S. In vivo efficacy of the recombinant anti-CD64 immunotoxin H22(scFv)-ETA' in a human acute myeloid leukemia xenograft tumor model. Int J Cancer. 2011 Sep 1;129(5):1277–82.

61. Thandeka Ndebele P, Barth Co-Supervisor S, Tai S. Determining the optimal host for affordable production of recombinant biopharmaceuticals exemplified by SNAP-tag based antibody fusion proteins. 2022.

62. Sodoyer R. TECHNOLOGY REVIEW Expression Systems for the Production of Recombinant Pharmaceuticals. Vol. 18, Biodrugs. 2004.

63. Frenzel A, Hust M, Schirrmann T. Expression of recombinant antibodies. Vol. 4, Frontiers in Immunology. 2013.

64. Khan KH. Gene expression in mammalian cells and its applications. Adv Pharm Bull. 2013;3(2):257–63.

65. Demain AL, Vaishnav P. Production of recombinant proteins by microbes and higher organisms. Vol. 27, Biotechnology Advances. 2009. p. 297–306.

66. Walker JM. METHODS I N MOLECULAR BIOLOGY TM Series Editor [Internet]. Available from: www.springer.com/series/7651

67. Mark JKK, Lim CSY, Nordin F, Tye GJ. Expression of mammalian proteins for diagnostics and therapeutics: a review. Vol. 49, Molecular Biology Reports. Springer Science and Business Media B.V.; 2022. p. 10593–608.

68. Barnes LM, Bentley CM, Dickson AJ. Stability of protein production from recombinant mammalian cells. Vol. 81, Biotechnology and Bioengineering. 2003. p. 631–9.

69. Bandaranayake AD, Almo SC. Recent advances in mammalian protein production. Vol. 588, FEBS Letters. 2014. p. 253–60.

70. Grillberger L, Kreil TR, Nasr S, Reiter M. Emerging trends in plasma-free manufacturing of recombinant protein therapeutics expressed in mammalian cells. Vol. 4, Biotechnology Journal. 2009. p. 186–201.

71. Malik A. Protein fusion tags for efficient expression and purification of recombinant proteins in the periplasmic space of E. coli. Vol. 6, 3 Biotech. Springer Verlag; 2016. p. 1–7.

72. Vincentelli R, Romier C. Expression in Escherichia coli: Becoming faster and more complex.
Vol. 23, Current Opinion in Structural Biology. 2013. p. 326–34.

73. Gill RT, DeLisa MP, Valdes JJ, Bentley WE. Genomic analysis of high-cell-density recombinant Escherichia coli fermentation and “cell conditioning” for improved recombinant protein yield. Biotechnol Bioeng. 2001 Jan 5;72(1):85–95.

74. Terpe K. Overview of bacterial expression systems for heterologous protein production: From molecular and biochemical fundamentals to commercial systems. Vol. 72, Applied Microbiology and Biotechnology. 2006. p. 211–22.

75. Martínez-Alarcón D, Blanco-Labra A, García-Gasca T. Expression of lectins in heterologous systems. Vol. 19, International Journal of Molecular Sciences. MDPI AG; 2018.

76. Arnold L. Demain, Preeti Vaishnav. Production of recombinant proteins by microbes and higher organisms. Biotechnology Advances . 2009 May;27(3):297–306.

77. Gary Walsh. Biopharmaceutical benchmarks 2014. nature biotechnology . 2014 Oct 9;32:992– 1000.

78. Zuppone S, Fabbrini MS, Vago R. Hosts for hostile protein production: The challenge of recombinant immunotoxin expression. Vol. 7, Biomedicines. MDPI AG; 2019.

79. Liu HF, Ma J, Winter C, Bayer R. Recovery and purification process development for monoclonal antibody production. Vol. 2, mAbs. 2010. p. 480–99.

80. Jain NK, Barkowski-Clark S, Altman R, Johnson K, Sun F, Zmuda J, et al. A high density CHO-S transient transfection system: Comparison of ExpiCHO and Expi293. Protein Expr Purif. 2017 Jun 1;134:38–46.

81. Pham PL, Perret S, Doan HC, Cass B, St-Laurent G, Kamen A, et al. Large-scale transient transfection of serum-free suspension-growing HEK293 EBNA1 cells: Peptone additives improve cell growth and transfection efficiency. Biotechnol Bioeng. 2003 Nov 5;84(3):332–42.

82. Remans K, Lebendiker M, Abreu C, Maffei M, Sellathurai S, May MM, et al. Protein purification strategies must consider downstream applications and individual biological characteristics. Microb Cell Fact. 2022 Dec 1;21(1).

83. Shukla AA, Hubbard B, Tressel T, Guhan S, Low D. Downstream processing of monoclonal antibodies-Application of platform approaches. Vol. 848, Journal of Chromatography B: Analytical Technologies in the Biomedical and Life Sciences. 2007. p. 28–39.

84. O'Kennedy R, Murphy C, Devine T. Technology advancements in antibody purification. Antibody Technology Journal. 2016 Aug;Volume 6:17–32.

85. Hober S, Nord K, Linhult M. Protein A chromatography for antibody purification. Vol. 848, Journal of Chromatography B: Analytical Technologies in the Biomedical and Life Sciences. 2007. p. 40–7.

86. Saraswat M, Musante L, Ravidá A, Shortt B, Byrne B, Holthofer H. Preparative purification of recombinant proteins: Current status and future trends. Vol. 2013, BioMed Research International. 2013.

87. Tripathi NK. Production and purification of recombinant proteins from Escherichia coli.
ChemBioEng Reviews. 2016;3(3):116–33.

88. Kinna A, Tolner B, Rota EM, Titchener-Hooker N, Nesbeth D, Chester K. IMAC capture of recombinant protein from unclarified mammalian cell feed streams; IMAC capture of recombinant protein from unclarified mammalian cell feed streams. Biotechnol Bioeng [Internet]. 2016;113:130–40. Available from: http://onlinelibrary.wiley.com/doi/10.1002/bit.25705/abstract

89. Spriestersbach A, Kubicek J, Schäfer F, Block H, Maertens B. Purification of His-Tagged Proteins. In: Methods in Enzymology. Academic Press Inc.; 2015. p. 1–15.

90. Dutta S and BK. Protein Purification by Affinity . In: The textbook of cloning, expression and purification of recombinant proteins . 2022. p. 141–71.

91. Karav S, Talak E, Tuncer M, Ozleyen A. The Effect of Fusion Tags on Enzyme Specificity and Protein Purification Efficiency. Vol. 6, International Journal of Agriculture Innovations and Research. 2017.

92. Young CL, Britton ZT, Robinson AS. Recombinant protein expression and purification: A comprehensive review of affinity tags and microbial applications. Vol. 7, Biotechnology Journal. 2012. p. 620–34.

93. Martínez Cristancho CA, David F, Franco-Lara E, Seidel-Morgenstern A. Discontinuous and continuous purification of single-chain antibody fragments using immobilized metal ion affinity chromatography. J Biotechnol. 2013 Jan;163(2):233–42.

94. Giese RW. Editorial on "Technology trends in antibody purification" by P.S. Gagnon. Vol. 1221, Journal of Chromatography A. 2012. p. 56.

95. Walls D, Loughran Editors ST. Protein Chromatography Methods and Protocols Second Edition Methods in Molecular Biology 1485 [Internet]. Available from: http://www.springer.com/series/7651

96. Fekete S, Beck A, Veuthey JL, Guillarme D. Ion-exchange chromatography for the characterization of biopharmaceuticals. Vol. 113, Journal of Pharmaceutical and Biomedical Analysis. Elsevier; 2015. p. 43–55.

97. Jungbauer A, Hahn R. Chapter 22 Ion-Exchange Chromatography. In: Methods in Enzymology.
Academic Press Inc.; 2009. p. 349–71.

98. Protein Purification Protocols.

99. Ishihara T, Yamamoto S. Optimization of monoclonal antibody purification by ion-exchange chromatography: Application of simple methods with linear gradient elution experimental data. In: Journal of Chromatography A. 2005. p. 99–106.

100. Gagnon Pete. Purification tools for monoclonal antibodies. Validated Biosystems, Inc; 1996. 254 p.

101. Kostanski LK, Keller DM, Hamielec AE. Size-exclusion chromatography - A review of calibration methodologies. J Biochem Biophys Methods. 2004 Feb 27;58(2):159–86.

102. Fekete S, Beck A, Veuthey JL, Guillarme D. Theory and practice of size exclusion chromatography for the analysis of protein aggregates. Vol. 101, Journal of Pharmaceutical and Biomedical Analysis. Elsevier; 2014. p. 161–73.

103. M. Potschka. Mechanism of size-exclusion chromatography: I Role of convection and obstructed diffusion in size-exclusion chromatography . 2001 Nov;648(1):41–69.

104. Wang Y, Teraoka I, Hansen FY, Peters GH, Hassager O. A theoretical study of the separation principle in size exclusion chromatography. Macromolecules. 2010 Feb 9;43(3):1651–9.

105. Protein Purification Protocols.

106. Duong-Ly KC, Gabelli SB. Gel filtration chromatography (size exclusion chromatography) of proteins. In: Methods in Enzymology. Academic Press Inc.; 2014. p. 105–14.

107. Karaan M, Barth S. Antibody engineering to evaluate binding, internalisation, and intracellular routing of tumour-targeting fusion proteins.

108. Mayuni G. Masters Thesis Generation of Glioblastoma specific SNAP based antibody fusion proteins for future radiolabelling application. 2022.

109. Mungra N, Barth S. Development of SNAP-tag based fusion proteins as novel auristatin Fcontaining immunoconjugates and photoimmunotheranostics in the detection and treatment of triple-negative breast cancer Plagiarism Declaration. 2021.

110. De S, Mukherjee A, Kaur R. Typing of Milk for A1 and A2 beta Casein [Internet]. 2011.
Available from: https://www.researchgate.net/publication/294581313

111. Zugazagoitia J, Guedes C, Ponce S, Ferrer I, Molina-Pinelo S, Paz-Ares L. Current Challenges in Cancer Treatment. Vol. 38, Clinical Therapeutics. Excerpta Medica Inc.; 2016. p. 1551–66.

112. Jin S, Sun Y, Liang X, Gu X, Ning J, Xu Y, et al. Emerging new therapeutic antibody derivatives for cancer treatment. Vol. 7, Signal Transduction and Targeted Therapy. Springer Nature; 2022.

113. Pucci C, Martinelli C, Ciofani G. Innovative approaches for cancer treatment: Current perspectives and new challenges. Vol. 13, ecancermedicalscience. ecancer Global Foundation; 2019.

114. Ibiayi Dagogo-Jack, Alice T Shaw. Tumor heterogeneity and resistance to cancer therapies. Nat Rev Clin Oncol. 2017 Nov 8;15:81–94.

115. Jungbauer A. Continuous downstream processing of biopharmaceuticals. Vol. 31, Trends in Biotechnology. 2013. p. 479–92.

116. Tripathi NK, Shrivastava A. Recent Developments in Bioprocessing of Recombinant Proteins: Expression Hosts and Process Development. Vol. 7, Frontiers in Bioengineering and Biotechnology. Frontiers Media S.A.; 2019.

117. Dosio FD, Brusa P, Cattel L. Immunotoxins and anticancer drug conjugate assemblies: The role of the linkage between components. Vol. 3, Toxins. 2011. p. 848–83.

118. Thomas A, Teicher BA, Hassan R. Antibody-drug conjugates for cancer therapy [Internet].
2016. Available from: www.thelancet.com/oncology

119. Mazor R, King EM, Pastan I. Strategies to Reduce the Immunogenicity of Recombinant
Immunotoxins. Vol. 188, American Journal of Pathology. Elsevier Inc.; 2018. p. 1736–43.

120. Mazor R, Onda M, Pastan I. Immunogenicity of therapeutic recombinant immunotoxins. Vol. 270, Immunological Reviews. Blackwell Publishing Ltd; 2016. p. 152–64.

121. Verma R, Boleti E, George AJT. Antibody engineering: Comparison of bacterial, yeast, insect and mammalian expression systems. Vol. 216, Journal of Immunological Methods. 1998.

122. Zhu J. Mammalian cell protein expression for biopharmaceutical production. Biotechnol Adv. 2012 Sep;30(5):1158–70.

123. Koc EC, Koc H. Regulation of mammalian mitochondrial translation by post-translational modifications. Vol. 1819, Biochimica et Biophysica Acta - Gene Regulatory Mechanisms. 2012. p. 1055–66.

124. Thomassstecklerreditors AMM. Handbook of Experimental Pharmacology 257 [Internet].
Available from: http://www.springer.com/series/164

125. Karaan M, Barth S. Antibody engineering to evaluate binding, internalisation, and intracellular routing of tumour-targeting fusion proteins.

126. Mayuni G. Masters Thesis Generation of Glioblastoma specific SNAP based antibody fusion proteins for future radiolabelling application. 2022.

127. Arruebo M, Vilaboa N, Sáez-Gutierrez B, Lambea J, Tres A, Valladares M, et al. Assessment of the evolution of cancer treatment therapies. Vol. 3, Cancers. 2011. p. 3279–330.

128. Barth S, Huhn M, Matthey B, Klimka A, Galinski EA, Engert AA. Compatible-Solute-Supported Periplasmic Expression of Functional Recombinant Proteins under Stress Conditions [Internet]. Vol. 66, APPLIED AND ENVIRONMENTAL MICROBIOLOGY. 2000. Available from: https://journals.asm.org/journal/aem

129. Barth S, Huhn M, Matthey B, Schnell R, Tawadros S, Schinköthe T, et al. Recombinant antiCD25 immunotoxin RFT5(scFv)-ETA' demonstrates successful elimination of disseminated human hodgkin lymphoma in SCID mice. Int J Cancer. 2000;86(5):718–24.

130. Martínez-Ceron MC, Marani MM, Taulés M, Etcheverrigaray M, Albericio F, Cascone O, et al.
Affinity chromatography based on a combinatorial strategy for rerythropoietin purification. ACS Comb Sci. 2011 May 9;13(3):251–8.

131. Goswami S, Wang W, Arakawa T, Ohtake S. Developments and challenges for mAb-based therapeutics. Vol. 2, Antibodies. MDPI; 2013. p. 452–500.

132. Describing the pathway for protein complex formation.

133. Remans K, Lebendiker M, Abreu C, Maffei M, Sellathurai S, May MM, et al. Protein purification strategies must consider downstream applications and individual biological characteristics. Microb Cell Fact. 2022 Dec 1;21(1).

134. Chang YC, Yang SY, Lin JY, Hanh NTD, Srinophakun P, Chiu CY, et al. Scaling down recombinant carbonic anhydrase isolation with immobilized metal ion chromatography (IMAC): Harnessing enzymatic carbon dioxide capture and mineralization. J Taiwan Inst Chem Eng. 2024 Dec 1;165.

135. Watanabe H, Matsumaru H, Ooishi A, Feng YW, Odahara T, Suto K, et al. Optimizing pH response of affinity between protein G and IgG Fc. How electrostatic modulations affect protein-protein interactions. Journal of Biological Chemistry. 2009 May 1;284(18):12373–83.

136. Timmick SM, Vecchiarello N, Goodwine C, Crowell LE, Love KR, Love JC, et al. An impurity characterization based approach for the rapid development of integrated downstream purification processes. Biotechnol Bioeng. 2018 Aug 1;115(8):2048–60.

137. Kesik-Brodacka M, Romanik A, Mikiewicz-Sygula D, Plucienniczak G, Plucienniczak A. A novel system for stable, high-level expression from the T7 promoter. Microb Cell Fact. 2012 Aug 16;11.

138. Xia W, Bringmann P, McClary J, Jones PP, Manzana W, Zhu Y, et al. High levels of protein expression using different mammalian CMV promoters in several cell lines. Protein Expr Purif. 2006 Jan;45(1):115–24.

139. Dan H, Balachandran A, Lin M. A Pair of Ligation-Independent Escherichia coli Expression Vectors for Rapid Addition of a Polyhistidine Affinity Tag to the N-or C-Termini of Recombinant Proteins. Vol. 20, Journal of Biomolecular Techniques. 2009.

140. Yuan LD, Hua ZC. Expression, purification, and characterization of a biologically active bovine enterokinase catalytic subunit in Escherichia coli [Internet]. Available from: www.academicpress.com

141. Hermening S, Kügler S, Bähr M, Isenmann S. Increased protein expression from adenoviral shuttle plasmids and vectors by insertion of a small chimeric intron sequence. J Virol Methods. 2004 Dec 1;122(1):73–7.

142. Wong S, Jimenez S, Slavcev RA. Construction and characterization of a novel miniaturized filamentous phagemid for targeted mammalian gene transfer. Microb Cell Fact. 2023 Dec 1;22(1).

143. Marques R, Lacerda R, Romão L. Internal Ribosome Entry Site (IRES)-Mediated Translation and Its Potential for Novel mRNA-Based Therapy Development. Vol. 10, Biomedicines. MDPI; 2022.

144. Reus JB, Trivino-Soto GS, Wu LI, Kokott K, Lim ES. SV40 large T antigen is not responsible for the loss of STING in 293T cells but can inhibit cGAS-STING interferon induction. Viruses. 2020;12(2).

145. Wang XY, Du QJ, Zhang WL, Xu DH, Zhang X, Jia YL, et al. Enhanced Transgene Expression by Optimization of Poly A in Transfected CHO Cells. Front Bioeng Biotechnol. 2022 Jan 24;10.

146. Kong J, Wang Y, Qi W, Huang M, Su R, He Z. Green fluorescent protein inspired fluorophores. Vol. 285, Advances in Colloid and Interface Science. Elsevier B.V.; 2020.

147. Nishizaki SS, McDonald TL, Farnum GA, Holmes MJ, Drexel ML, Switzenberg JA, et al. The Inducible lac Operator-Repressor System Is Functional in Zebrafish Cells. Front Genet. 2021 Jun 18;12.

148. Lee H, Song ES, Lee YH, Park JY, Kuk MU, Kwon HW, et al. A novel hybrid promoter capable of continuously producing proteins in high yield. Biochem Biophys Res Commun. 2023 Apr 2;650:103–8.

149. Panagopoulos I, Andersen K, Gorunova L, Eilert-Olsen M, Lund-Iversen M, Wessel-Aas T, et al.
Presence of a t(12;18)(q14;q21) Chromosome Translocation and Fusion of the Genes for High-mobility Group AT-Hook 2 (HMGA2) and WNT Inhibitory Factor 1 (WIF1) in Infrapatellar Fat Pad Cells from a Patient With Hoffas Disease. Cancer Genomics Proteomics. 2022 Sep 1;19(5):584–90.

150. Prabhakant A, Panigrahi A, Krishnan M. Allosteric Response of DNA Recognition Helices of Catabolite Activator Protein to cAMP and DNA Binding. J Chem Inf Model. 2020 Dec 28;60(12):6366–76.

7. Appendix

Table 13: Elements of the plasmid and their function

Elements	**Function**
T7 promoter	Regulate the transcription of the target gene(136)
Cytomegalovirus (CMV) promoter	Induces transient expression of the fusion protein(137)
Ig-*Kappa* leader	Allows secretion of the fusion protein
N-terminal polyhistidine tags (His x 6)	Facilitates detection and purification of recombinant proteins(138)

Enterokinase (EKS) cleavage site	Permits the elimination of N-terminal histidine tags and the isolation of the fused protein(139)
SNAPf	A rapid-labelling version of SNAP-tag, exhibiting a reactivity boost of up to tenfold towards benzylguanine (BG) substrates
Chimeric intron	Increase transgene expression by enhancing mRNA processing (140)
F1 origin	Allows rescue of single-stranded DNA (141)
Internal ribosome entry site (IRES)	Facilitate the translation EGFP gene(142)
SV40 Ori	Origin of replication (143)
Bovine growth hormone polyadenylation (bGH poly(A)) signal	Allows termination of transcription and initiate the polyadenylation process during the expression of a gene(144)
Green fluorescent protein (GFP)	Enable the visualization of successful transfection in mammalian cells and of the tagged proteins within living cells(145)
BleoR	Allows selection of transient transfectants in mammalian cells (using Zeocin)
Lac operator	Inhibit the transcription of lac genes in the absence of the lac gene(146)
Lac promoter	functions as a regulatory element that controls the expression of genes involved in lactose metabolism(146)
SV40 promoter	enabled sustained expression at stable levels(147)
Ampicillin resistance gene	Used as a genetic marker and allows the selection of transformed cells
M13 rev	Single-stranded oligonucleotide sequence used in polymerase chain reactions (148)
CAP binding site	Site where catabolite activator protein (CAP) binds, playing a role in the transcription of multiple genes, including those encoding enzymes crucial for sugar metabolism(149)
*Sfi*I/*Not*I	Restriction sites

Table 14: Binding validation steps for H22(scFv)-ETA

Mix	Group / Cell line	Volume	Objective	Cell number to be stained
1	U937 stimulated unstained	200 µl		5 x 10^5 cells
2a	U937 stimulated + ethanol + Viability-Live/dead Stain Alexa Flour 405	200 µl	Use to gate and separate live cells from dead cells	2.5 x 10^5 cells

2b	U937 stimulated + Add to 2a after removal of ethanol	200 ul	(Compensation)	2.5 x 10^5 cells
3	U937 stimulated + H22-ETA + Anti-His PE+Alexa646	200 µl	Single Stain (Compensation)	5 x 10^5 cells
4	U937 stimulated + H22dETA + Anti-His PE+Alexa646			
5	U937 stimulated + H22SNAP + Anti-His PE+Alexa646			
6A	U937 stimulated + Viability-Live/dead Stain Alexa Flour 405 + H22-ETA+ Anti-His PE+Alexa646	200 µl		5 x 10^5 cells
6B	U937 stimulated + ViabilityLive/dead Stain Alexa Flour 405 + H22-ETA + Anti-His PE+Alexa646	200 µl		5 x 10^5 cells
	U937 unstimulated + Viability-Live/dead Stain Alexa Flour 405 + H22-ETA + Anti-His PE+Alexa646	200 µl		5x 10^5 cells
6	U937 stimulated + Viability Live/dead stain Alexa 405 + Anti-CD64 Antibody – Alexa Flour 647	200ul	Positive Control	5x 10^5 cells
7	U937 stimulated + AntiCD64 antibody – Alexa Flour 647	200ul	Single Stain (Compensation)	5 x 10^5 cells
8A	U937 stimulated + Viability-Live/dead Stain Alexa Flour 405 + H22-dETA + Anti-His PE	200ul		5 x 10^5 cells
8B	U937 stimulated + Viability-Live/dead Stain Alexa Flour 405 + H22-dETA + Anti-His PE	200ul		5 x 10^5 cells
9A	U937 stimulated + Viability-Live/dead Stain Alexa Flour 405 + H22-SNAP + Alexa 647	200ul		5 x 10^5 cells
9B	U937 stimulated + Viability-Live/dead Stain Alexa Flour 405 + H22-SNAP + Alexa 647	200ul		5 x 10^5 cells

10	U937 stimulated + Anti-His PE	200ul	Control/Secondary Antibody Baseline	5 x 10^5 cells

Table 15: Equipment needed

Equipment	Manufacturer /brand
Weighing balance	Radwag
pH meter	Dostmann Electronic
centrifuge	Beckman coulter
Pipettes	Discovery Pro
Pipettes tips	Merck
Heating block	Eppendorf
Mini Trans-Blot Cell system	Bio-Rad, USA
Gel Doc™ XR Gel	Bio-Rad, USA
MiniProtean Tetra Cell system	Bio-Rad, USA
Vacuum filtration system	Conxport
ZOE™ Fluorescent Cell Imager	Bio-Rad Laboratories, UK
ÄKTA Avant protein purification system	GE Healthcare, USA
HisTrap™ Excel column	GE Healthcare, USA
HiTrap Chelating HP	GE Healthcare, USA
HiTrap Chelating HP	GE Healthcare, USA
HiTrap Q	GE Healthcare, USA
HiLoad™ Superdex™ 200 pg	GE Healthcare, USA
TC biosafety cabinet	Labgard
Cell counter	Bio-rad
Tissue Culture incubator	Nuaire

Vortex	LMS Co Ltd
UV spectrophotometry	DeNovix, USA
Shaking incubator	Yinder Co Ltd
Water purification system	Milli-Q

Table 16: Tissue culture Media

Media	Composition	Concentration
RPMI-1640 culture medium	Phenol red	15 mg/L
	Fetal Bovine serum Penicillin Sodium Pyruvate Streptomycin GlutamMAX	10 % v/v 100 I. U/ mL 3.7 g/L 100 ug/ Ml 2 mM

Table 17: Cell lines used for the expression of SNAP-tag fusion antibody

Protein purified	**Expression system**	**Cell line**
αASPH(scFv)-SNAP	Mammalian	HEK 293T
αL243(scFv)-SNAP	Mammalian	HEK 293T

Table 18: E.coli strain used to express H22(scFv)-ETA

Strain	Genotype	Source
Escherichia coli (*E. coli*) BL21(DE3)	*F- ompT hsdSB (rB- mB-) gal dcm- lon-*	New England Biolabs, USA

Table 19: Reagents used for bacterial expression

Terrific broth Composition	Quantity
Terrific broth powder	47.6
Glycerol	8 mL
ddH20	1 L

Table 20: Additional buffers used for experiments

Buffers	**Composition**
1X PBS (pH7.4)	8.1mM Na2HPO4 8.1mM KH2PO4 137mM NaCl 2.7mM KCL Sterile dH2O

1x SDS-PAGE Running Buffer pH 8.3	SDS powder(10g) dH2O(100mL)
Transfer buffer	Tris Base (30g) Glycine(144g)
1x Phosphate-Buffered Saline (PBS)	
10x running buffer	Tris Base (30.3g) SDS (10g) Glycine (144g) dH2O (fill up to 1L)
10% Ammonium per sulphate (APS)	Ammonium per sulphate powder (5g) dH2O (50mL)
10X Tris-buffered saline (TBS)	Tris Base(200mM) NaCl (1.5M) dH2O
1X buffer transfer	10X Transfer Buffer: 100% Methanol: dH2O (1:2:7)
10X Tris-buffered saline (TBS)	Tris Base(200mM) NaCl (1.5M) dH2O
1X TBS-Tween(TBST)	1 (TBS): 9 (dH2O) 1mL Tween 20
4% Polyacrylamide gel	4 % Acrylamide/Bis-acrylamide 190 mM Tris-Cl, pH 6.8 0.1 % SDS 0.1 % Ammonium persulphate 0.1 % TEME
10% Polyacrylamide gel	10 % Acrylamide/Bis-acrylamide 375 mM Tris-Cl, pH 8.8 0.1 % SDS 0.1 % Ammonium persulphate 0.1 % TEMED
Luria-Bertani (LB) broth	1.0 %Casein peptone 0.5 % Yeast extract 1.0 % NaCl